Republic of Iraq
Ministry of Higher Education and Scientific Research
University of Babylon
College of Materials Engineering
Department of Ceramics Engineering and Building Materials

Optimizing the Porosity of Geopolymer based on metakaolin

A Thesis
Submitted to the Council of the College of Materials Engineering/University of Babylon in Partial Fulfillment of the Requirements for the Master Degree in Materials Engineering/ceramic

By
Shahad Abdulzahra Jawad Midan

Supervised by
Prof. Imad Ali Disher Al-Hydary (Ph.D.)
Prof. Mohammed A. Ahmed Al-Dujaili (Ph.D.)

2021 A.C 1443A.H

بسم الله الرحمن الرحيم

﴿وَمَا تَوْفِيقِي إِلَّا بِاللَّهِ عَلَيْهِ تَوَكَّلْتُ وَإِلَيْهِ أُنِيبُ﴾

صدق الله العظيم

الآية (٨٨) - سورة هود

Supervisor Certification

We certify that this thesis entitled **(Optimizing the porosity of Geopolymer based on metakaolin)**, which was prepared by "shahad Abdulzahra Jawad", had been carried out under our supervision at the University of Babylon/College of Materials Engineering/Department of Ceramics Engineering and Building materials in partial fulfillment of the requirements for the degree of Master in Ceramic Engineering.

Supervisor
Signature:
Prof. Imad A. Disher Al-Hydary (Ph. D)
Date: / / 2021

Co-Supervisor
Signature:
Prof. Mohammed A. Ahmed (Ph. D)
Date: / / 2021

In view of the available recommendations. I forward this thesis for debate by the examination committee.

Signature:
Prof. Mohsin Abbas Aswad (Ph. D)
Head of Ceramics Engineering and Building Materials
Date: / /2021

Dedication

To my parents, sisters and brothers who give me the biggest love and support…

Shahad 2021

Acknowledgments

First of all, profusely all thanks be for **ALLAH** Lord of all creations who enable me to achieve this work. I would like to express my deep thanks to the College of Materials Engineering/ University of Babylon for giving me the chance to complete my study.

I would like to express my deep gratitude and appreciation to my supervisors **Prof. Imad Ali Disher Al-Hydary (Ph.D.) and Prof. Mohammed A. Ahmed (Ph.D)** for their advice, support and encouragement they gave me during the course of work. Their suggestions and moral support in difficult times have been essential for completing this work. I am very proud to know you and learn under your supervision. I want to express my appreciation and gratitude to the head of department **Dr. Mohsin Abbas Aswad**, all the professors, and the ceramics department staff. My deep appreciation goes to the members of ceramic materials laboratories **especially Eng. Ashwaq, Eng. Mahmood, Eng. Khaidaa, Eng. Homam, Eng. Ibtisam, Eng. Rehab, Eng. Khansaa**.

I would also like to thank all my friends and colleagues during the study in the college, for creating an unforgettable environment in which my research was carried out, especially library staff in College of Materials Engineering, University of Babylon.

My deeply gratitude and thanks for my family to their support, patience, and help. My mother and father, my first teachers, there are neither enough words in the world nor a good actions to show you how much I am grateful to everything you did to me and still doing. I will always seeking for you satisfaction. Every woman needs a supporter in her life, but imagine that she has three. My brothers, anything I reached, did or gained, was easy without your help and cooperation.

Examination Committee Certification

We certify that we had read this thesis entitled **(Optimizing the porosity of Geopolymer based on metakaolin)** and as an examination committee, we examined the student **(Shahad Abdulzahra Jawad)** in its contents and that in our opinion it meets the standard of a thesis and is adequate for the award of the degree of Master in Ceramic Engineering.

Signature:
Prof. Dr. Elham Abd Al Majeed (Ph.D)
Date: / /2021
(Chairman)

Signature:
Assist.Prof. Besma Mohammed Fahad(Ph.D)
University of Al Mustansiriyah
Date: / /2021
(Member)

Signature:
Prof. Hayder Algibory(Ph.D)
University of Babylon
Date: / /2021
(Member)

Signature:
Prof. Imad A. Disher (Ph.D)
University of Babylon
Date: / / 2021
(Supervisor)

Signature:
Prof. Mohammed A.Ahmed(Ph.D)
University of Babylon
Date: / / 2021
(Supervisor)

Signature:
Prof. Mohsin Abbas Aswad(Ph.D)
Head of ceramics engineering and Building materials
Date: / / 2021

Signature:
Prof. Imad A.Disher Al-Hydary(Ph.D)
Dean of Materials Engineering collage
Date: / / 2021

وزارة التعليم العالي والبحث العلمي
جامعة بابل
كلية هندسة المواد
قسم هندسة السيراميك ومواد البناء

ايجاد امثل مسامية للجيوبوليمر المتكون من الميتاكاؤلين

رسالة

مقدمة الى كلية هندسة المواد جامعة بابل كجزء من متطلبات نيل درجة الماجستير
في هندسة المواد /السيراميك

من قبل
شهد عبد الزهرة جواد ميدان

باشراف
أ.د. عماد علي دشر الحيدري
أ.د. محمد عاصي احمد

١٤٤٣ هـ ٢٠٢١م

الخلاصة

الجيوبوليمرات مع الصيغة الكيميائية (Na2O.Al2O3.nSiO2.xH2O)هي مواد رابطة الومينوسيليكات ثلاثية الابعاد يمكن انتاجها في درجة حرارة الغرفة عن طريق الانحلال والتكثيف المتعدد وترسيب مصدر الالومينوسيليكات. عادة مايتضمن انتاج الجيوبوليمرات المسامية اضافة عوامل رغوية مثل بيروكسيد الهيدروجين (H_2O_2).

من المتوقع ان يؤثر دمج عوامل الرغوة في انتاج الجيوبوليمرات على حركية البلمرة الجيولوجية،بالاضافة الى انسيابية المعاجين من خلال تفاعل غير مقيد في بيئة قلوية عالية من الجيوبوليمرات مما يؤدي الى تكوين مادة مسامية مع فراغات خشنة غير مرغوب فيها وقوة ميكانيكية منخفضة.

الدراسة الحالية هي محاولة لتحسين المسامية ومقاومة الانضغاط للجيوبوليمر.تم استخدام طريقة تاجوشي لتصميم وتحليل التجارب ولتحديد نسب المزج المثلى لمواد البدء لتركيب الجيوبوليمرالمسامي .ومع ذلك، لايمكن لطريقة تاجوشي التقليدية حل التحسين المتعدد الاهداف بحيث في هذه الدراسة طريقة تاجوشي مقترنة بسبعة طرق يمكن ان تساعد في هذة المشكلة.

تم تحضير الجيوبوليمر المسامي عند درجة الحرارة المحيطة من مسحوق الميتاكاؤلين ($Al_2Si_2O_7$)كمصدر للالمنيوم والسليكون،وهلام السيليكا كسيليكا خالية،وسيليكات الصوديوم وهيدروكسيد الصوديوم كسلائف للمحلول القلوي، واستخدم بيروكسيد الهيدروجين مع الخميرة الفورية كعوامل رغوية واستخدم الزيت النباتي كعامل استقرار(السطحي). تم اقتراح التركيبة المثلى للعوامل المؤثرة من اجل تحقيق قوة ضغط ومسامية اعلى. فحصت المواد الاولية والجيوبوليمرات المسامية المحضرة بانحراف الاشعة السينية(XRD) وتحليل(DTA) وتحليل حجم الجسيمات والفحص المجهري الضوئي وتحديد بعض الخواص الفيزيائية مثل الكثافة الظاهرية والمسامية الكلية وامتصاصية الماء وقوة الانضغاط.

تميزت عينات النتائج بامتلاكها مقاومة الضغط عالية (2.4-88.3Mpa) مع كثافات ظاهرة تتراوح من ($0.47\text{-}1.21 g/cm^3$) ومسامية عالية (22-77%) .تم اقتراح العينات المثلى (4, 8, 10, 11) من خلال طرق utility concept والdesirability geometric mean ،بينما تم اقتراح العينات الاقل جودة المتبقية من خلال طرق التحسين الاخرى مثل (level weight, principal component analysis, grey rational analysis, data envelopment analysis, engineering judgment, principal component analysis)

Abstract

Geopolymers with the chemical formula ($Na_2O.Al_2O_3.nSiO_2.XH_2O$) are three-dimensional aluminosilicate binder materials made by dissolving, polycondensing, and precipitating an aluminosilicate source at ambient temperatures. Blowing agents, such as hydrogen peroxide (H_2O_2), are commonly used in the synthesis of porous geopolymers. The inclusion of foaming agents in the production of geopolymers is expected to affect the geopolymerisation kinetics as well as the rheology of the pastes, resulting in a porous matrix with undesirable coarse voids and low mechanical strength.

The current study is an attempt to optimize the porosity and compressive strength of the geopolymer. Taguchi method is used for the design and analysis of experiments and to determine the optimum mix proportion of starting materials to synthesize strong and porous geopolymer. However, traditional Taguchi method cannot solve multi-objective optimization so that in this study Taguchi method is coupled with seven approaches which can assist this problem.

The porous geopolymer was prepared at ambient temperature from metakaolin powder ($Al_2Si_2O_7$) as a source of aluminium and silicon, silica gel as free silica, and sodium silicate and sodium hydroxide as precursors of alkaline solution. Hydrogen peroxide with the instant yeast were used as blowing agents and the vegetable oil used as stabilizing agent (surfactants). Optimal combination of process parameters has been proposed in order to achieve higher compressive strength and porosity. The starting materials and porous geopolymer were characterized by X-ray Diffraction (XRD), DTA analysis, particle size analysis, optical Microscope and some physical properties such as bulk density, total porosity, water absorption, compressive strength were also tested. The resulting samples found to have higher compressive strength varied

between (2.4–88.3 MPa) with apparent densities varying from (0.47) to (1.21 g/cm^3) and high porosity of (22-77 %). The optimal samples (4,8,10,11) were suggested by the utility concept and Desirability based methods, while the remaining lower quality samples were suggested by the other optimization methods (Grey rational analysis, Principal component analysis, Data envelopment analysis, level weight, engineering judgment).

Table of Content

List of Figures

List of Tables

List of Latin Symbols

Symbol	Meaning
Δ	Deviation sequence
I	Value of input
o	Value of output
η	S/N ratio
λ	Wavelength
ρ	Bulk density
σ	Standard deviation
σc	Compressive strength
ω	Importance of response
v	Weight function
μ	Response mean

List of English Symbols

Aw	Water absorption
D	Desirability function
E	General Efficiency
h	Hour
L	Quality loss
PA	Apparent porosity
Pi	Preference number
T	Target value
U	Utility function
y	Observed data
Z	Normalization function

List of Abbreviation

AAMs	alkali activated materials
ANOVA	Analysis of variance
DEA	Data envelopment analysis
DGM	Desirability Geometric Mean
DMU's	decision-making units
DOE	Design of Experiment
DTA	Differential Thermal Analysis
GP	Geopolymer
GRA	Grey Relational Analysis
GRC	Grey Rational Coefficient
GRG	Grey Rational Grade
LTB	Larger-The-Best
NTB	Nominal-The-Best
OA	Orthogonal Array
OPC	Ordinary Portland cement
PCA	Principal Component Analysis
PGs	Porous geopolymers
PSA	Particle Size Analysis
QL	Quality Loss
R&D	Research &development
S/N	Signal-to-noise ratio
STB	Smaller-The-Best
TNQL	Total Normalized Quality Loss
XRD	X-Ray Diffraction

CHAPTER ONE

INTRODUCTION

1.1Overview

Portland cement is used exclusively in the construction industry. In the process of producing cement clinker, which is calcined, cement is a significant pollutant to the atmosphere [1-3]. The amount of carbon dioxide created during the manufacturing of Ordinary Portland Cement OPC is on the order of one ton for every ton of OPC produced due to the calcination of limestone and the burning of fossil fuels. Furthermore, as compared to steel and aluminum, OPC takes the least amount of energy to manufacture [4-6].

The geopolymer is an alternative material that can be utilized to replace cement in a more environmentally friendly manner without the need for combustion [7]. Davidovits describes geopolymer as an amorphous, three-dimensional short range order inorganic polymer when a highly concentrated aqueous alkali hydroxide-silicate solution is applied to aluminosilicate raw materials such as metakaolin, fly ash, or slag [8]. For silicon (Si) and aluminum (Al), thermally activated natural resources, such as metakaolinite, or industrial byproducts, such as fly ash or slag, are used to make the geopolymers. The binder is made by dissolving silicon and aluminum in an alkaline activating solution, which subsequently polymerizes into molecular chains [9]. Metakaolin's application in geopolymers may be justified by the fact that it is a common industrial mineral that can be manufactured in large quantities with uniform properties [10-12].

Porous geopolymers (PGs) are one of the fastest-growing research areas in the field of porous inorganic nonmetallic materials because of the good global availability and low cost of the starting materials, the ability

to produce components without requiring a sintering step, and promising properties such as low thermal conductivity and good chemical stability [13-15].

A variety of ways have been investigated to construct reproducible porous geopolymer sponges, foams, graded and/or hollow structures. Some of the processing procedures are direct foaming, sacrificial template, emulsion templating, additive manufacturing, replica templating, and combinations of these [16-18]. The simplest and most promising technology for large-scale manufacture is direct foaming [13]. Foam stabilizer include calcium stearate, olive oil, vegetable oil, protein, Tween-80,Triton X-100, oleic acid [19-25], sodium dodecyl benzene sulfonate (SDBS) [13], and pore foaming agents like hydrogen peroxide or Aluminum powder [26], In the manufacture of porous geopolymer, Silicon powder, as well as other Si-containing materials including FeSi, SiC, and silica fume are essential.

The performance of geopolymer foam materials can be influenced by a variety of factors. These factors include raw material quality, mix proportion design, and the amount and type of foam agents/stabilizer [19]. In cement and geopolymer foams, hydrogen peroxide has long been utilized as a chemical foaming agent. In the extremely alkaline environment of geopolymers, hydrogen peroxide decomposition can be an unconstrained process, resulting in a porous matrix with undesired coarse gaps [27]. The trapped gas bubbles in the paste expand and create voids. The amount of oxygen created by the following reaction determines the volume expansion of this substance [28]:

$H_2O_2 \rightarrow H_2O + ½\ O_2$

High alkalinity is known to catalyze hydrogen peroxide breakdown [29], and sodium silicate solution is known to stabilize it by reducing hydrogen peroxide decomposition and slowing down the reaction [30].

1.2 The Problem of the Study

It is well known that the presence of the pores reduces the mechanical strength of the geopolymer [31], [32]. However, in many applications, it is desired to have a material that combines high porosity and high mechanical strength. Such material can be used, for example, as load bearing thermal insulator, load bearing light weight material and highly porous catalyst or adsorbent that can be used under high pressure conditions. A study that combines the optimization of both porosity and mechanical strength is not well reported in the literatures.

1.3 The Scope of the Current Study

The current research work is an attempt to imply the Taguchi method in the design of the experiment for optimizing the porosity and compressive strength of the metakaolin-based geopolymer. Three common factors were selected to design the experiments including the concentration of hydrogen peroxide, the quantity of hydrogen peroxide and the quantity of vegetable oil as stabilizer. Furthermore, for the first time, two additional factors were tackled in the current study; these are (i) the time of polymerization elapse before adding the hydrogen peroxide to the produced geopolymer paste prior to casting and (ii) the amount of yeast added to the mix which has been used to catalyze the decomposition of the hydrogen peroxide to produce pores. The first factor, i.e. the time of polymerization, is expected to affect the pore size, pore shape and the distribution of the pores along the geopolymer body; this is due to its effect on the viscosity of the geopolymer paste. The later factor, i.e. the

amount of yeast, is chosen to have a controllable factor that affect the decomposition of hydrogen peroxide rather than the uncontrollable factors of the alkalinity and the amount of sodium silicates, which have fixed values based on the preselected composition of the geopolymer, that have been optimized in a previous work in our department [33]. Five levels, having strongest impact on the performance of the specimens, for each of the five factors were selected in the design of the experiments based on primary rough experiments. The effect of these parameters on the density, porosity and compressive strengths at age of 28 days were examined and used with the help of Taguchi method to find the optimal sample in terms of porosity and compressive strength.

The Taguchi approach, However, can only be utilized for a single response situation. It can't be utilized to solve problems with many responses. Therefore, in this study more effective approaches were used to solve such complicated problem these approaches includes:

1.4 The Objectives of the Current Study

The current research project aims to produce geopolymers with high compressive strength and high porosity by Taguchi method.

1.5 Structure of the thesis

The thesis was divided into five chapters. The first chapter contains an introduction that briefly discusses the topic, its importance, and the current work technique. The second chapter is devoted to reviewing various theoretical concepts related to the study's issues and the literature review. Chapter three involves experimental methods utilized to fabricate the samples and the instrumentations used for testing. The results of the study are presented in Chapter 4 along with a discussion of the findings.

In Chapter 5, the current work's conclusions were presented, as well as new scopes for future investigation.

CHAPTER ONE: INTRODUCTION

CHAPTER TWO

THEORETICAL ASPECTS & LITERATURE REVIEW

2.1 Introduction

This chapter is divided into two parts; the first part deals with the theoretical aspects related to the current work and the second part is literature review of previous research.

2.2 Theoretical Part

2.2.1 Overview

Ordinary Portland Cement, the most common cementitious building material, is responsible for a significant amount of global CO_2 emissions due to the decomposition of limestone and the combustion of fossil fuels during production[1]. Geopolymer and other similar binders such as alkali activated materials (AAMs) have attracted a lot of attention as suitable alternatives due to their significantly lower emissions during production. An additional benefit of the use of geopolymer compared with OPC concrete is based on the possibility of using high-volume industrial waste in high- performance concretes, with a significant reduction in CO_2 emission[2].

The concept of geopolymer concrete was first introduced by a French scientist Joseph Davidovits in 1978 who proposed alkaline liquid as an activator to be used to react with some source material rich in silicon and aluminium, such as industry and agro waste products like fly ash, ground granulated blast furnace slag or rice husk ash to produce geopolymer mortar which act as binder [35-37]. Commercially available geopolymers could be utilized in fire- and heat-resistant coatings and

adhesives, medicinal applications, high-temperature ceramics, novel binders for fire-resistant fiber composites, encapsulation of toxic and radioactive waste, and new concrete cements [38-40]. Many scientific and industrial fields are investigating the properties and applications of geopolymers, including current inorganic chemistry, physical chemistry, colloid chemistry, mineralogy, geology, and other forms of engineering process technologies. Geopolymers is a branch of polymer science, chemistry, and technology that is one of the most important branches of materials science. Geopolymers fall into a variety of categories, including:

• Geopolymer cement based on slag.

• Geopolymer cement based on rock.

• Geopolymer cement based on ferro-sialate.

• Geopolymer cement based on metakaolin.

• Fly ash-based geopolymer cement entails the following:

Type 1; Alkali-activated fly ash geopolymer

Type 2; slag/fly ash-based geopolymer cement

Geopolymers possess many favourable properties such as rapid setting and hardening, good long-term properties and durability, as well as a good ability to immobilize toxic metals, and improved resistance to acids and the action of fire.[5]

Pure inorganic geopolymers and organic-containing geopolymers are the two main types of geopolymers. Inorganic geopolymer is a mineral chemical molecule or mixture of compounds made up of repeating units, such as silico-oxide (-Si-O-Si-O-), silico-aluminate (-Si-

O-Al-O-), ferro-silico-aluminate (-Fe-O-Si-O-Al-O), or alumino-phosphate (-Al-O-P-O-) [42].

Organic polymers are macromolecules composed of many repeating monomer units. Both synthetic and natural polymers play a crucial role in everyday life. Polysaccharides, polypeptides, and polynucleotides are the main types of biopolymers in living cells. The geopolymer reaction mechanism is depicted in Fig. 2.1, with the actual starting units of sodium-based alumino-silicate [6].

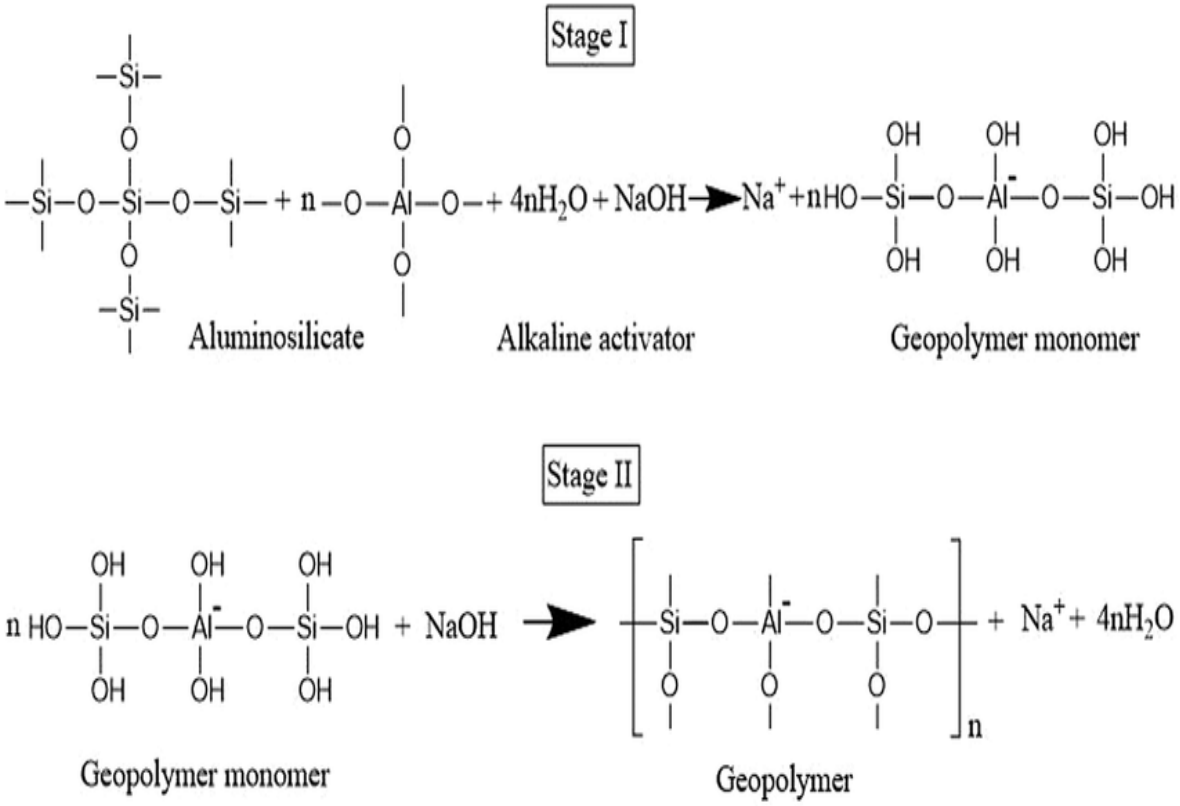

Figure (2.1) Geopolymer-reaction mechanism between the sodium hydroxide activator and the Si−Al source materials[6].

Geopolymer microstructure is largely temperature sensitive; at room temperature, it is X-ray amorphous, but at temperatures above 500 °C, it transforms into a crystalline matrix. There are two synthesize routes used in the production of geopolymer [7]:

1- Alkaline route: in this route the geopolymer synthesize by using an alkaline medium (Na^{+}, Ca^{++}, K^{+}, Cs^{+}) hydroxide or a mixture of two or more of them.

2- Acidic route: This will produce poly (alumino-phospho) types by using phosphoric acid H_3PO_4 [7].

2.2.2 Properties of Geopolymer

The following are some of the general features of geopolymers[44]:

1) Geopolymers have a high degree of polycondensation, which gives them outstanding mechanical strength.
2) Long-term durability: geopolymer concrete or mortars can withstand thousands of years of exposure to the elements without losing much function.
3) Unique high-temperature features
4) Quick setting: Geopolymer achieves 70% of its final compressive strength during the first four hours of setting.
5) It is referred to be a "green substance" because of its minimal energy usage and waste gas emissions during production. Thermal processing of natural alumino-silicates at low temperatures yields a viable geopolymeric raw material that uses 3/5 the energy of Portland cement.
6) Recyclable with a variable coefficient of thermal expansion.
7) Hazardous waste disposal binder for heavy metal fixation, particularly for the solidification of nuclear waste.
8) Fire resistance: geopolymer can tolerate temperatures ranging from 1000 to 1200 degrees Fahrenheit without losing performance.

2.2.3 The Limitations of Geopolymers

The main limitations for the use of geopolymer are:

1-The high cost for the alkaline solution.

2-The risk associated with the high alkalinity of the activating solution.

3-difficulties in applying steam curing/high temperature curing process [8].

2.2.4 The Applications of Geopolymers

There exist a wide variety of potential and existing applications such as:

1-Construction and repair of highway, road and airport runway

2-Cement and binder materials

3-Storage of toxic and radioactive wastes

4-Fire proof and heat resistant composites

5-Potential utilizations in art and decoration

6-Sustainable Repair Material

2.2.5 Geopolymerization

Natural silico-aluminates are used in geopolymerization, which is a geosynthesis (chemically integrating mineral process). Any pozzolanic chemical or source of silica and alumina that dissolves rapidly in alkaline solution serves as a source of geopolymer precursor species and hence lends itself to geopolymerization[44].

Because the alkali component is a compound from the first group of elements in the periodic table, the substance is also known as alkali activated aluminosilicate binders or alkali activated cementitious material[45].

Chemically and architecturally, silicon and aluminum atoms react to generate compounds that are similar to those found in natural rocks. The inorganic polymeric substance can be thought of as an amorphous version of geological feldspars, but it's made in the same way as thermosetting organic polymers are. As a result, these materials are referred to as "geopolymers.". It is an appealing alternative for basic industrial applications requiring the stabilization of huge volumes of waste materials. It gets its name from its resemblance to organic condensation. In terms of their hydrothermal synthesis conditions, polymers are unique. The alkaline value depends on the chemical makeup of the starting components. Cements are divided into two categories [46]:

(1) Binders made from calcium-rich materials, such as blast furnace slag, that when activated with an alkaline solution form a calcium silicate hydrate (CSH) gel.
(2) Ingredients made from low-calcium, high-SiO_2 and Al_2O_3 raw materials, such as metakaolin. When activated with alkaline solution, these materials create an amorphous material (alkaline aluminosilicate) with good mechanical strength at a young age after a mild thermal curing [44].

In general, geopolymerization can be divided into three stages, see Fig (2.2). First of them is dissolution, when the solid alumino-silicates material is dissolved because of the water and alkali activator presence. After eliminating a small amount of water, the reorientation starts, now the group atoms take their place in the structure. The water is nearly completely removed during solidification and the substance takes on its final shape [44].

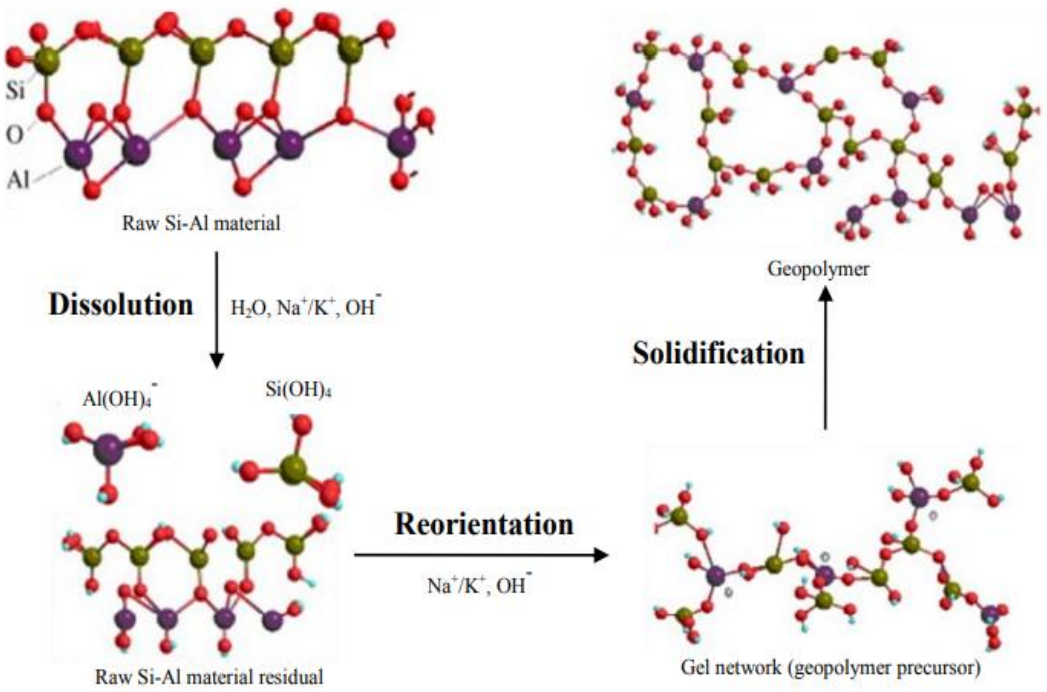

Figure (2.2) Stages of geopolymerisation process[9]

2.2.6 Important Issues in Geopolymer Synthesis

Aside from alkali activators, which play an important role in altering the characteristics of geopolymers [48], the most critical factor in achieving desired outcomes is raw material selection. Metakaolin and fly ash are two common raw materials used in geopolymer synthesis because they both have a lot of reactive amorphous Al and Si in them. Early geopolymer synthesis used metakaolin as a common raw material, but as the applications focus has shifted to construction, fly ash is becoming more prominent. At 500–900 ^{o}C, the dehydration product of kaolinite clay is metakaolin ($Al_4[Si_4O_{10}](OH)_8$)[49]. Plate-like particles make up metakaolin powder, which comprises 4-coordinated Si and a variety of Al coordination environments [50]. It has a specific surface area of 9–20 m^2/g as assessed by N_2 sorption. Fly ash, on the other hand, is composed of small, spherical, generally glassy particles with a surface area of only 0.6–4.2 m^2/g, depending on the source [54].

As a result of this morphological distinction, the liquid demand of metakaolin-based geopolymer paste is significantly higher than that of fly ash-based geopolymer paste. In comparison, a liquid/ash ratio of 0.30 to 0.65 is required for fly ash geopolymer paste and 0.40–0.96 is required for concrete, depending on the fly ash properties and activator type. A greater amount of liquid is necessary to moisten the area of the surface and interlayers of metakaolin particles, which can be determined by the binder's yield stress, in order to provide good workability [54].

The second difference is that metakaolin-based geopolymers have a faster reaction time and stronger development of strength than Geopolymers made from fly ash, especially at low temperatures. Particle surface area and reaction temperature have a significant impact on metakaolin, the secondary minerals contained in original kaolinite clay, reaction rate, and strength development. The amount of fly ash available, the surface area of the reaction, and the reaction temperature are all essential considerations [52].

For geopolymer synthesis, ambient temperature (20–25^{o}C) and a considerably elevated temperature (30–150^{o}C) are used as curing conditions. Despite the development of high-pressure and high-vacuum settings, they are not frequently employed. Heat treatment promotes strength growth, although heat-treated binders had lower 28-day strengths than mixes treated at ambient or slightly lowered temperature, which is likely owing to the restricted reaction extent of metakaolin at high temperature [53].

According to a recent study of the reaction kinetics and thermochemistry of geopolymerisation, increasing the reaction temperature from 20 to 40 degrees Celsius speeds up the reaction rate, but the final reaction extent is greater at 20 degrees Celsius, especially for low alkali systems. Due to the reduced reactivity of most fly ashes when

compared to metakaolin, elevated temperature curing is preferable for Geopolymers made from fly ash. It's worth noting that curing under sealed and covered circumstances appears to be crucial for achieving high strength [54].

2.2.7 Porous Geopolymers

In recent years, porous geopolymers have gained a lot of attention because of unique properties associated with thermal and chemical resistance. Moreover, porous materials can be described through pore type, morphology and orientation. Besides the classification to open (interconnected) and closed (isolated) porosity the shape of the pores can be design as honey-comb, lotus-type, reticulated or bubble-like foamed materials and/or combination of these.[10]

A foaming agent is used to produce the pores. The foaming agent used must be able to produce air bubbles with a high level of stability, resistant to the physical and chemical processes of mixing, placing and hardening. In cement and geopolymer foams, hydrogen peroxide has long been utilized as a chemical foaming agent [27].

Although the foaming agent additives are useful for producing the bubbles in the geopolymer, the reaction of the foaming agent in the GP is unstable so it can produce large pores and a large variety of pore diameters. To ameliorate this problem, Surfactants, fibers, and other stabilizing agents and particles have been chosen to be incorporated to the GP slurry in order to lower the gas/slurry system's surface energy and protect the coalescence of the bubbles (Ostwald ripening). Furthermore, the agents can control the pore size, pore distribution, and the amount of open and closed pores. Surfactants act as wetting agents, emulsifiers, and dispersants which help to reduce the surface tension on the surface. The

surfactants, such as Tween, protein, and vegetable oil are classified in the hydrophilic group and have been used for this propose. One of the interesting surfactants is vegetable oils due to its low cost and easy availability [20].

The larger pore size is created by the release of O_2 gas during H_2O_2 decomposition. If the released bubble size can be efficiently controlled, the mechanical strength of the foamed geopolymer will be improved [26]. Porous geopolymer materials have an excellent thermal insulating property due to their high volume of pores and voids, in addition to other desirable properties such as reduced shrinkage, enhanced heat resistance, and fire prevention [55]. The performance of geopolymer foam materials can be influenced by a variety of factors. These factors include raw material quality, mix proportion design, foam agent/stabilizer content and kind, and so on. The foam stabilizer, as a surfactant, is particularly important because it can lower the surface free energy of the bubble and increase its toughness, preventing bubble break and coalescence. It has a significant impact on geopolymer foam material stability, optimization, and development [19].

2.2.8 Porosity-Strength Relationship

Geopolymer porosity refers to a structure's ability to allow water, air, acid, and base to pass through. The volume of all the pores in a material divided by the volume of the bulk substance is known as porosity. The presence of pores in the concrete is due to insufficient compaction during the placing of the mixtures into the mold. These pores can alter the strength of concrete, which is the most significant quality. The effect of porosity on the strength of cement paste has been explored in several studies [56].

Lian et al., for example, claimed that the porosity of an interior structure could impair concrete strength. They claimed that the mathematical model obtained from Griffith's theory could accurately reflect the link between concrete compressive strength and porosity [2].
Lian et al, in a different study discovered that the investigation of the compressive strength of porous concrete might be used to characterize the mechanical capacity of porous concrete. This is because, in comparison to the other factors, porosity has a greater impact on concrete strength. As a result, porosity has been recognized as a key factor in determining the strength of concrete. Furthermore, overall porosity and pore size distribution are the most important elements that can affect the compressive strength of the samples, according to Sidney Mindess. Another reason is due to the phase makeup of the sample. He concluded that when the number of big pores rose, the sample's compressive strength dropped [3,4].

2.2.9 Processing Routes of Porous Geopolymer

During the last several decades, considerable effort has been devoted to new processing of porous geopolymers, as well as research of their characteristics and prospective applications in different sectors, spurred by the enormous need for low-cost, environmentally friendly engineering components. Different processing routes for porous geopolymer materials have been developed[13]:

a) Direct foaming

b) Sacrificial template

c) Emulsion templating

d) Additive manufacturing

e) Replica templating and combination of these.

Direct foaming consists in the generation of bubbles inside liquid containing a ceramic precursor solution to create foam which then needs to be set without collapsing obtained porous network before setting[14].

The direct foaming process has been used for so many applications as shown in fig (2.3). This process has a lot of advantages, for example: high porosity and control of pore sizes and permeability. Different shapes can be easily goaled, because of that, many are the applications for materials produced by this method, for example: Filters, membranes, catalytic supports, etc.[15]

Hydrogen peroxide is a well-known blowing agent that produces more uniform foam by generating gas at the molecular level. In basic media, it is thermodynamically unstable and easily decomposes into water and oxygen gas. The trapped gas bubbles in the paste expand and create voids (macropores). The amount of oxygen created by the following reaction[28] determines the volume expansion of this substance:

$H_2O_2 \rightarrow H_2O + ½\ O_2$

High pH and high temperatures are known to catalyze this reaction. The addition of H_2O_2 has no effect on the geopolymerization rate, which is solely determined by the alkali solution concentration and the liquid/solid ratio. However, the amount of swelling, apparent density, pore size, homogeneity, and, as a result, the material's ultimate qualities vary significantly depending on the H_2O_2 level. Other factors influencing its mechanical and physical qualities include the synthesis temperature, the type of alkali activators utilized, and the surfactant content [28].

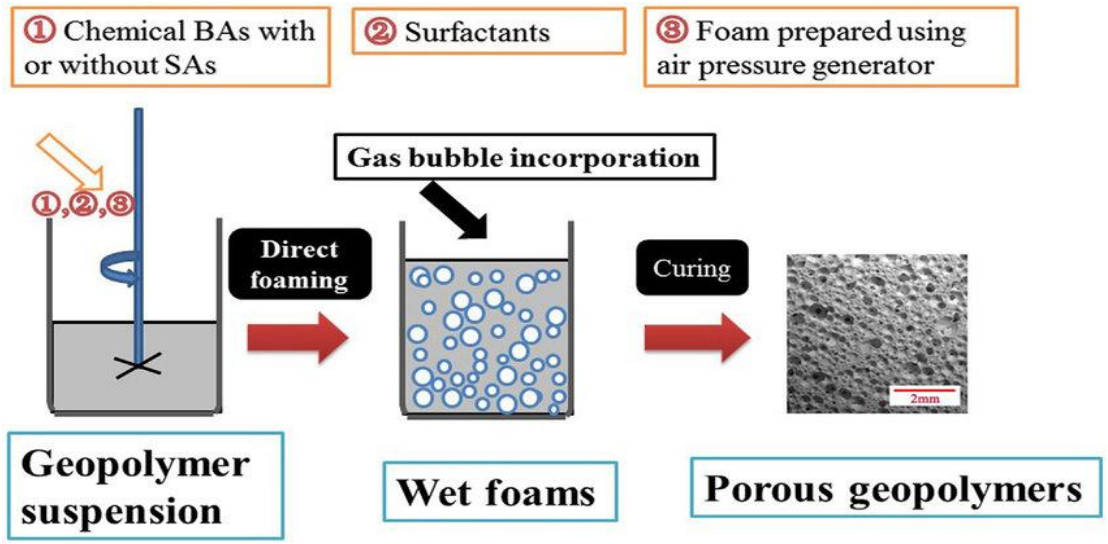

Figure (2.3) (direct foaming process) [14]

When gas-releasing agents and pre-foaming chemicals are introduced into geopolymerisation systems, their effects on the phase evolution of the binder remain unclear from a chemical standpoint. Al powder, for example, has been used in geopolymer foam concrete experiments and is a common gas-releasing component in OPC foam concrete. The quantity and responsiveness (microstructure, surface treatment) of aluminum powder will impact the creation of geopolymers at the atomic and nanostructure level, and regulate the time of aluminate release, since it releases soluble aluminate while releasing H2 gas. However, more research is needed on the effect of aluminum powder and its hydrolysate on the kinetics of geopolymerization, and the effect of a large aluminum concentration on geopolymer performance at high temperatures. It's also worth mentioning that when utilizing pre-foamed organic foaming agents in geopolymer binders, a lot of foam is needed because bubbles tend to be formed during the mixing process due to the paste's high viscosity. It will crack, leading in inefficient foaming [26].

From a microstructure point of view, It's also important noting the distinction between solid geopolymers and foamed geopolymers. Although numerous research have looked at the pore structure of OPC foam concrete and how it affects the material's mechanical and thermal insulation properties, the impact of pore structure on porous geopolymers has yet to be fully explored. As seen in fig (2.4) [54].

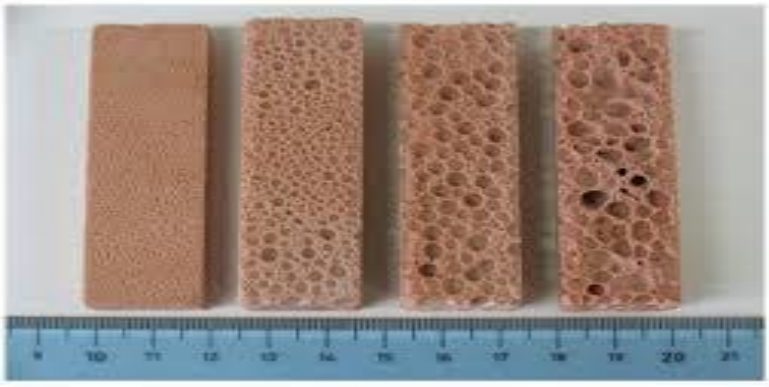

Figure (2.4) Porous metakaolin based Geopolymer [16]

2.2.10 H_2O_2-Yeast Reaction

Hydrogen peroxide is a molecule made up of hydrogen atoms and oxygen atoms. It can be expressed using the chemical formula, H_2O_2. Under the right conditions, hydrogen peroxide will undergo a chemical reaction to break down into two parts, oxygen (O_2) and water (H_2O). When a chemical that is made up of only one molecule breaks down into two different, smaller molecules, it is called a decomposition reaction. This particular decomposition reaction is also an ’exothermic’ reaction, meaning it gives off heat. Yeast contains an enzyme called catalase. The enzyme works as a ’catalyst’ in this reaction. A catalyst is a substance that speeds up the rate of a chemical reaction without changing its products. The yeast is added to the hydrogen peroxide to speed up the reaction. The catalase in the yeast speeds up the process of breaking

down the hydrogen peroxide and thus produces oxygen and water more quickly[17].

2.3 Experimentation Design (DOE)

Experimentation design is a systematic method to determine the relationship between factors affecting a process and the output of that process. In other words, it is used to find cause-and-effect relationships. This information is needed to manage process inputs in order to optimize the output [60].

2.3.1 Taguchi Method

Dr. Genichi Taguchi was advancing this design [60]. He proposed breaking down the design process into three stages: systems design, parameter design, and acceptability design. This method was erected depending on tradition experiment design. DOE is used to investigate the various variables impact simultaneously. The method of Taguchi simplified the procedure of DOE [60]. Taguchi Method is a process/product optimization method that is based on 8-steps of planning, conducting and evaluating results of matrix experiments to determine the best levels of control factors. The primary goal is to keep the variance in the output very low even in the presence of noise inputs. Taguchi method is robust design techniques widely used in industries as it can improve the processing quality, reduce the number of experiments, minimize the processing variation and maintenance and promote the quality stability.

In Taguchi approaches, the experiments number were decreased by array of orthogonal (OA) and decrease the uncontrollable factors impacts[19]. Fig.(2.5) demonstrates flow chart of Taguchi technique [62].

The Taguchi design quality is confirmed in the design stage itself. The technique of Taguchi is utilized to decrease trails‟ number, reduce the time of experiment, reduce the manufacture price, increasing profit, and to identify the important factors in a least time. The design of Taguchi allow us to view the variability resulting from noise factors that are normally unnoticed in the traditional DOE method.

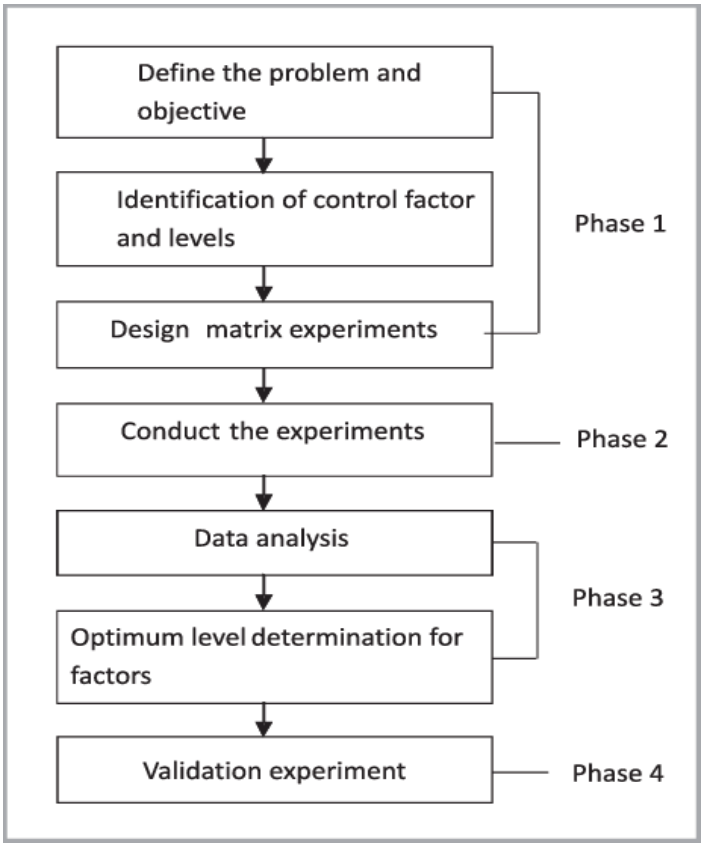

Figure (2.5) flow chart representing the Taguchi method for optimization. Phase 1 (Planning), Phase 2 (Conducting), Phase 3 (Analysis), Phase 4 (Validation). [62]

The method of Taguchi could be utilized to improve any product design or operation by three steps: design of tolerance, parameter and concept and system. In first step, the technical experiences and knowledge arecalm to help designers to improve the concept design drawing. The optimal process parameters setting levels are stated in the step number two. Step number two is the most important step, whereas

the factors impacting quality characteristics in the manufacturing process that is stated. The major objective of this step is to detect the best conditions, which yield the best magnitude. Step number three is achieved after implementation the design‟s parameter, it determining the design‟s parameter outcomes by tightening the significant factors tolerance [63].

The technique of Taguchi utilized to determine loss function. The function of loss is the variance between the desired and experimental magnitudes. At that time, the function of loss is transformed in the proportion of signal/noise (S/N) form. The optimum levels of controlling factor are those with maximize proportions of signal/noise (S/N) that are desired output log functions, work as optimization objective functions, and contribution with analysis data and optimal prediction outcomes. Usually, three kinds of quality S/N proportion properties written in equations (2.1-2.3.), when the feature is nonstop [62].

a. The best method is nominal one

$S/N= 10 \log \bar{y}^2/s^2$ …… (2.1)

b. Better method is lesser one

$S/N= -10 \log 1/n(\sum y^2)$…….. .(2.2)

c. Better method is greater one

$S/N=-10 \log 1/n(\sum \frac{1}{y^2})$ …… (2.3)

Whereas: $\bar{y}$ is the average of the detected data, S_{y2} the y variance, n is the number of observation, and y the detected data of every characteristic.

The response could be the output of the product or some other suitable characteristic. A block diagram representation of the product is shown in fig (2.6) the response of the product is denoted by y. Recall that the response that consider for the purpose of optimization in a robust design experiments is called a quality characteristic.

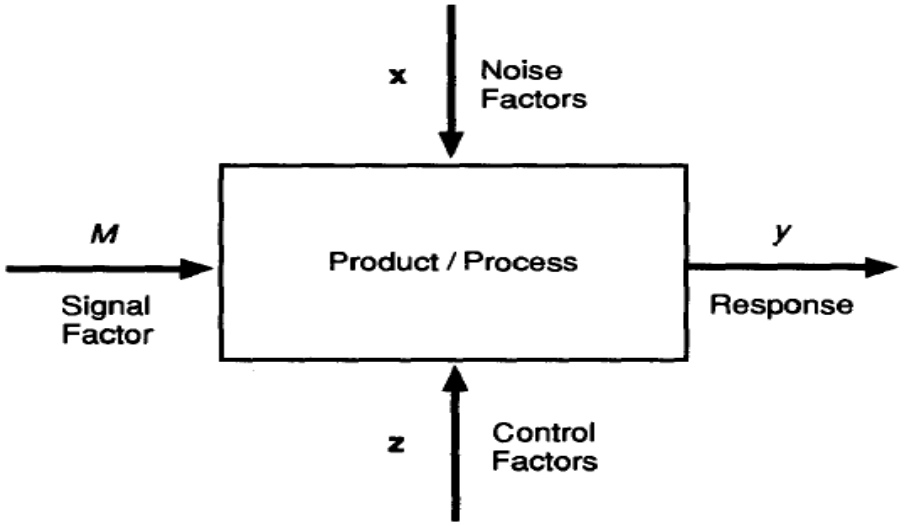

Figure (2.6) Block diagram of a product/process[75]

The array of orthogonal, proportion of Signal/Noise, and the Variance Analysis (ANOVA) help gears in method of Taguchi. By collecting all the tools of helping and analysis, the design of Taguchi could be effectively utilized to obtain the optimum performance for machine in any machining process [60]. The Variance Analysis (ANOVA) is a numerical method applied to identify the individual interactions for all factors of control in the design test. ANOVA could be useful in determining the input parameters impact and interpret data of experiment. ANOVA contributions in appropriately testing the significance of all major parameters and the interactions of these factors by comparison the average square against the errors of experiment estimation at exact sureness levels. Lastly, a validation experiment should be carried out to confirm the optimum parameters.

2.3.2 Multi Response Optimization

When utilizing the Taguchi technique to improve multi-response systems, the following points should be kept in mind:

• In many cases, the properties and loss function of each response are always different. As a result, each response's loss cannot be easily compared and averaged.

• In many circumstances, the unit of measurement for each response is always different. As a result, the loss suffered by each unit for each reaction may vary.

• In many circumstances, the importance of each response could be varied.

• When there is a nominal optimal quality characteristic in the case of multiple responses, an adjustment factor should be selected. This is particularly true if one of these criteria is utilized to alter the goal average while other quality metrics' values fluctuate considerably. Optimization strategies are utilized to overcome the four problems outlined above [64].

The Taguchi method [65] is a practical method to improve individual quality responses. However, manufactured items have more than one major quality reaction in today's current procedures [63]. However, traditional Taguchi method cannot solve multi-objective optimization. In practice, many industrial processes are multi-stage in nature. Engineers, often, try to optimize individual processes and then expect an optimized system, which is neither systematic nor provides a realistic result.

A production process constitutes a set of inputs and outputs as shown in Fig. (2.7). The inputs X_1, X_2, …, X_n are controllable factors whereas the inputs Z_1, Z_2, …, Z_n are uncontrollable or difficult to control factors. The production process transforms these inputs into outputs that will have several quality characteristics. The output variable ‘Y’ is measure of process quality. The Taguchi method is an approach for robust

experimental design that seeks to obtain a best combination set of factors/levels with lowest variation while the mean is close to the desired target[66].

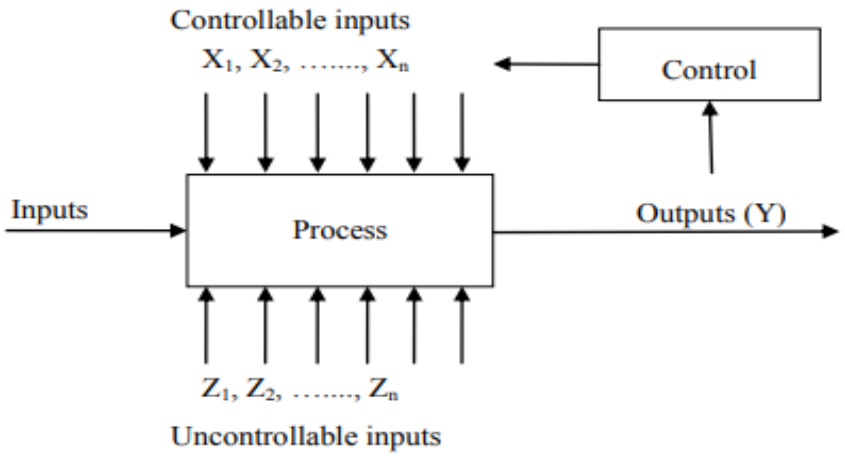

Figure (2.7) a process as a system

The optimization of multi-response problems has recently gotten a lot of attention. In the Taguchi Method, several ways were employed to solve the multi-response problem, including:

2.3.2.1. Grey Rational Analysis Method

Grey Relational Analysis (GRA) is a normalization evaluation technique to solve a more complicated multi-performance characteristics optimization effectively. To address multi-response issues, it can be used with the Taguchi technique. Based on the orthogonality, orthogonal experimental design selects some representative points from the comprehensive experiments, these points have uniform dispersion and uniformity. In the orthogonal tests, the factors are the parameters that affect the properties of product, and the level in the orthogonal tests refers to the specific conditions for each factor to be compared. The Taguchi design method converts the experimental results to a signal-to-noise (S/N) ratio. The value of S/N ratio indicates the dispersion around the

desired results and includes three types of performance characteristics: lower-the- better, nominal-the-better and higher-the-better. S/N ratios of the higher-the-better can be calculated using Equations (2.1-2.3). The (S/N) ratio were normalized, to distribute the data evenly and scale it into an acceptable range for further analysis [67], using Equation (2.3), to obtain Z_{ij} which represents the normalized value of S/N ratio for the larger is better.

$$Z_{ij} = \frac{y_{ij} - \min(y_{ij})}{\max(y_{ij}) - \min(y_{ij})}; i = 1,2, \dots, m; j = 1,2, \dots, n \qquad (2.4)$$

According to GRA, equation (2.5) is used to calculate the deviation sequences, equation (2.6) is used to calculate the grey relational coefficient (GRC) and equation (2.7) is used to calculate the grey relational grade (GRG) [100].

$$\Delta = \left(Z_{max} - Z_{ij}\right); i = 1,2, \dots., m; j = 1,2, \dots, n \qquad (2.5)$$

$$GRC_{ij} = \frac{\min(\Delta) + \lambda \max(\Delta)}{\Delta_{ij} + \lambda \max(\Delta)}; i = 1,2, \dots, m; j = 1,2, \dots, n \qquad (2.6)$$

$$GRG_i = \sum_{j=1}^{n} \varphi_j GRC_{ij} \; ; i = 1,2, \dots.., m \qquad (2.7)$$

where:

Δ_{ij} is the difference between the optimum value of the normalized S/N ratio and the i^{th} normalized S/N ratio value for the j^{th} response, λ is the identification coefficient that ranges from 0 to 1, and φ_j is the normalized non-negative coefficient assigned to the j^{th} response with the sum of all φ_j is equal to 1. All the responses (characteristics) considered in this research are equally weighted [100].

2.3.2.2. Utility concept

Though the Taguchi approach is used for a single response problem, most of the researchers proposed various methods for multi-response problem by modifying it[68]. Quality is a key attribute that customers require into the product or service. So the modern quality control and improvement program focus that their product should be made as par the customer requirements. On the other hand, customer evaluates a product performance based on number of diverse quality characteristics of the product. To able make rational choice, these performances evaluation on different characteristics should be combined to give a composite index. Such a composite index shows the utility of the product. The utility of a product on a particular characteristic measures the usefulness of that particular characteristic of product/service[69].

It is assumed that the overall utility of the product is the total sum of utilities of each particular quality characteristics of the product. Thus if x_i is the measure of effectiveness of an attribute (characteristic) i and there

are n attributes evaluating the outcome space, then the combined utility function can be expressed as [69]:

$U(x_1,x_2,x_3,\ldots,x_n) = f[U_1(x_1), U_2(x_2), \ldots\ldots U_n(x_n)]$ ……(2.8)

Where $U_i x_i$ is the utility of the i^{th} attribute.

The overall utility function is the sum of individual utilities. If the attributes are independent, then

$U(x_1,x_2,x_3,\ldots..,x_n) = \sum_{i=1}^{n} Ui(xi)$ …….(2.9)

Depending upon the customer's requirements, the characteristics might be given priorities. The priorities could be adjusted by providing a weight to the individual utility index. The overall utility function by assigning weights to attributes could be written as:

$U(x_1,x_2,x_3,\ldots,x_n) = \sum_{i=1}^{n} WiUi(xi)$ ……..(2.10)

Where, W_i is the weight assigned to attribute i and the total sum of the weight for all the attributes is equal to one. The utility function is of "higher- the- better" type characteristic. If the composite measure, the overall utility, is to be maximized. The quality characteristics considered for the evaluation of utility index will be optimized (minimized or maximized). The S/N ratio of the orthogonal test results was calculated using the corresponding equation, given by Equations (2.3). A preference scale for each quality attributes is constructed to determine the overall utility value, these scales given weight to calculate the overall utility. The preference scale may be linear, logarithmic or exponential. The minimum acceptable quality level for each quality attributes is set at a preference scale of 0 and the best available quality is assigned a preference number of 9. In this study, logarithmic scale was used. The preference number is given by [69]:

$pi = A \times log(x_i / x_i')$……..(2.11)

Where x_i is the value of quality characteristics or attribute i, x_i' is the minimum acceptable value of quality characteristics or attributes i, and A is a constant. Arbitrarily, A has been chosen such that $pi = 9$ at $x_i = x^*$, where x^* is the optimum value of x_i with the assumption that such a number exist. The assessment of weights depending on the end of the product, the weight should be assigned such that it can hold following condition:

$\sum_{i=1}^{n} Wi = 1$ …… (2.12)

The overall utility value can be calculated by using following equation:

$U=\sum_{i=1}^{n} Wi\ Pi$ …… (2.13)

2.3.2.3. Method of Data Envelopment Analysis (DEA)

It is an effective procedure on the basis of the data envelopment analysis (DEA) to optimize the multi-response problems. In the Taguchi method, to solve the multi response problem, engineering judgment is the primary method. But, without doubt an engineer's judgment will increase uncertainty during the decision-making process. In order to solve the multi response problem, an approach of assigning weight to each response is submitted[70].

DEA is a linear programming based technique for measuring the relative efficiency of a set of competing decision-making units (DMU) where the presence of multiple inputs and outputs makes the comparisons difficult. The relative efficiency of the DMU's "many inputs and outputs" is usually expressed as a ratio (weighted sum of DMU outputs divided by weighted sum of DMU inputs). As a result, in order to obtain a greater absolute efficiency performance, the ratio inputs must be lower and the ratio output result must be higher. Alternatively, when the inputs is confined to a set value and the output result is larger, the absolute efficiency improves [71].

A DMU is a combination of factors/levels with 1 as the input data. and the value of the answers' SN ratios as the output data. The higher the output value, the higher the DMU's relative efficiency rating will be. It will aid in the solution of the multi-response problems [71] the higher the relative efficiency number, the easier it is for the item's qualitative attributes to stand out in relief. The following Eq. summarizes the general efficiency metric employed by DEA (2.14)

$$E_{ks} = \frac{\sum_y o_{sy}\ v_{ky}}{\sum_x I_{sx} u_{ks}} \quad \dots \dots \dots \dots \dots \dots \dots \dots \dots \dots \dots \dots \dots \dots \dots \dots \dots \dots \dots (2.14)$$

where

E_{ks}; the weights of the DMU k that has been examined are used to calculate the efficiency of DMU s.

O_{sy}; the DMU s output y values

I_{sx}; the input x values for DMU s

v_{ky}; trial DMU k's weights for output y

u_{kx}; the input x weights allocated to trial DMU k

The objective is to maximize the relative efficiency value of a trial DMU k from among a reference set of DMU s; by selecting the optimal weights associated with the input and output measures. The maximum relative efficiencies are constrained to 1. The formulation is represented in expression (2.14) [71]:

$$max \quad E_{kk} = \frac{\sum_y O_{ky}\ v_{ky}}{\sum_x I_{kx} u_{ks}}$$

S.t. $E_{ks} \leq 1 \quad \forall\ designs\ s \quad \ldots\ldots\ldots\ldots\ldots\ldots\ldots\ldots\ldots (2.15)$

u_{kx} , $v_{ky} > 0$

This nonlinear programming formulation (2.15) is equivalent to the following linear programming (LP) formulation (2.16) by setting its denominator equal to 1 and by maximizing its numerator.

max $E_{kk} = \sum_y O_{ky}\ v_{ky}$ $\ldots\ldots\ldots\ldots\ldots\ldots\ldots\ldots\ldots\ldots\ldots\ldots\ldots\ldots (2.16)$

s.t. $\sum_x I_{kx} u_{ks} = 1$

$E_{ks} \geq 1$ ∀ designs s

u_{kx} ; v_{ky} >0

The optimal efficiency value ($E^*_{KK}=1$) obtained from formulation (2.16) is only one. If $E_{kk} = 1$, no other DMUs with the same weights as DMU k are more efficient. That is, in ($E_{kk} = 1$), DMU k is on the optimum boundary and is not controlled by other DMU. If DMU k is not on the optimal frontier, and at least another DMU is more efficient under E_{kk} 1, DMU k is not on the optimal boundary (2.16).The formula (2.16)

[71] is used to compute the relative efficiency of the DMU in comparison to its own optimum set of weights. Because the experimental result comprises censored data, which is constrained and difficult to analyze, the BP model was utilized to predict the SN ratios of all combinations of factors/levels. On the other hand, the BP model may generate estimations based on incomplete data. The knowledge representation in this case is to utilize the BP model to define the relationship between the controllable factors/levels and the multi-SN response ratios. The input values are the levels of the control factors, and the number of input nodes is equal to the number of control factors. The output values are the multi-SN response ratio numbers, and the number of multiple responses is equal to the number of output units. The following is how the SN ratios are calculated [71]:

For the j_{th} response during the i_{th} trial, let the SN ratio be X_{ij}. For i = 1;…;m; j =1;…; n:

$$x_{ij} = -10\log_{10}\left[\frac{1}{l}\sum_{k=1}^{l} y^2{}_{ijk}\right], 0 \le y_{ijk} \le \infty \quad \text{..... (2.17)}$$

$$(for\ the\ smaller - the - better\ response)$$

$$x_{ij} = -10\log_{10}[\frac{1}{l}\sum_{k=1}^{l}\frac{1}{y^2{}_{ijk}}], 0 \le y_{ijk} < 1 \text{ ..... (2.18)}$$

$$(for\ the\ larger - the - better\ response), and$$

$$x_{ij} = -10\log_{10}[\frac{y^{-2}{}_{ij}}{s^2{}_{ij}}], 0 \le y_{ijk} \le \infty \text{ ... ... (2.19)}$$

$$(for\ the\ nominal - the - best\ response)$$

where yijk =observed data in full data for the ith trial's jth response, the k_{th} repetition, $\acute{y} = \frac{1}{l}\sum_{k=1}^{l} y_{ijk}$(the average observed data for the jth answer during the ith trial in full data), $S^2{}_{ij} = \frac{1}{l-1}\sum_{k=1}^{l}(y_{ijk} - \acute{y}_{ij})^2$(the variation of observed data in complete data for the jth response at the ith trial) for i = 1,…,m ; j = 1,…,n ; and k = 1,…, l.

The learning rate and momentum network parameters will be tuned to help the trained network attempt convergence and stabilization in prediction behavior. To halt the trained network, the stopping criterion should be chosen to simultaneously reduce the root mean square error (RMSE) of training and testing. Selecting the RMSE of training and testing among the examined estimation models yields the best estimation model. For the normalization X_{ij}. X_{ij} is the SN ratio for the i_{th}(i =1; 2,…,m) response in the j_{th}(j = 1, 2,…, n) experiment. X_{ij} is normalized as Z_{ij}($0 \leq Zij \leq 1$)by the following formula to avoid the effect of adopting different units [71].

$$Z_{ij} = \frac{X_{ij}}{\max\{X_{ij}, j=1,2,\ldots\ldots,n\}}, \text{for } i = 1, 2, \ldots, m;\ j = 1, 2, \ldots, n \ldots\ldots\ldots (2.20)$$

(To be used for responses using a larger-is-better and nominal-is-best approach.)

$$Z_{ij} = \frac{\max\{X_{ij}, j=1,2,\ldots\ldots,n\}}{X_{ij}}, \text{for } i = 1, 2, \ldots, m;\ j = 1, 2, \ldots, n \ldots\ldots\ldots (2.21)$$

(To be used for responses in which the lower the number, the better).

The relative efficiency of each experiment can be calculated using the formula (2.16). To compute the relative efficiency of each trial (DMU), the inputs is set to 1 and the output results is set to Zij.

To find the best factors/levels combination, the DMU must be graded according to its relative efficiency. The higher the relative efficiency value, the higher the quality of the product. It will be possible to combine a collection of factors/levels with 100 percent relative efficiency. Based on the price, acceptability, and other factors, the professional will pick the preferable and best mix of variables/levels. By analyzing and testing the estimated SN ratios with ANOVA, professional may decide if control factors are important or not at the j_{th} response, as well as get the significant and non-significant controllable factors for these numerous responses (analysis of variance).

2.3.2.4. Desirability Based Method

The desirability function is one of the most commonly used approaches for dealing with multi-response surfaces difficulties. Because all responses may be optimized at the same time by integrating them into a single objective function that shows the relationship between all the responses that need to be improved [72].

D(Y) is a desire function that is generally a geometric mean of n desirability functions (weighted), d_i (y_i), one for each element, y_i of Y. Each di (yi) value is scaled between 0 and 1 and converted from the corresponding response yi. The related response's quality is optimum, with a score of 0 indicating low quality and 1 representing great quality. The mathematical link between responses and the desirability function may be expressed in the following way:

$$max \;\; D(Y) = (d_1(y_1)^{k1} \times d_2(y_2)^{k2} \times \ldots\ldots \times d_n(y_n)^{kn})^{\frac{1}{\sum_i ki}} \ldots\ldots (2.22)$$

yi stands for the calculated response value. The i'th response's translated desirability value is i di(yi), with ki representing the relative significance of response i compared to the others. If all responses possess the same significance, without weights, D(Y) becomes the geometric mean of all n modified responses. D(Y) is the geometric mean of the di(yi)′s, As a result, if all of the responses are near to their ideal values, the total desirability value can only be close to 1. Similarly, if any of the di(yi)′s are sufficiently close to zero, D(Y) will be small. As a result, to optimize several responses at the same time, one looks for x values that enhance D(Y) [73].

Desirability functions can be generated for any of the three types of experiments, despite the fact that optimisation might take three kinds. Weighted linear transformations, according to Aksezer, are beneficial for determining the risk of variations from expected response levels. Due to

the L type of responses in this problem, Aksezer's research uses a larger-is-better desirability function and transformation [72]. If the interest response is a maximizing problem, the recommended particular larger-the-better desirability function is appropriate.

$$di(yi) = \begin{cases} 0 & yi < LSL \\ \left(\frac{yi - LSL}{USL - LSL}\right)^{s} & LSL \leq yi \leq USL \\ 1 & yi > USL \end{cases} \quad \ldots\ldots\ldots\ldots\ldots (2.23)$$

The bottom and top description ranges of the related response yi are LSL and USL, respectively, as shown in fig (2.8). The weight exponents inside the region of interest influence the form of the response. With this desirability function, USL becomes the required largest value instantly. It's the practical upper limit, and anything higher won't make the reaction stronger.

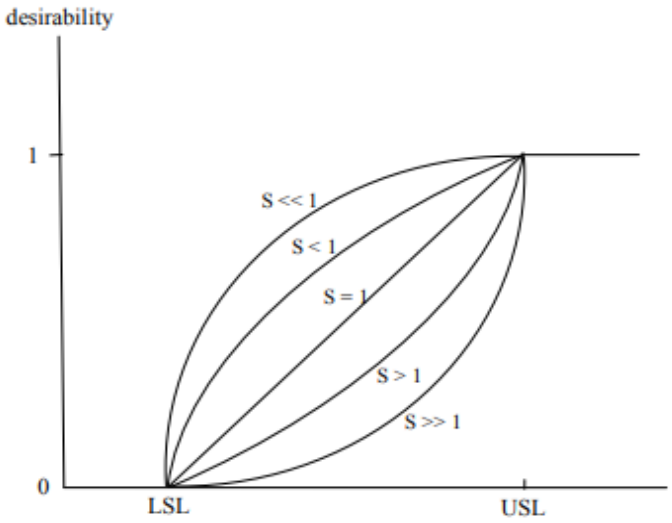

Figure (2.8) the higher the desirability function, the better.

The shape of the particular desirability function for different values of its major factors demonstrates this. Clearly distinguishing, for the user-specified value s = 1, the desirability function rises linearly, is positive for s = 1, and is negative for s > 1. Weights, on the other hand, provide you greater leeway when it comes to distributing individual

desirability within the scope of your interest. The significant coefficient, ki ′s, for each response relates the priority sequence of all responses, allowing them to be compared [72]. The important coefficient of each response, ki ′s, links the priority sequence of all responses so that they may be compared. Desirability-based criteria, such as Derringer and Suich's popular geometric mean (DGM), have solved multi-response optimization issues and are defined as[101]:

$$D=[(d_1)^{\omega_1}\ (d_2)^{\omega_2}\ \ldots.(d_p)^{\omega_p}]^{\frac{1}{\Sigma\omega i}} \ldots\ldots (2.24)$$

Where di is the i-th response's individual desirability function (i=1,...,p) and ω_i are user-specified parameters for assigning priority to di. The goal is to maximize D, which is one (D =1) when all responses are correct (d1=1) and zero (D = 0) when at least one response is outside of the specified boundaries (d i= 0, for any i).

Derringer and Suich devised one-sided desirability transformations for the larger-The-Best (LTB) response type (the anticipated response value is expected to be greater than a lower bound L; $\hat{y} > L$):

$$d = [\frac{\hat{y}-L}{\hat{y}-L}]^r, L \leq \hat{y} \leq U \ldots\ldots\ldots (2.25)$$

Where r is a user-specified parameter (r > 0), $\hat{y}$ is the predicted response model, and U is the upper bound, and d=1 for $\hat{y} \geq U$ and $d = 0$ for $\hat{y} \leq L$.

The expected response value for the smaller-The-Best (STB) response type is supposed to be smaller than the upper bound U; $\hat{y} < U$) as follows:

$$d = [\frac{\hat{y}-U}{\hat{y}-U}]^r, L \leq \hat{y} \leq U \ldots\ldots\ldots (2.26)$$

Such that $d = 1$ for $\hat{y} \leq L$, and $d = 0$ for $\hat{y} \geq U$.

Individual desirability functions for two-sided transformations, which occur when the estimated answer's value is predicted to reach a specified target value (T), are as follows:

$$d = \begin{cases} \left(\frac{\hat{y} - L}{T - L}\right)^{s}, L \le \hat{y} \le \mathrm{T} \\ \left(\frac{\hat{y} - U}{T - U}\right)^{t}, T \le \hat{y} \le \mathrm{U} \\ 0 \quad , \quad otherwise \end{cases} \quad \ldots\ldots\ldots (2.27)$$

Where s and t are user-specified parameters (s, t >0), d =1 for $\hat{y} = T$, and $d = 0$ for $\hat{y} < L$ or $\hat{y} > U$. For product or process quality control, specification limitations designated by U and L are commonly available.

2.3.2.5. Engineering Judgment Method

The objective of engineering design, a major part of research and development (R&D), is to produce drawings, specifications, and other relevant information need to manufacture products that meet customer requirements. Many Taguchi users have coupled excellent engineering skills with knowledge for multi-response scenarios. In a much more integration (VLSI) circuit-manufacturing system, for example, Phadke [75] enhanced three responses by combining pure technical knowledge with his applicable expertise (surface flaws, wafer thickness, and deposition rate).When engineering judgment is combined with prior experience, the decision-making process is frequently fraught with uncertainty. Furthermore, engineering assessment is subjective. Taguchi's quality loss function (TQLF) and principal component analysis (PCA), a strong multivariate statistical approach [76], may easily address this problem. The design parameters and noise variables are organized in orthogonal arrays using experimental design. For each experimental combination, the signal-to-noise (SN) ratio is calculated. The optimal

options (i.e. control variables and associated levels) for the design factors are then determined using SN ratios. The Taguchi approach, on the other hand, can only be used to optimize a single-response problem; it cannot be used to improve a multi-response problem see fig(2.9)[64].

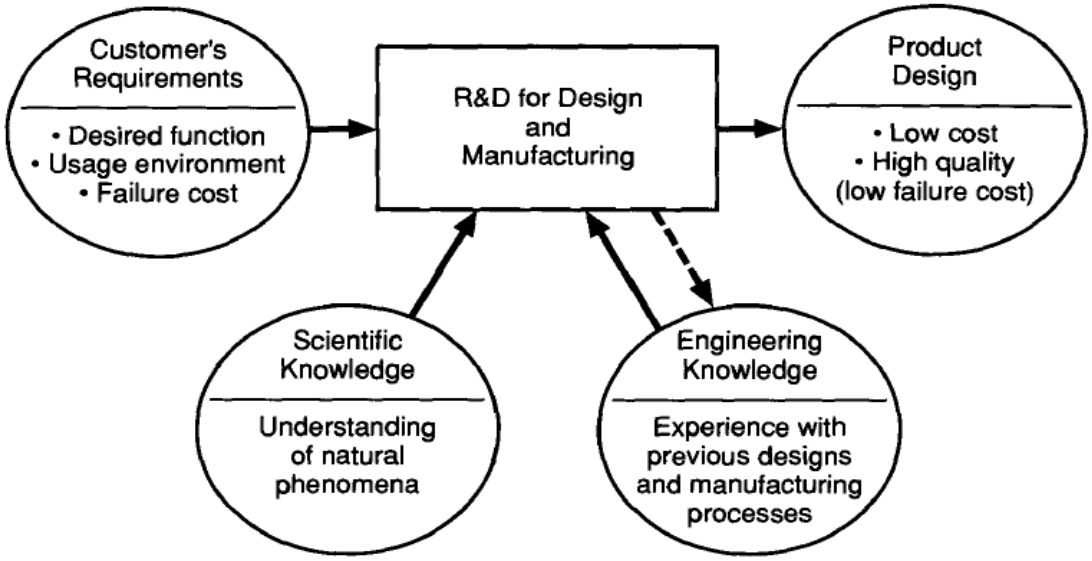

Figure (2.9) block diagram of (R&D) activity [75]

There are three phases to this optimization process:

Phase 1: Calculate the loss in quality.

For each response, the quality loss is calculated in this step. The following three formulas are provided by Taguchi [77]:

$L_{ij} = K_1 \frac{1}{n_i} \sum_{k=1}^{n_i} y^2{}_{ijk}$ The smaller the response, the better ……. (2.28)

$L_{ij} = K_2 \frac{1}{n_i} \sum_{k=1}^{n_i} y^2{}_{ijk}$ for the larger-the-better response……..(2.29)

$L_{ij} = K_3 \left(\frac{s_{ij}}{y_{ij}}\right)^2$ in the case of the nominal-best-response..…(2.30)

Where:

L_{ij} = quality loss for i_{th} response at j_{th} trial

y_{ij} =observed data for i_{th} respsonse at j_{th} trial, k_{th} repetition

n_i = replications for ith response

$$\bar{y}_{ij} = \frac{1}{n_i}\sum_{k=1}^{n_i} y_{ijk}$$

$$s_{ij} = \frac{1}{n_i - 1}\sum_{k=1}^{n_i}\left(y_{ijk} - \bar{y}_{ij}\right)^2$$

k_1 k_2 k_3 = quality loss coefficients.

Taguchi [77] does not define SN for the nominal-the-best quality feature as:

$$-10\log_{10}(MSD) = -10\log_{10}[\frac{1}{n}\sum(y-\bar{y})^2 + (\bar{y}-T)^2] \quad \ldots\ldots\ldots (2.31)$$

Where T is the target value
But

$$SN = -10\log_{10}\frac{\bar{y}^2}{s^2} \quad \ldots\ldots\ldots\ldots\ldots\ldots\ldots\ldots\ldots\ldots\ldots\ldots\ldots\ldots (2.32)$$

The main issue is that determining the best factor amounts based on maximizing SN = –10log10(MSD) does not necessarily minimize both $\frac{1}{n}\sum(y-\bar{y})^2$ and $(\bar{y}-T)^2$.

Equation (2.32) demonstrates that maximizing SN must imply lowering SN $s^2/\bar{y}^2$, which is a desirable quality for any process [78]. As a result, for this investigation, in the case of the nominal - best - response, the quality loss is calculated using the formula L=k($s^2/\bar{y}^2$).

Phase 2. The MRSN (multi-response signal to noise) ratio should be calculated.

To reduce variability, we should first normalize the magnitude of each response's quality loss. The quality loss at every test for each response is divided by the greatest quality loss in the j tests. As a result, the maximum normalized value is 1. The quality loss is proportional to the size of the normalized value. As a result, the normalized quality loss spans from 0 to 1. As a consequence, each response's quality loss may be promptly appended. Second, each response is given an appropriate weight

for determining each experiment's total normalized quality loss (TNQL). Consequently, TNQL may be used to calculate the MRSN ratio. The following is a summary of these three steps[64]:

Step 1: For each response, normalize the quality loss on each trial.

$C_{ij}=\frac{L_{ij}}{L_i^*}$ …………………………………….. (2.33)

Where $L_i^* = max\{L_{i1}, L_{i2}, \dots \dots \dots, L_{ij}\}$

Step 2. Calculate each trial's total normalized quality loss (TNQL):

$TNQL_j = \sum_{i=1}^{m} w_i\, c_i$ ……………………………………… (2.34)

Where wi represents the weight of the i_{th} normalized response (i = 1, 2,..., m).

Step 3. For each trial, calculate the MRSN ratio:

$MRSN_j = -10\log (TNQL_j)$ …………………………………..(2.35)

Phase 3. Determine the best mix of factors and levels.

Taguchi [77] recommended immediate minimization of the expected quality loss in both the smaller-the-best and larger-the-best instances. Taguchi devised a two-stage optimization approach for the nominal-the-best condition, first improving the signal-to-noise ratio and then adjusting the mean on target. The following approach for determining the optimal factor/level combination in a multi-response situation is based on these ideas:

Step 1: Calculate the effects of the factors.

(1) On the MRSN, plot factor effects and tabulate major effects.

(2) For nominal-the-best condition, graph variable impacts and summarize key factors on the mean response.

Step 2: Find the most efficient control variables and their concentrations.

(1) Determine the control factor, which is a variable that has a significant influence on the MRSN.

(2) For each control factor, determine the optimum level as the one with the highest MRSN value.

Step 3: Figure out the best adjusting variables:

The necessary adjusting variables should be discovered if the nominal-the-best feature arises in multi-response problems. There are four possibilities:

(1) When there are qualities to be improved that are smaller-is-better and nominal-is-best.

(2) When it comes to optimizing larger-is-better and nominal-is-best characteristics.

(3) When smaller-is-better, larger-is-better, and nominal-is-best qualities must be optimized.

(4) When all of the theoretically excellent features need to be improved.

For situations 1, 2, and 3, an adjustment factor that meets the following two requirements can be chosen. To begin, any component with a significant impact on the mean response for nominal-the-best attributes but no impact on MRSN might be considered a modification factor candidate. Second, when applying the modification factor to get the mean back on track, the manner in which quality attributes are enhanced should simultaneously fulfill the goals of both the smaller-is-better and larger-is-better scenarios. As an adjustment factor for scenario 4, any component with no substantial impact on MRSN, a high influence on the mean response for its quality attribute, and no significant impact on the mean response for the other quality attributes can be used [64].

2.3.2.6. Level Weight Method

In the Taguchi approach, it is a basic yet effective way for dealing with the multi-response problems. The basic idea is that for each factor level, the average S/N ratio of each response is valued in proportion to the factor with the greatest average S/N ratio. To determine optimal factor values, the average weight of all responses is utilized as a quality indicator. That is, among all factor levels, the factor level with the highest average weight is determined to be the best for that factor. The main benefit of this method is that it is characterized by simple and uncomplicated computations that do not necessitate statistical knowledge or prior knowledge of response weights or importance. To summarize, this methodology's simplicity and efficiency substantially assist practitioners in handling multi-response issues in a variety of Taguchi method applications [76]. The optimum factor level is the one that maximizes the S/N ratio independent of the response type. That is to say, the objective function that must be improved is:

For the STB type response

$$\eta = -10\log_{10}\left[\frac{1}{n}\sum_{i=1}^{n} y^2{}_i\right] \quad \text{..... (2.36)}$$

For the NTB type response

$$\eta = -10\log_{10}\frac{\mu^2}{\sigma^2} \quad \text{..... (2.37)}$$

For the LTB type response

$$\eta = -10\log_{10}\left[\frac{1}{n}\sum_{i=1}^{n}\left(\frac{1}{y_i{}^2}\right)\right] \quad \text{..... (2.38)}$$

Where n is the number of times y has been replicated, μ is the response mean, and σ is the standard deviation. As a result of the foregoing, this methodology can be used to solve the multi-response problem in the Taguchi method.

The number of replies in an OA is denoted by r. Let η_j (j =1,..., r) be the response j's S/N ratio. Then, using a suitable formula from Eqs (2.36 – 2.38), compute η_j for all j values. Assume that at K levels, a process factor *l* is allocated. Let η_{ijk} be the average of η_j for the trails at level *k* (*k* = 1, ..., *K*) of factor *l*, and let $\tilde{\eta}_{ijk}$ be the average of η_{ijk}. Determine η_{ijk} of every factor level for all response. Let w_{ijk} be the weight of level *k* for factor *l* from response *j*, which is calculated as [76]:

$$w_{ijk} = \begin{cases} \frac{max_k \tilde{\eta}_{ijk}}{\tilde{\eta}_{ijk}} & for\ STB\ type\ response \\ \frac{\tilde{\eta}_{ijk}}{max_k \tilde{\eta}_{ijk}} & for\ NTB, LTB\ type\ response \end{cases} \quad (2.39)$$

For each response j, calculate w_{ijk} values of factor *l*. The value of w_{ijk} almost certainly between zero and one. Let w_{lk} be the $\acute{w}_{lk}$ average of w_{ijk} over all responses. Calculate the $\acute{w}_{lk}$ values for all levels of factor *l*. Typically, larger $\acute{w}_{lk}$ indicates higher performance. As a results, determine the factor level equal to the maximum of $\acute{w}_{lk}$(k =1, 2, … , k) as the ideal level of factor *l*. Calculate each response's predicted improvement as a result of optimizing process parameters, and compare the overall expected improvements to those found in previous research. The predicted improvement is calculated using the S/N ratios at optimal factor level versus the S/N ratio at beginning factor level [76].

2.3.2.7. Principal Component Analysis (PCA)

When numerous responses must be tuned, it is a powerful multivariate statistical method for identifying the ultimate optimal state. It is a realistic and systematic methodology based on Taguchi's methodology for dealing with multi-response problems in industrial experiments. The approach employs Taguchi's quality loss function

(TQLF) and principal component analysis (PCA). Data analysis, data extraction, and data categorization are the three main goals of PCA. Pearson [79] was the first to introduce the methodology, and Hotelling [80] was the first to describe actual computing methods in PCA. It's a data extraction approach for identifying a limited number of factors that account for a substantial degree of variability in the response variable [81].The steps in the methodology are as follows:

1. Figure out what influences control, signal, and noise.

A thorough brainstorming session is required to discover the controlling, signal, and noise variables that influence the condition(s) of importance.

2. Determine which response types or quality factors need to be improved.

Typical forms of continuous quantifiable responses or quality attributes include:

(a) Smaller-the-better (STB) responses.

The goal of a smaller-is-best response is to achieve a measurement of zero. Tool wear, engine noise, speed of response to customers complaining, wastage permeability, deformation, and surface integrity are all examples of this type of feature.

(b) Larger-the-better (LTB) responses.

When the goal of the study is to optimize the response while staying within acceptable design constraints, this sort of response is usually explored. Strength, efficiency, an automobile's miles per gallon, resistance to corrosion, product or parts dependability, product durability, and so on are examples of this type of feature.

(c) Target-is-the-best (TTB) responses.

When the goal of the study is to attain a certain response performance target, this attribute is considered. Measurements (diameter, depth, length, etc.), strength, stress, fluidity, resistivity, energy,

electricity, susceptibility, and so on are examples of this type of characteristic. The variation around the objective should be maintained to a minimal because this feature has a goal value.

3. Determine the quality loss (QL) per unit product for each response.

This phase should determine the quality loss per unit product for every response or quality attribute. Taguchi's quality loss functions make this simple to achieve (TQLFs). Let L_{ij} denote the quality loss for the i_{th} response (or quality attribute) at the j_{th} trial condition or test period, with Li_* denoting the highest quality loss and $Li_\bullet$ denoting the least quality loss.

4. Compute the loss in terms of quality in normalized units (NQL)

The following equation may be used to calculate the normalized quality loss [81]:

$$y_{ij} = \frac{Li_* - Lij}{Li_* - Li_\bullet} \quad \ldots\ldots\ldots\ldots (2.40)$$

The NQL is represented by yij. The goal of the NQL computation is to reduce any response to a single non dimensional number. This is owing to the fact that each answer is measured in a different way. The NQL scale runs from 0 to 1, with 0 being the lowest and 1 representing the greatest *(i.e. $0 \leq NQL \leq 1$).*

5. Use PCA to analyze the NQL data.

Given that $k \leq p$, PCA may be considered an effective method for identifying a smaller amount of components (say k) that explain the majority of the variability in the original p responses in multi-response cases. Let X1, X2,..., Xp be a set of responses; using PCA, we may obtain the statically independent linear function of principal components as follows [81]:

$$Z_1 = a_{11}X_1 + a_{12}X_2 + \_\_\_ + a_{1p}X_p$$

Subject to the condition that $a_{11}{}^2 + a_{12}{}^2 + \cdots + a_{1p}{}^2 = 1$. The first major component is referred to as Z1. The essential parts are constructed in decreasing order of variability, in the first principle factor accounting for the most variability, the second for less, and so on. The major components are completely self-contained. The eigenvalues are the variations of the principle components, and it's worth noting that the sum of the variations of the primary components equals the variances of the original responses. The eigenvectors are the values of the major components (i.e. a11, a12, etc.). It is a matter of personal taste as to how many components must be considered. As a general guideline, choose components with eigenvalues higher than or equal to one. We may use PCA on the NQL data obtained in step 4 to solve multi-response problems in commercial experiments. The greater the Z number, the better the product's effectiveness (also known as the multi-response performance statistic).

6. Determine the optimal condition

The ideal circumstance is one that produces the highest Z number. At every factor level, the Z number (multi-response performance data) must be obtained, and then the factor/interaction impacts that have a major effect on the multi-response performance data must be identified. In this case, the multi-response performance data can be regarded as a single response for statistical analysis.

2.4 Literature Review

This review deals with the previous studies related to the synthesis of porous geopolymer and the impact of various parameters on the geopolymer characteristics. Also, it reviews the use of Taguchi method to optimize the properties of geopolymer.

In 2009, Kiyoshi Okada et al. prepared geopolymers by reaction of sodium silicate and metakaolinite in alkaline solution at temperatures close to ambient, using a range of Na_2O/Al_2O_3 and H_2O/Al_2O_3 ratios. The porous properties, water absorption and water release, and the mechanical properties of the resulting geopolymers were determined , they found that The H_2O/Al_2O_3 ratio exerts a major effect on the physical properties, higher ratios result in increased pore volumes and pore sizes, and therefore thus higher water absorption ability, whereas lower H_2O/Al_2O_3 ratios increase the bulk density and mechanical strength, and at the lowest H_2O/Al_2O_3 ratio used (14.2), the highest mechanical strength (about 14MPa), The water retention properties of the samples depend on their pore size, larger sizes giving both higher water absorption and water release rates. Thus, the slow water release properties required in materials for remediation of heat island effects will be better satisfied by geopolymers with lower H_2O/Al_2O_3 ratios[83].

In 2010, V. Vaou, D. Panias. prepared foamy geopolymers from non-expanded perlite that have excellent thermophysical properties, including that they are non-flammable and safe for humans and environment. The alkaline activator used for the synthesis of geopolymers was a sodium hydroxide solution that was prepared by dissolving anhydrous sodium hydroxide pellets in deionised water, hydrogen peroxide (H_2O_2) solution 30% w/w was used as a chemical blowing agent. The results showed that the foamy geopolymers from perlite have almost similar thermal conductivity (0.03 W/m K), superior compressive strength (780 kPa at 2% deformation) and a fracture behaviour resembling the one of rocks, superior fire resistant properties (100% noncombustible), superior maximum application temperature (700 °C) [84].

In 2011, K. Pimraksa et al. studied the synthesis of lightweight geopolymer and the reaction of highly porous silica obtained from two sources materials diatomaceous earth (DE) and rice husk ash (RHA). Various starting Na_2O/Al_2O_3 and SiO_2/Al_2O_3 ratios, reduction of unit weight, strength development and microstructure evolution resulting from chemical polymerization reactions were studied. The results showed that the optimum calcination temperature of DE was 800 ◦C and the finer DE was more reactive due to the increase in the surface area. Pastes activated with 10 M NaOH possessed higher compressive strength than that with 10 M KOH. The optimum curing temperature and time were 75 ◦C and 5 days. At starting SiO_2/Al_2O_3 ratio of 13.0-33.5, the increase in starting Na_2O/Al_2O_3 ratios from 1.0 to 3.0 increased the compressive strength from 11 to 60 kg/cm^2 but the samples with Na_2O/Al_2O_3 ratios of 2.0 and 3.0 were not stable as indicated in water immersion test, the bulk density values also increased from 0.93 to 1.5 g/cm^3. High SiO_2/Al_2O_3 ratios used resulted in the lightweight geopolymer materials[85].

In 2012, E. Kamseu et al. investigated the relations between the bulk composition, the pore size-distribution, pore volume fraction and the effective thermal conductivity of the porous geopolymer. The final material results with improved insulating behavior, insulating material with thermal conductivity of 0.15 W m^{-1} K^{-1} was achieved. The results demonstrated that gel compositions with better mechanical properties and chemical stability are those where homogeneously dispersed fine pores can be easily introduced[86].

Also in 2012, Monita Olivia et al. presented an optimization of fly ash geopolymer mixtures by Taguchi method, and a study on the mechanical properties and durability of concrete produced from the

optimal mixes. A total of nine mixtures were evaluated by considering the effects of aggregate content, alkaline solution to fly ash ratio, sodium silicate to sodium hydroxide ratio, and curing method. Ordinary Portland Cement (OPC) concrete of 55 MPa strength was used as a control mix. Results showed that the geopolymer concrete can be produced with of 55 MPa at 28 days and Moduli of elasticity were 14.9–28.8% lower than those of the OPC control mix [87].

In 2013, Prune Steins et al. analyzed the effect of age and an alkali activator on a geopolymer's porosity structure. For this purpose, Nitrogen sorption was used to characterize the porous structure of the geopolymer and to measure the specific surface area and the distribution of pore size as a function of time and alkali nature. According to the results, the pores that are not accessible to this technique represent a small part of the total porosity but tend to increase over time as a result of a refinement of the porosity. The use of two alkali ions (Na+ and K+) differing by their size and by their kosmotropic or chaotropic properties allowed them to demonstrate that pore size, shape and distribution depend on the alkali activator. The potassium geopolymer has a greater specific surface area than the sodium geopolymer because the pores are smaller and more numerous. According to the scattering results, the kinetics are much slower for the sodium geopolymer than for the potassium geopolymer in the six months of observation[88].

In 2014, Marcelo Strozi Cilla et al. devised a new method for making porous open cell geopolymer foams with a high specific surface area. They used saponification /peroxide/ gelcasting combined route. The findings revealed that geopolymer foams with a void ratio of 85% and an expansive porosity of 70% could be made. and possessing a specific

surface area of 50 m^2/g. The in situ formation of surfactants by the saponification reaction of oil in the geopolymer alkaline environment led to increased total and open porosity in comparison to alternative methods for the fabrication of geopolymer foams[89].

At the same year, Giulia Masi et al. presented a study on different foaming techniques to synthesis low density geopolymers. Varying concentrations of three foaming agents (surfactant, aluminium powder and hydrogen peroxide) were added to a fly ash based geopolymer matrix. They were investigated in order to assess their influence on the final properties of low density geopolymers. They found that homogeneous microstructures with small pores can be obtained by adding surfactant and hydrogen peroxide. The combination of hydrogen peroxide (0.1wt%) and surfactant (1.0wt%) produced geopolymer foams with density and compressive strength values of $0.94g/cm^3$ and 4.6MPa , respectively. Water absorption values for the samples foamed with 2.0 wt% of surfactant are in the range of 36–40% for increasing concentration of the foaming agent, porosity ranges between 50 and 80%, independent of the foaming agent and its concentration used in mixes, whereas for the un-foamed geopolymer is 46% [34].

Also, in 2014 , Ze Liu et al. used circulating fluidized bed combustion fly ash (CFA) as a raw material for geopolymer foam synthesis. Hydrogen peroxide was employed as a foaming agent to prepare CFA-based foam geopolymer. The CFA-based foam geopolymer was successfully fabricated with different contents of hydrogen peroxide and exhibited uncompleted alkali reaction and reasonable strength with relative low atomic ratios of Si/Al and Si/Na. The results showed that the particle sizes of CFA mainly distribute from 5 to 40 μm, and the average

particle size of CFA is about 13.33 μm. Also, with the increase in foaming agent (H_2O_2) content from 0 to 5wt%, the density of the foaming agent decreases from 1593.7 to 276.6 kg/m^3, and the macro-porosity increases from 11.2% to 63.0% [90].

In 2015, Palmero et al. produced and investigated dense and lightened geopolymer materials based on calcined kaolin and different alkali activators. They added four different concentrations of hydrogen peroxide to four distinct geopolymer mixes that had been optimized before foaming. The results showed improved compressive strength up to 46 MPa and the thermal conductivity ranged from 0.12 to 0.78 W/m K, in function of the density of the samples: the lowest values, presented by the macroporous materials, were comparable with those of most commonly used building insulation materials [91].

In 2016, Rui M. Novais et al . produced lightweight biomass fly ash-containing geopolymers using H_2O_2 as blowing agent. They looked examined how hydrogen peroxide concentration, NaOH molarity, and water content affected the characteristics of FA-containing geopolymers in both the fresh and hardened state properties. Results demonstrated that the blowing agent decreases the slurries yield stress. They also found that the geopolymerisation rate is only slightly affected by the blowing agent, while a strong impact is exerted by the activator molarity. The proper association between NaOH molarity and blowing agent content leads to the production of lightweight geopolymers exhibiting very low thermal conductivity (up to 0.08 W/m K) and apparent density (440 kg/m^3) [93].

In 2017, Ankur Mehta et al. presented the influence of various parameters on strength and absorption properties of fly ash based

geopolymer concrete. The optimization of mixtures was achieved by using Taguchi method considering the parameters such as different contents of OPC as fly ash replacement, different concentrations of sodium hydroxide (NaOH) and different curing temperatures. Results show that maximum 7 days compressive strength of 64.39 MPa and minimum water absorption of 3.04% was obtained for fly ash based geopolymer concrete with the considered parameters[94].

Also in 2017, Ailar Hajimohammadi et al. Prepared several foamed geopolymer mix designs using the same amount of hydrogen peroxide foaming agent and under the same reaction conditions. To manage the porosity of the geopolymer foam matrix, they looked at the effect of mix design on both the geopolymerisation reaction and the H_2O_2 foaming reaction. They discovered that when the mix design creates a chemically stable environment for the foaming reaction while also allowing the binders to set quickly, the outcome is fine pores that are evenly distributed throughout the matrix. The presence of more sodium silicate in the solution results in more stable H_2O_2 decomposition and foaming during the foaming process, whereas a large amount of sodium hydroxide in the mix design leads in an unlimited decomposition of the H_2O_2. They modeled the behavior of geopolymer foams and discovered that the size and location of pores affect the strength of foamed geopolymer by distributing stress throughout the sample [27].

In 2018, Yong Cui et al. studied the effect of calcium stearate based foam stabilizer on pore characteristics and thermal conductivity of geopolymer foam material. The purpose of this study was to look into the properties of geopolymer foamed materials (GFMs) as they were affected by a calcium stearate based foam stabilizer (CSFS) by looking at the

regular pattern of foam characterization, compressive strength, bulk density, geopolymerization products, pore distribution, and thermal conductivity. The foam time and first setting time were found to be ideal with 1.0 percent CSFS content. At this moment, the foam duration and volume of GFMs had both grown by 42.8 percent and 28.6 percent, respectively. GFMs with a bulk density of 0.31 g/cm^3 have a compressive strength of 1.45 MPa, which is better than the standard of 1.0 MPa for 0.325 g/cm^3. When no CSFS was present, the total porosity was minimum at ~70%. The total porosity was the largest at ~82% at a CSFS content of 1.0%, which was the matched point in this study. However, the total porosity was decreased to ~74% when the CSFS dosage was 2.0% [19].

In the same year 2018, Chengying Bai et al. focuses on the production and characteristics of very porous geopolymers (porosity 50 vol% or bulk density 0.7 g/cm^3), in which macro-porosity is purposefully incorporated into the micro- and meso-porous geopolymer matrix. Direct foaming (DF), replica method (RM), sacrificial filler technique (SFM), additive manufacturing (AM), and other methods are the five processing methods utilized to fabricate porous geopolymer (OM). They discovered that direct foaming is the simplest and most commonly utilized method for producing porous geopolymers, in their many forms. Porous geopolymers were also shown to be potential low-cost options for technologically significant applications such as catalyst supports or films, liquid or gas filtration, absorption, and insulating. [14]

Also in 2018, Michal Lach et al. developed foamed geopolymers based on fly ash as cheap and fire resistant material for buildings and applications in civil engineering structures. They used sodium hydroxide flakes and an aqueous sodium silicate solution. The results showed the

foamed geopolymers has low coefficient thermal conductivity between 0.068 and 0.126 W/(m·K). They have excellent fire and heat resistant facilities, including resistance of this type of materials to the erosive action of fire. Moreover, they have reasonable mechanical properties – they were characterized by compressive strength between 0.5 and 3.5 MPa depending on the density, which ranged from 250 to 700 kg/m^3. The conducted research confirmed that geopolymers have the highest fire resistance classes and can be used as a material for protection against various types of fire and as fire-resistant insulation materials in construction. [95]

In 2019, Kozo Onoue et al. studied the optimization of the design parameters of fly ash-based geopolymer using the dynamic approach of the Taguchi method. The purpose of the optimization in this study is to set design parameters' level properly so that SN ratios become high. This would result in a robust input–output system. The results showed that the compressive strength of the optimized FAGP mortar ranged from 28.8 N/mm^2 to 47.1 N/mm^2 at 2 days, corresponding to the input values[96].

Also in 2019, Svetlana Petlitckaia et al. designed lightweight metakaolin based geopolymer foamed with hydrogen peroxide and surfactants to stabilize the resulting gas bubbles. The direct foaming procedure was used to create geopolymer foams. They used a sodium silicate solution, sodium hydroxide, an aluminosilicate source (metakaolin) with deionized water. Hydrogen peroxide, at a 50 percent w/w concentration, was utilized as a foaming agent. The results demonstrated that regardless of the surfactant employed, the initial concentration of H2O2 (R=0.25–2.5 percent) controls the level of volume expansion (40–475 percent), the volume fraction of produced gas (28–83

percent), and the pore size (150–3000 μm). For equal apparent densities (ranging from 0.23 to 1.1 g/cm^3), the samples were found to have a substantially higher compressive strength (0.57–5.9MPa) [28].

At the same year, Asmaa Kaddami et al. proposed a new approach to counteracting aging processes of fresh geopolymer foams and to maintaining the microstructure that has been set initially by mixing metakaolin suspension with precursor aqueous foam. It was then shown that the use of the latter surfactant is not sufficient for controlling the morphology of the hardened geopolymer foam. This is mainly due to the drainage process, which is induced by the density difference between the gas bubbles and the metakaolin suspension, and to the ripening process, which results from gas exchange between bubbles. The major result is that arrest of foam drainage can be achieved if the metakaolin concentration in the suspension is larger than a critical value which depends on both bubble size and gas volume fraction.[98]

In 2020, Z. Zayer Hassan et al. studied the optimization the properties of Metakaolin-based (Na, K)-Geopolymer using Taguchi design method. This study aimed to find out the mixes, and their processing parameters, which are suitable to produce geopolymer paste with one of the following features: Highest compressive strength, highest/lowest porosity, highest/ lowest initial and final setting time. The results of study found that the Geopolymer paste with high compressive strength of (107.2MPa) can be obtained with the formula ($0.2K_2O.0.8Na_2O.\ Al_2O_3.3.6SiO_2.xH_2O$) using proper processing condition. The results revealed that the use of alkali solution of K-ions and Na-ions improves the compressive strength of the geopolymer remarkably as compared with the use of Na-ions solution alone. In

addition, it has been noticed that the setting time is reduced, for geopolymers with silica content of less than 3.8, when K-ions is used. Similarly, the bulk density of geopolymers is found to be reduced by adding K-ions[32].

In 2021, Yingjie Qiao et al. studied the effects of surfactants/stabilizing agents on the microstructure and properties of porous geopolymers by direct foaming. In this study, porous metakaolin-based geopolymers (PMGs) were fabricated using different surfactants. Effects of different surfactants on total porosity, bulk density, cell size and cell size distribution, pore microstructure as well as mechanical and thermal properties of PMG samples were reported. The results show that porous geopolymers (PGs) with high porosity (~50 < ε < ~86 vol%), low bulk density (0.35< ρb < 1.2 g/cm3), various average cell size (~101 μm< d <~374 μm), acceptable compression strength (0.35 < σ < 56.5 MPa), and low thermal conductivity (0.13 < λ < 0.32 W/mK) were successfully prepared by direct foaming adding only different types of stabilizing agents/surfactants, or by adding a combination of blowing agents(H_2O_2) and stabilizing agents[13].

2.5 Remarkable Notes

Depending on the pervious review, the subsequent notes could be mentioned:

1- Most of the previous research did not use the approved optimization methods to get the best results.
2- Research that used optimization approaches, including Taguchi, did not take multiple responses into account.
3- There is no clear mechanism in the research to control the reaction of H_2O_2.

4- Some factors affecting the results have not been studied before, such as polymerization time.
5- The use of yeast as catalyst for the decomposition of H_2O_2 was not mentioned before in previous studies.
6- Specimen formed of alkaline sodium silicate and hydrogen peroxide as foaming agent had a microstructure of heterogeneous with a significant pores number.
7- A study that combines the optimization of both porosity and mechanical strength is not well reported in the literatures. Based on that, the current study was suggested to fill these gaps.

CHAPTER THREE

EXPERIMENTAL WORK

3.1 Introduction

This chapter explains the procedure for creating geopolymers, the materials used in that process, the design of experiments, the optimization method followed in the current work and a brief description of the characterization techniques used in this study.

3.2 The Starting Materials and Chemicals

Metakaolin was made by calcining kaolin clay at 750°C for three hours in an air environment at a 5°C/min heating rate. The Kaolin was supplied from Dwaikhla, a local area in the western desert of Iraq. Sodium silicate ($Na_2SiO_3.5H_2O$) sodium hydroxide (NaOH), silica gel ($SiO_2.nH_2O$), hydrogen peroxide (50%-H_2O_2, Thomas Barker) were used as received without further treatment or purification. Instant yeast and sun flower vegetable oil were supplied from local market and used as catalyst and stabilizing agent, respectively, to synthesis the porous geopolymer. Table (3.1) shows the materials used in this investigation, as well as their source, purity, and chemical formula.

Table (3.1) the materials source, pureness, and chemical formula of starting materials

Material Name	Chemical Formulas	Purity (%)	Supplier
Caustic soda	NaOH	97.99%	THOMAS BARKER
Sodium silicate	$Na_2SiO_3.5H_2O$	97.98%	THOMAS BARKER
Silica gel	SiO_2	98.99%	THOMAS BARKER
Water	H_2O	Distilled water	Lab distillator

3.3 Synthesis of Geopolymer

$Na_2O. Al_2O_3. 3.8SiO_2. xH_2O$ formula describes the composition of the geopolymer synthesized in the current study. This formula and the processing parameters, including the amount of water of 11ml per 10.73g of metakaolin, mixing time of 5 min and the sodium silicates to sodium hydroxide ratio of 3.02 were obtained from a previous study on the optimization of the composition and the processing parameters of geopolymer in the ceramics and building materials department university of Babylon college of material engineering.[32]

In order to optimize the porosity and compressive strength of the geopolymer, five factors were selected. These are H_2O_2 concenteration, the quantity of H_2O_2, the time of polymerization, the amount of yeast added to the mix and the amount of oil. Based on primary preliminary trials, five levels have the most impact on the performance of the specimens for each of the five variables. These five factors were chosen based on previous research, and include those that have a major influence on porous geopolymer production. The maximum and lower limits for each element were determined using previous research findings as well as many primary experiments. These factors and their corresponding levels are shown in Table (3.2).

Table (3.2) Five factors and five levels of orthogonal test design

N	**A:**Concenteration of H_2O_2%	**B:**Quantity of the yeast(g)	**C:**Quantity of H_2O_2(ml)	**D:**Polymerization time(min)	**E:**Quantity of vegetable oil(ml)
1	10	0.1	0.2	0	0.1
2	20	0.2	0.4	30	0.2
3	30	0.3	0.6	60	0.3
4	40	0.4	0.8	90	0.4
5	50	0.5	1	120	0.5

This study used a mixture of sodium hydroxide and sodium silicate as an alkaline liquid. Water is first added to the beaker then hydroxide salt is weighed and added to get the necessary molarity. The silicate salt was then added while the solution was agitated at 80 degrees Celsius and 600 revolutions per minute. After dissolving the silicate salts, silica gel was added to the solution and agitated for an hour. The solution was then cooled naturally to room temperature after a desired volume of water was supplied to compensate for the water lost owing to evaporation. The metakaolin was added to the alkaline solution after it had cooled to room temperature and was mixed for 5 minutes with a mechanical mixer at a set speed of 3550rpm. Finally hydrogen peroxide, yeast and vegetable oil were added to the solution under stirring for 2 min, after the desired polymerization time to form the geopolymer paste. The polymerization time was considered to start when the the geopolymer paste has been completely poured into the molds. Molds constructed of PVC plastic with a diameter of 2 or 5 cm and a height of 4.2 cm were used to shape the geopolymer pastes. The molds were stored in a particular environment at the lab for one day at a temperature of 23 °C±2 and then demolded. Before testing, these samples were cured for 28 days at room temperature (Air curing). Fig (3.1) shows the fractured surface of the samples obtained according to the prementioned preparation method.

Figure (3.1) Porous geopolymer samples with different porosity

Figure (3.2) shows a flowchart that summarizes the experimental work achieved in the current study.

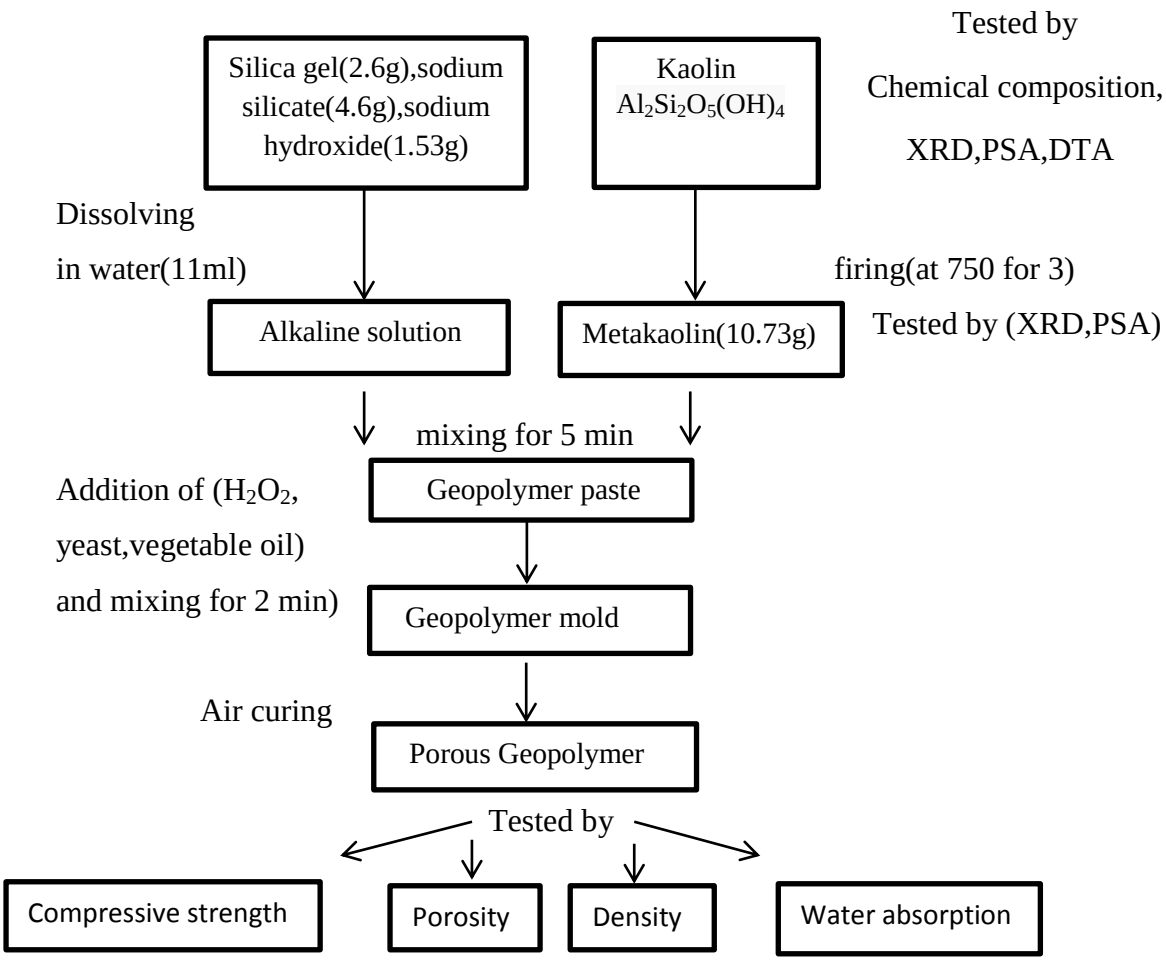

Figure 3.2 flowchart of the experimental work performed in the current work.

3.4 Experiments' Design

Designing studies for the stated set of process variables using the full factorial technique necessitates a high number of samples, up to 625 samples in addition to the work, time, and high cost. To solve these flaws, the Taguchi method was applied. For the geopolymer mix, the Taguchi method proposed 25 tests. Table (3.3) lists the circumstances of each experiment.

Table (3.3) The Conditions of The experiments produced by Taguchi method

Experiment No.	**A:**Concenteration of H_2O_2%	**B:**Quantity of the yeast(g)	**C:**Quantity of H_2O_2(ml)	**D:**Polymerization time(min)	**E:**Quantity of vegetable oil(ml)
1	10	0.1	0.2	0	0.1
2	10	0.2	0.4	30	0.2
3	10	0.3	0.6	60	0.3
4	10	0.4	0.8	90	0.4
5	10	0.5	1.0	120	0.5
6	20	0.1	0.4	60	0.4
7	20	0.2	0.6	90	0.5
8	20	0.3	0.8	120	0.1
9	20	0.4	1.0	0	0.2
10	20	0.5	0.2	30	0.3
11	30	0.1	0.6	120	0.2
12	30	0.2	0.8	0	0.3
13	30	0.3	1.0	30	0.4
14	30	0.4	0.2	60	0.5
15	30	0.5	0.4	90	0.1
16	40	0.1	0.8	30	0.5
17	40	0.2	1.0	60	0.1
18	40	0.3	0.2	90	0.2
19	40	0.4	0.4	120	0.3
20	40	0.5	0.6	0	0.4
21	50	0.1	1.0	90	0.3
22	50	0.2	0.2	120	0.4
23	50	0.3	0.4	0	0.5
24	50	0.4	0.6	30	0.1
25	50	0.5	0.8	60	0.2

The Taguchi method is an efficient approach for optimizing a single quality response[65]. In today's complicated industrial processes, we frequently have to optimize multiple responses at once rather than one at a time. In this work, the Taguchi approach was used with a number of different assistance methods [99]:

1-Grey rational analysis

2-Utility concept

3-Data envelopment analysis

4-Desirability based method

5-Engineering judgment method

6-Level weight method

7-Principal component method

3.4.1 The Procedure of the Taguchi-Grey Relational Analysis Method:

Step 1: Using Equations (2.3), calculate the S/N ratio of the orthogonal test results and evaluate the variation in the S/N ratio.

Step 2: Using Equation (2.4), normalize the S/N ratios of each response to produce Zij, which reflects the normalized value of the S/N ratio for the greater is better.

Step 3: The deviation sequences was calculated using equation (2.5).

Step 4: The grey rational coefficient (GRC) was calculated using equation (2.6).

Step 5: The grey rational grade (GRG) was calculated using equation (2.7).

3.4.2 The Procedure of the Utility Concept Method:

Step 1: Calculate the S/N ratio of the orthogonal test results using the associated equation (2.3).

Step 2: *A* is an arbitrarily constant has been chosen such that $pi = 9$ at $x_i = x^*$, where x^* is the optimum value of x_i with the assumption that such a number exist.

Step 3: A preference scale for each quality attributes is constructed to determine the overall utility value using equation (2.11).

Step 4: The overall utility value can be calculated by using equation (2.13).

3.4.3The Procedure of the Desirability based Method (DGM):

Step 1: Using the relevant equation, Equations, calculate the S/N ratio of the orthogonal test results (2.3).

Step 2: For Larger-The-Best (LTB) response type (the estimated response value is expected to be larger than a lower bound L; $y\hat{} > L$) according to equation (2.25).

Step 3: Determine the importance of response ω_i by the users and limited between 0.1-0.9.

Step 4: the desirability function of the responses can be calculated using equation (2.24).

3.4.4 The Procedure of the Engineering Judgment Method:

Step 1: Calculate the S/N ratio of the orthogonal test results using Equations (2.3) and evaluate the variation in the S/N ratio.

Step 2: Using Equation (2.4), normalize the S/N ratios of each answer to produce Zij, which reflects the normalized value of the S/N ratio for the greater is better.

Step3: The importance of response is determined between 0.1-0.9.

Step4: The combined responses were calculated according to equation (2.34).

3.4.5 The Procedure of the Level Weight Method:

Step1: Calculate the S/N ratio of the orthogonal test results using Equations (2.3), and evaluate the variation in the S/N ratio.

Step2: Calculate the S/N ratio averages with the help of Taguchi (ANOVA) analysis.

Step3: The values of the level weights represent the value corresponding to it in the previous step relative to the highest value within the same variable according to equation (2.39).

Step4: In the final level weight each value represents the average of the two corresponding values in the previous step that share the same variable and level.

3.4.6 The procedure of the Principal Component Analysis Method:

Step1: Calculate the S/N ratio of the orthogonal test results using Equations (2.3) and evaluate the variation in the S/N ratio.

Step2: Using Equation (2.4), normalize the S/N ratios of each answer to get Zij, which indicates the normalized value of S/N ratio for the bigger is better.

Step3: The values of eigenvector calculated by the principle component analysis located in Minitab for the each normalized value.

Step4: The value of the principle component calculated according to the following equation:

$$Z_1 = a_{11}X_1 + a_{12}X_2 + \_\ \_\ \_ + a_{1p}X_p$$

3.5 Confirmatory Experiments

Confirmatory experiments are carried out to ensure that the final optimal factor settings are correct and that the optimal condition generated from the experiment genuinely improves product quality[81].Confirmation experiments were conducted by synthesis porous geopolymer samples according to the optimal conditions which are expected to improve the compressive strength and porosity of the geopolymer. The proposed experiments from all methods were standardized by taking one experiment from the similarities and excluding the experiments within the initial (25) experiments.

3.6 Testing methods

3.6.1 Chemical Analysis

The wet chemical method was used to determine the chemical composition of kaolin. The Iraq geology and mining survey in Baghdad conducted this investigation. The wet chemical analysis uses the procedure to decompose a sample with a reagent such as acids to dissolve in a solvent and identifies and quantifies the targeted elements using various measurement methods. Separation and isolation of the sample is performed if needed. The wet chemical analysis can be divided in two types of analysis, the qualitative analysis to identify the elements and the quantitative analysis to determine the quantity.

3.6.2 X-Ray Diffraction (XRD)

XRD analysis was used to determine the phases that make up the samples, as well as to confirm the creation of the amorphous metakaolin phase and the geopolymer's phase composition.

The x-ray was produced via utilizing high voltage power (40kv/30mA) which fast-tracks the electrons from heated tungsten filament to strike the target which is made from copper. The x-ray is generated and goes through a nickel filter before hitting the specimen, which is rotating in a circular motion at a speed of 5°/min. When the incident beam diffracts according to Bragg's law (equation 3.1), diffraction occurs [60].

$$n\lambda = 2d \sin\theta \quad \text{.....(3.1)}$$

Where (λ) is the incident wavelength ray (λ=1.5406 angstrom), (d) is the inter-planar distance (A˚), the angle (θ) is located between the incident beam and the surface of specimen, and (n) is a positive integer. The x-ray diffracted is received from the sample by the rotating detector that rotated at (2θ) as a speed. As a final point, the data of diffraction (the intensity of the diffracted ray and the values of diffraction angels) was acquired utilizing a computerized system. The d-spacing values of the tested samples that have comparing with the d-spacing standard data of ceramic materials which are given by International Center of Diffraction Data (ICDD). This test was performed using diffractometer of x-ray (type: XRD 6000, made in Shimadzu, Japan) that exists in the department of ceramics and building materials engineering at Babylon University's Materials Engineering College.

3.6.3 Particle size Analysis

Using a laser particle size analyzer accessible at the Department of Ceramic and Building Materials Engineering / Materials Engineering / University of Babylon, this test was performed to determine the particle size distribution of kaolin and metakaolin powder. The basic diffraction

standard for lasers was straightforward: Diffraction, or light scattering on the particles, produces an angle behind of the particle, dependent on the distribution intensity, which involves a ring system with dark and bright patches. The shifting intervals areas between dark and light are dependent on particle size, where the relationship between particle size and ring intervals is negative. Small particles create massive rings, whereas big particles cause intensity distributions with finely edged rings. The rings distances may be calculated exactly using the Mie (theory), and with sufficiently big diameters particles, the Fraunhofer-estimate theory could be applied. The procedure of this test involved taking a small amount of powder and added it to 500 ml of distilled water and place the mix inside the device and take the result from the computer device connected to the device.

3.6.4 Differential Thermal Analysis (DTA)

Using tiny quantities of solid powder, DTA is used to examine phase transitions, crystallizations, and decomposition temperatures. This experiment was carried out at the Ceramics and building Materials engineering/Materials Engineering College / Babylon University. This device measures the temperature differences between the sample to be examined and the reference material (a thermally inert material that is not subject to phase transition) by heating it to above 950 degrees Celsius. With a 10 °C/min air heating frequency, the temperature is improved. The temperature is then shown alongside the variable thermal measurement (V). If the relative thermal analysis was zero or stable, there was no thermal case, but a positive (T) indicates that the sample temperature was higher than the study material, causing the exothermic maximum to form on the top side, and a negative (D) indicates that the sample temperature

was lower than the control temperature, causing the endothermic peak to form on the lower side.

3.6.5 Compression Test

This test was performed for geopolymer paste and concrete at age of 28 days. At first, to ensure that the samples are flat, the specimen should be polished with a polishing machine. This test was performed at Ceramics and building Materials engineering/Material Engineering College / Babylon University. The compressive strength can be determined depending on the next formula [60].

$\sigma c = P/A$ ……………………………………………………………(3.2)

Where:

σc =compressive strength (MPa)

P = load that used (KN)

A= sample's area (mm^2)

3.6.6 Density Measurements

The Archimedes method was used to determine the density, porosity, and water absorption of the synthesized samples. Firstly all of the samples were dried at 150°C for 6 hours before being cooled in desiccators to room temperature. The dry weight (D) was calculated to within 0.001 g. Secondly the samples were put in purified water for 24 h where the samples submerged in the water during the specific period. Then, the samples suspended weight (S) were measured to the nearest 0.001 g. Next, After identifying (S), the samples were lightly rolled on a moisted cotton cloth to get rid of the extra water from the surface. Directly, the samples were weight to identify the mass after saturating (M) to the closest 0.001g. During this step, it is worth mentioning that the samples immersed in water were subjected to a vacuum process to allow

the water to penetrate into the pores. The density was calculated according to the equation (3.3):[60]

$\rho = D/(M-S)$ ……...… (3.3)

Where ρ is the bulk density. The percent proportion of the open pores volume to the sample bulk volume can be used to determine apparent porosity. The apparent porosity was calculated by utilizing the next formula.

$$P_A = (\frac{M-D}{M-S}) \times 100 \quad \text{……(3.4)}$$

Where P_A is apparent porosity (%). Water adsorption was calculated by using the following equation:

Aw(%)= (M-D/ D) ×100 ……..(3.5)

3.6.7 Optical Microscope Imaging

Imaging was applied in order to evaluate the porosity of the samples. Imaging was carried out using optical microscope with a magnification around ×200. The cross section of the samples was mildly polished by the use of appropriate emery papers.

CHAPTER FOUR

RESULTS AND DISCUSSION

4.1 Introduction

This chapter displays the results which were gained from the experimental works and their discussion. It includes the description of the impact of different process parameters on the paste geopolymer characteristics as well as the process condition required to obtain the highest compressive strength and porosity.

4.2 Result and Discussion

4.2.1 The Chemical Analysis

The results of the chemical analysis of the kaolin utilized in this investigation are shown in Table (4.1). This analysis was carried out using the wet chemical technique. The amount of SiO2 in the clay is more than the stoichiometric amount in the kaolinite, as can be shown (48.77 percent). This supports the XRD result that free quartz is present and aids in the estimation of the amount of free quartz that should be omitted when calculating the composition of geopolymer. This is due to the inertness of quartz, which renders it an inert component in the geopolymer synthesis.

Table (4.1) the chemical composition of kaolin

SiO_2 (%)	Fe_2O_3 (%)	Al_2O_3 (%)	TiO_2 (%)	CaO (%)	MgO (%)	SO_3 (%)	P_2O_5 (%)	K_2O (%)	Na_2O (%)	Cl (%)	LOI (%)
48.77	1.76	34.27	1.47	0.43	0.08	0.11	0.02	0.43	0.17	0.03	12.46

4.2.2 XRD Analysis

Fig (4.1) demonstrates the XRD pattern of the kaolin powder. The pattern indicates the powder's crystalline structure. According to (ICCD=00-001-0527) and (ICCD=00-033-1161), the common characteristic peaks of kaolin were observed for kaolinite and SiO_2 minerals, respectively. The production of metakaolin is well-known as a result of heat treatment of kaolin at moderate temperatures. As shown in Fig. (4.2), this was validated for the kaolin heat treated at 750^{o}C for 3 hours (MK-750) [60]. The pattern emphasizes metakaolin powder's amorphous form. A strong peak in the XRD analysis of metakaolin corresponds to the free quartz in the kaolin powder.

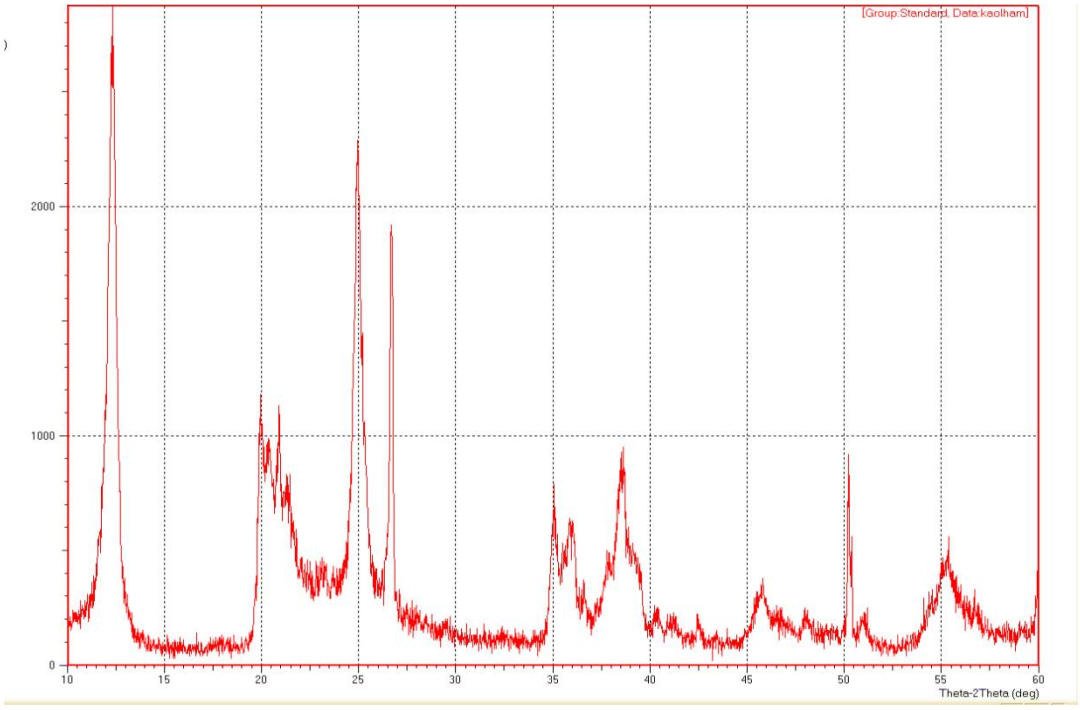

Figure (4.1) X-ray diffraction profile for the kaolin

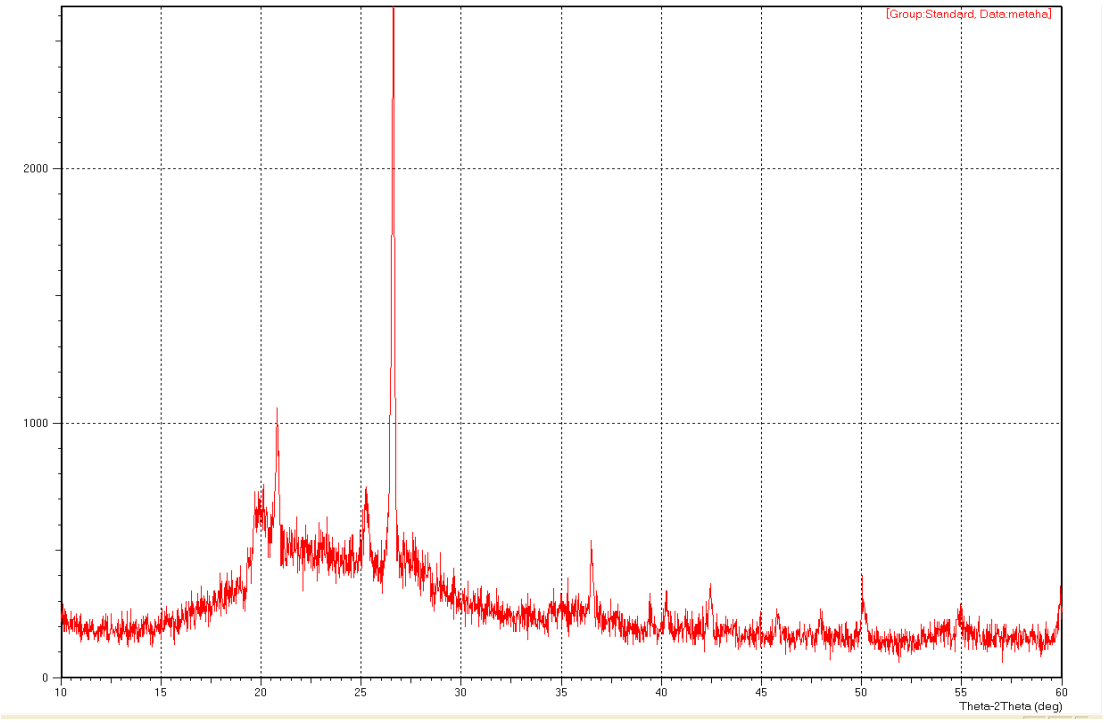

Figure (4.2) X-ray diffraction profile for the metakaolin

4.2.3 Analysis of the Particle Size

The particle size distribution of kaolin powder is shown in Figure 4.3. The findings revealed that kaolin is mostly made up of micro-sized particles smaller than 20 micrometers. With a D50 of 3.8µm, the particle size distribution is multimodal. Figure (4.4) depicts the particle size distribution of MK-750. Metakaolin, as compared to kaolin, is noted for having finer particle sizes due to the shattering of the kaolinite structure. Agglomeration and aggregation, on the other hand, result in the creation of massive secondary particles, as shown in Fig (4.4).

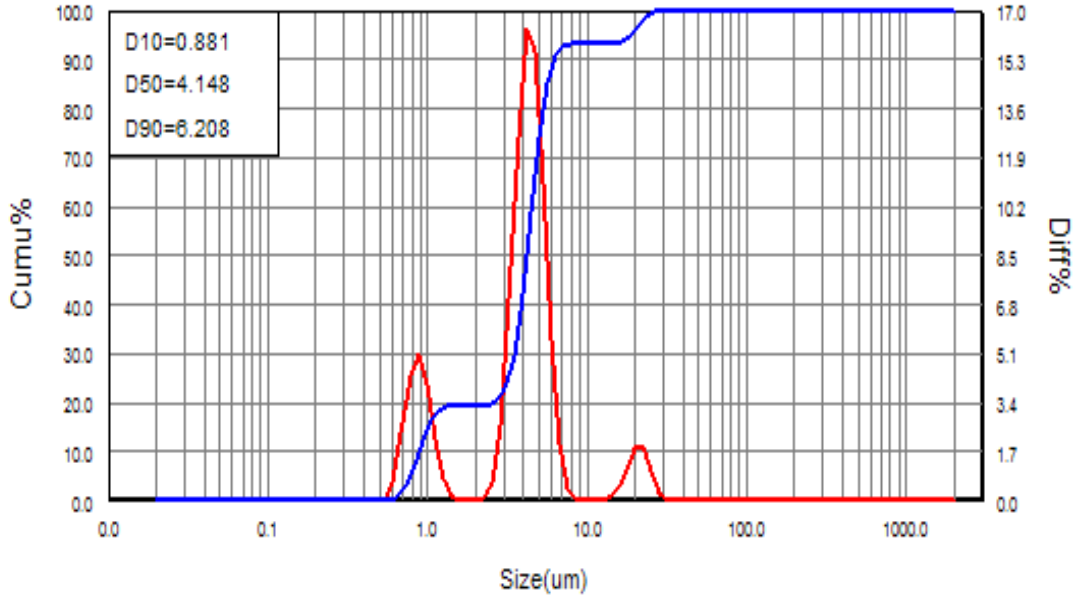

Figure (4.3) the particle size distribution of kaolin powder

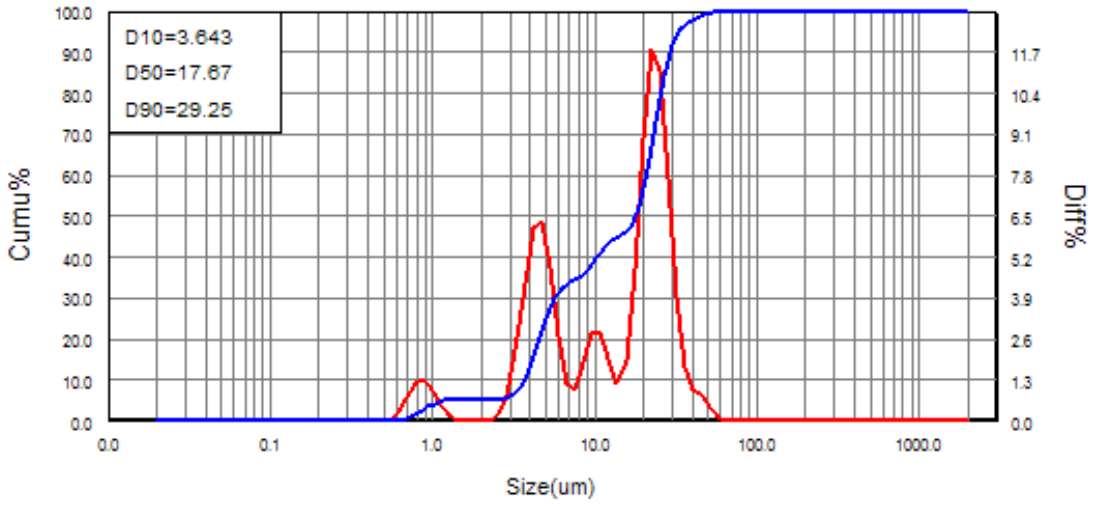

Figure (4.4) the particle size distribution of metakaolin powder

4.2.4 DTA Analysis

The differential thermal analysis (DTA) curve for kaolin is shown in Figure (4.5). The endothermic peak for kaolin calcination to generate metakaolin was measured at 530 °C. This event ended at 575°C, and no

other thermal events were recorded, indicating that 750°C is a good temperature for metakaolin production.[83,85,88]

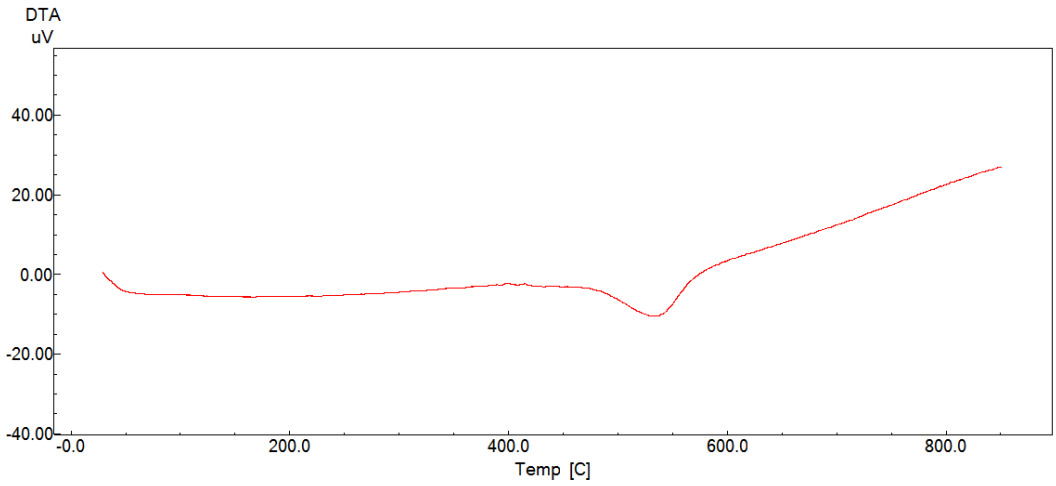

Figure (4.5) Variation of peak temperature with heating rate in differential thermal analysis measurements for the kaolin

4.2.5 Optical Microscope Images

Optical microscope imaging was performed on the porous geopolymer samples produced using different H_2O_2, yeast, vegetable oil contents and different polymerization time according to L25 experiments in order to evaluate the porosity of the samples as shown in fig (4.6). From the optical micrographs the significant differences for each sample can be observed. It is also evident that the pore diameter increased with increasing the amount of H_2O_2, leading to larger amount of open porosity. This can be seen when comparing images (a) and (b) in one side, that have concenteration of foaming agent of (20%), while those in (c) and (d), in the other side, with similar samples except the concenteration of H_2O_2 (30%). The steady addition of H_2O_2 and yeast to the pastes causes a chemical reaction between them, resulting in an increase in the number of pores and thus the overall pore volume Fig. 4.6 (g,h). This accounts for

the fact that H_2O_2-rich samples have the lowest apparent density and compressive strength values. The pores appear to be spherical across the whole H_2O_2 foam range.

However, as the amount of H_2O_2 in the pores increases, the shape of the pores changes from spherical to irregular, as shown in (e) and (f), possibly due to the increased intensity of the gaseous oxygen release. The amount of foaming agent has an important influence on pore size. There are two types of pores that can be seen in the samples, which are closed and open to contain holes fig 4.6(c-f). The pore size distributions of samples with variable H_2O_2 and yeast levels reveal that as H_2O_2 incorporation increases, the distributions narrow and move to smaller pore diameters. It appears that adding additional H_2O_2 to geopolymer pastes results in foams with higher porosity and smaller, more homogeneous pores [90,91].

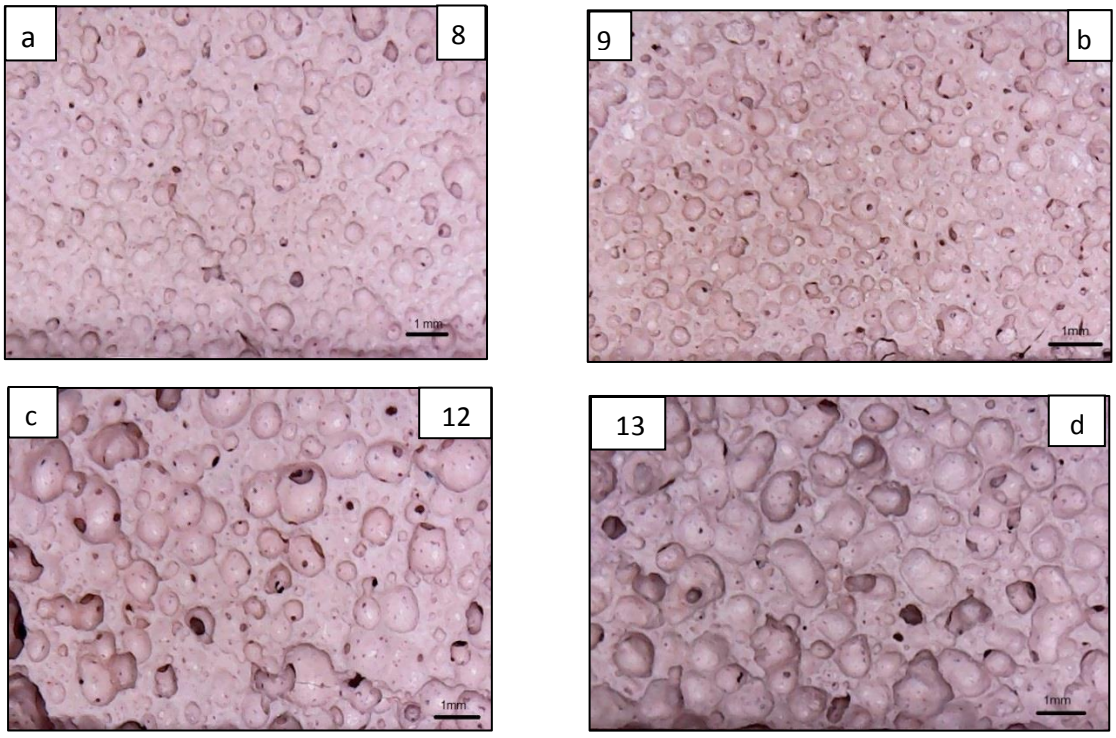

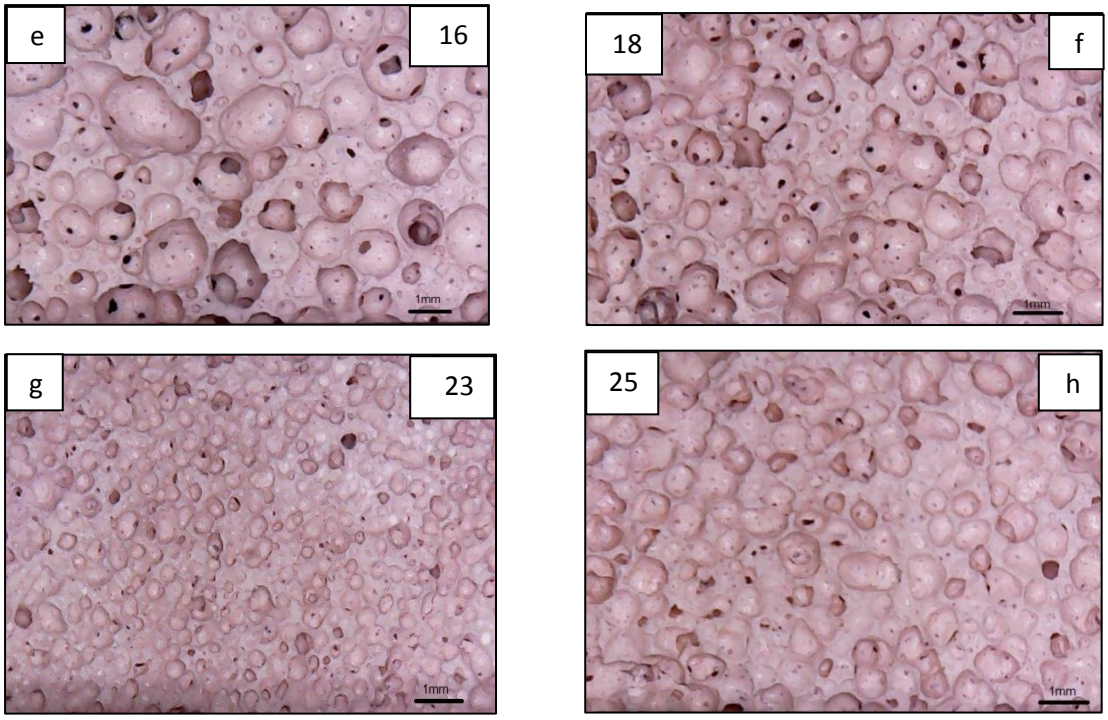

Figure (4.6) some optical microscope images of the produced porous geopolymer synthesized according to L25 experiments

4.3 Results of Optimization Methods

4.3.1 Taguchi method

The average value of the experimentally obtained results for compressive strength and porosity, density, water absorption are given in table (4.2).

Table (4.2) experimental results for the compressive strength and the porosity, density, water absorption

Experiment No.	Compressive strength(Mpa)	Porosity(%)	Density g/cm^3	Water absorption(%)
1	66.95	30.67	1.25	25.0

2	50.34	31.91	1.09	26.3
3	33.60	30.83	0.97	32.7
4	25.56	21.57	0.94	25.3
5	21.39	9.52	1.009	10.0
6	30.20	26.29	0.96	29.7
7	19.94	16.84	0.86	20.1
8	6.12	24.35	0.79	38.0
9	9.99	34.51	0.79	48.8
10	6.32	19.58	0.87	22.5
11	7.37	28.26	0.79	36.6
12	3.09	59.43	0.53	117.9
13	3.51	65.76	0.48	148.0
14	24.41	35.00	0.92	37.6
15	12.40	21.64	0.89	24.1
16	2.76	74.66	0.45	164.7
17	6.28	65.25	0.61	128.6
18	2.65	84.10	0.37	213.3
19	5.95	31.06	0.85	36.5
20	4.39	41.09	0.81	50.7
21	8.85	80.12	0.46	184.9
22	10.66	60.98	0.82	74.7
23	4.57	42.02	0.81	50.9
24	7.69	65.00	0.64	110.2
25	2.76	76.18	0.46	166.2

These raw data can be transformed into S/N ratio by using equation (2.3). The corresponding S/N ratio values for experimental parametric setting according to L_{25} orthogonal array are shown in table (4.3).

Table (4.3) signal –to- noise (S/N) ratio values

Experiment No.	(S/N) ratio (compressive strength)	(S/N) ratio (Porosity)
1	36.52	29.73
2	34.04	30.08
3	30.53	29.78
4	28.15	26.68
5	26.60	19.58
6	29.60	28.39
7	25.99	24.53
8	15.74	27.73
9	19.99	30.76
10	16.01	25.84
11	17.35	29.02
12	9.79	35.48
13	10.91	36.36
14	27.75	30.88
15	21.87	26.71
16	8.82	37.46
17	15.96	36.29
18	8.46	38.49
19	15.49	29.84
20	12.85	32.27
21	18.94	38.07
22	20.56	35.70
23	13.19	32.47
24	17.72	36.26
25	8.82	37.64

The normalized values of the S/N ratio, calculated according to equation (2.4), are given in table (4.4).

Table (4.4) normalized S/N ratio values

Exp. no	Compressive strength	porosity
1	1.00	0.54
2	0.91	0.56
3	0.79	0.54
4	0.70	0.38
5	0.65	0.00
6	0.75	0.47
7	0.62	0.26
8	0.26	0.43
9	0.41	0.59
10	0.27	0.33
11	0.32	0.49
12	0.05	0.84
13	0.09	0.89
14	0.69	0.59
15	0.48	0.38
16	0.01	0.94
17	0.27	0.88
18	0.00	1.00
19	0.25	0.54
20	0.16	0.67
21	0.37	0.98
22	0.43	0.85
23	0.17	0.68
24	0.33	0.88
25	0.01	0.95

4.3.2 Grey-based Taguchi analysis

The grey relational coefficient for the normalized S/N ratio values, which were calculated according to equation (2.6) are given in table (4.5). These values are corresponding to the value of λ as (0.5) for compressive strength and porosity. Next, the grey relational grade can be computed by Equation (2.7). Finally, the grades are considered for optimizing the multi response parameter design problem. The S/N ratio plot of compressive strength and porosity with respect to concenteration of H_2O_2, quantity of the yeast, quantity of H_2O_2, polymerization time, quantity of oil are shown in Fig (4.7). In this figure (a) it can be easily seen that, for λ value of 0.5, the optimal parameter conditions are (A_5,B_1,C_1,D_3,E_2),in the same fig (b) for λ value of 0.9, the optimal conditions are (A_5,B_1,C_1,D_4,E_2), while in (c) for λ value of 0.4, the optimal conditions are (A_1,B_1,C_1,D_3,E_2) and in (d) for λ value of 0.1 the optimal conditions are (A_1,B_1,C_1,D_1,E_1). The subscribt number indicates the level of the factor at which the optimal response could be obtained. Similarly, the optimal multi response parameter where obtained for different values of λ as given in table (4.6).

Table (4.5) grey relational coefficient and grey grade values for λ values of 0.5

Exp. no	GRC_{1j}	GRC_{i2}	GRG_i
1	1	0.52	0.76
2	0.85	0.53	0.69
3	0.70	0.52	0.61
4	0.63	0.44	0.53
5	0.59	0.33	0.46
6	0.67	0.48	0.58
7	0.57	0.40	0.49
8	0.40	0.47	0.44
9	0.46	0.55	0.50
10	0.41	0.43	0.42

11	0.42	0.49	0.46
12	0.34	0.76	0.55
13	0.35	0.82	0.58
14	0.62	0.55	0.58
15	0.49	0.45	0.47
16	0.34	0.90	0.62
17	0.41	0.81	0.60
18	0.33	1.00	0.67
19	0.40	0.52	0.46
20	0.37	0.60	0.47
21	0.44	0.96	0.70
22	0.47	0.77	0.62
23	0.38	0.61	0.49
24	0.43	0.81	0.62
25	0.34	0.92	0.63

Table (4.6) optimal parameter levels for different values of λ for compressive strength

Exp. no	λ	A	B	C	D	E
Exp-1	0.1	10	0.1	0.2	0	0.1
Exp-2	0.2	10	0.1	0.2	60	0.1
Exp-3	0.3	10	0.1	0.2	60	0.1
Exp-4	0.4	10	0.1	0.2	60	0.2
Exp-5	0.5	50	0.1	0.2	60	0.2
Exp-6	0.6	50	0.1	0.2	60	0.2
Exp-7	0.7	50	0.1	0.2	60	0.2
Exp-8	0.8	50	0.1	0.2	90	0.2
Exp-9	0.9	50	0.1	0.2	90	0.2

(a) λ=0.5

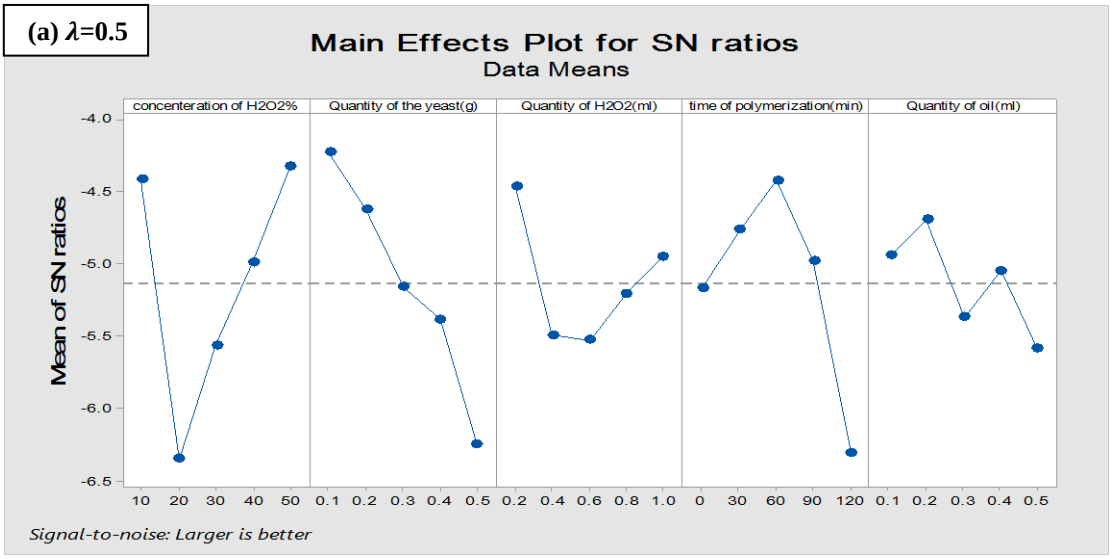

(b) λ =0.9

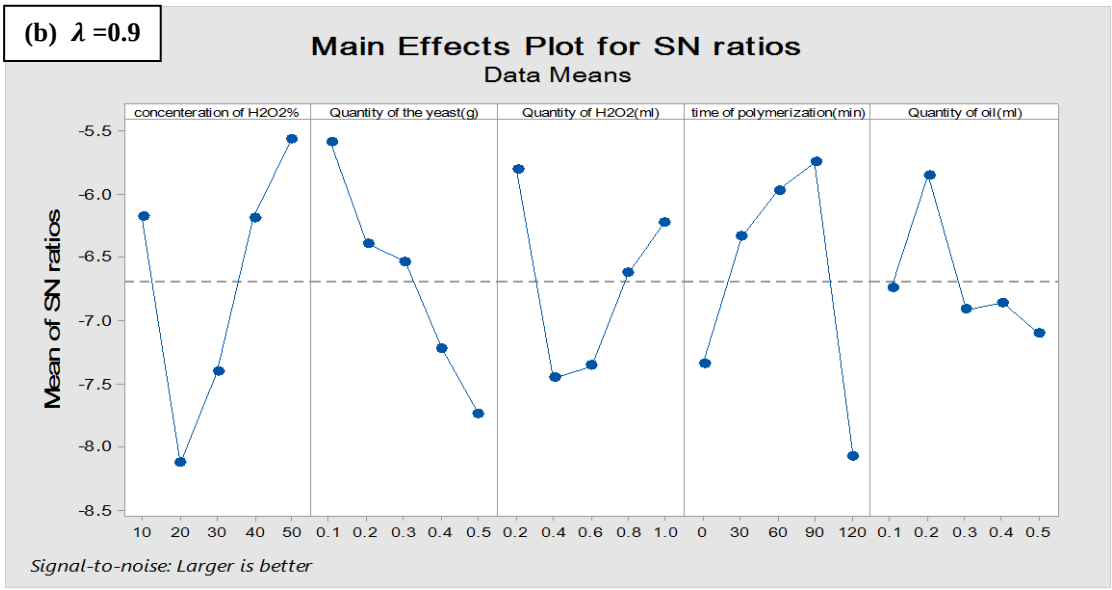

(c) λ=0.4

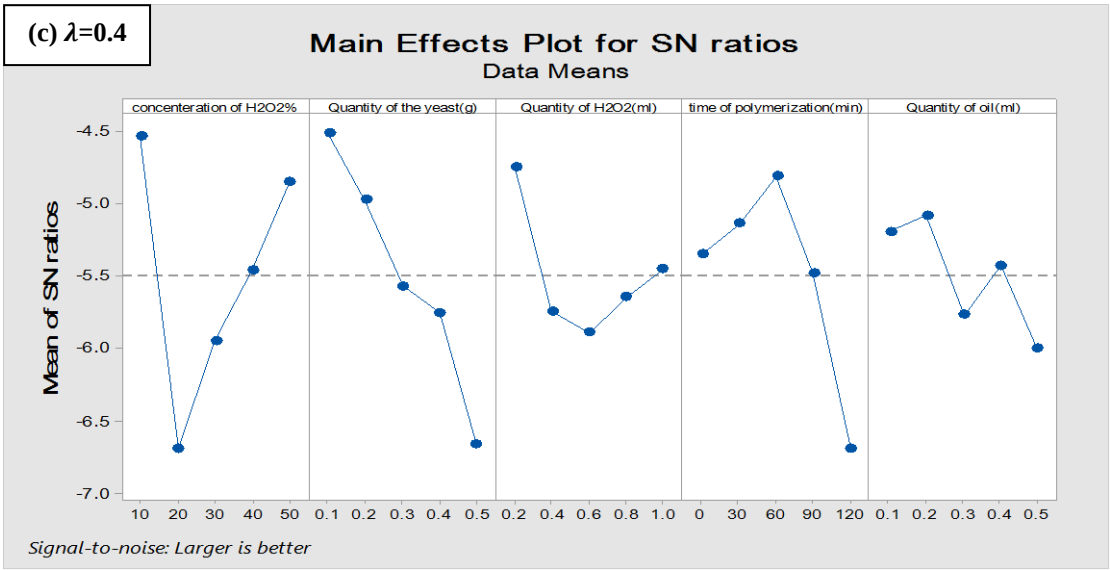

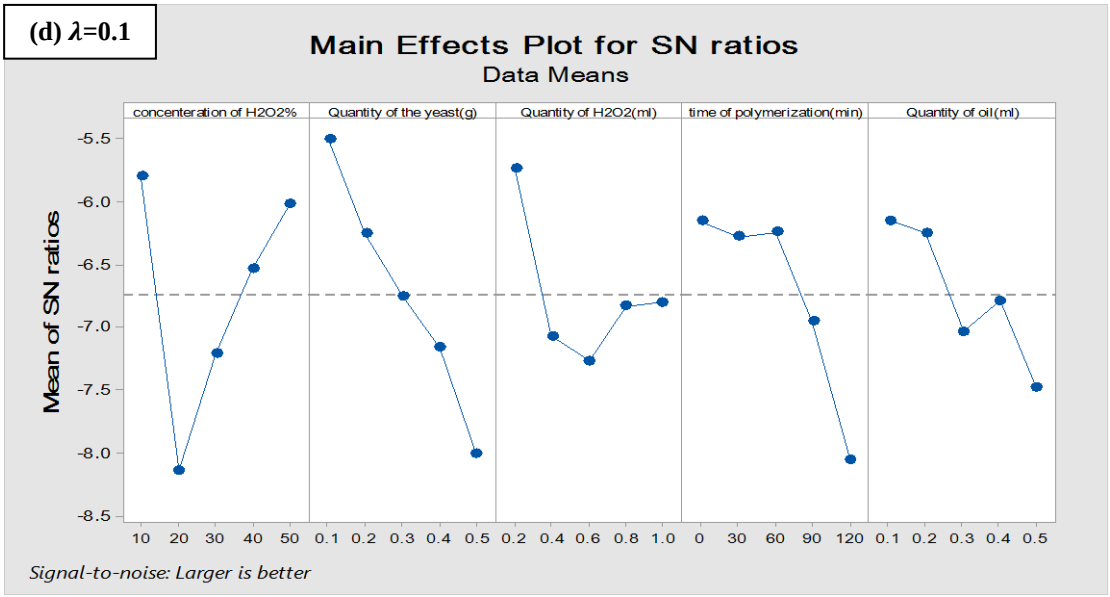

Figure (4.7) the main effect plot for SN ratio according to grey rational analysis method

4.3.3 Utility Concept Method

The S/N ratio of the orthogonal test results from using the corresponding equation, given by Equations (2.3) are the same as that obtained in grey rational analysis method see table(4.3). First step the arbitrarily constant value (A) has been determined for all the experiments and it was14.94 for compressive strength and 27.49 for porosity. The second step is to determine the preference number (*pi*) according to equation (2.11), the results shown in table **(**4.7).Next, the utility value can be computed by Equation (2.13) the results are given in table (4.8). Finally, the utilities are considered for optimizing the multi response parameter design problem. The S/N ratio plot of compressive strength and porosity with respect to concenteration of H_2O_2, quantity of the yeast, quantity of H_2O_2, polymerization time, quantity of vegetable oil are shown in Fig (4.8).

Table (4.7) the preference number and utility value results

No. Exp	Compressive strength	porosity	U
1	12.34	-3.17	18.66
2	10.49	-2.69	17.04
3	7.86	-3.10	14.64
4	6.09	-7.37	12.61
5	4.93	-17.13	10.60
6	7.17	-5.00	13.82
7	4.48	-10.32	10.87
8	-3.18	-5.92	4.41
9	-0.00	-1.76	7.69
10	-2.97	-8.52	4.33
11	-1.98	-4.15	5.67
12	-7.62	4.72	1.48
13	-6.79	5.93	2.34
14	5.79	-1.59	12.92
15	1.39	-7.33	8.39
16	-8.35	7.45	1.09
17	-3.02	5.84	5.73
18	-8.62	8.87	1.00
19	-3.37	-3.02	4.53
20	-5.34	0.32	3.09
21	-0.79	8.29	7.98
22	0.41	5.03	8.74
23	-5.08	0.58	3.35
24	-1.70	5.79	6.91
25	-8.35	7.69	1.11

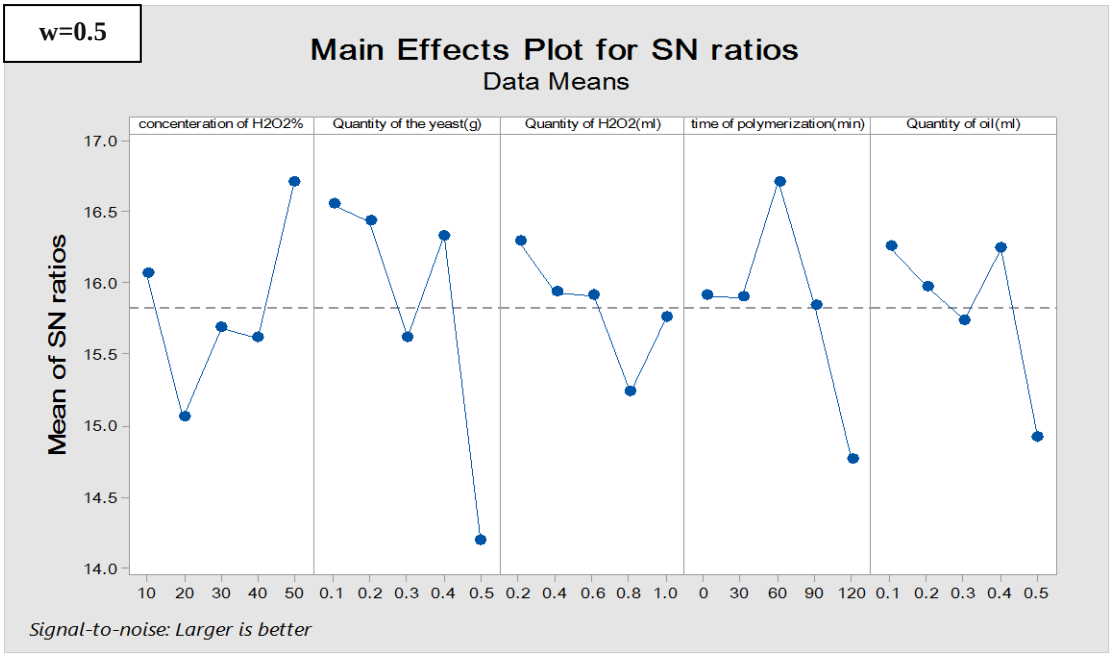

w=0.5

Figure (4.8) the main effect plot for SN ratio according to utility concept method

It can be easily seen that, for *w* value of 0.5, the optimal parameter conditions are (A_5,B_1,C_1,D_3,E_1). Similarly, the optimal multi response parameter where obtained for different values of *w* as given in table (4.8).

Table (4.8) optimal parameter levels for different values of *w* for compressive strength

Exp. no	*w*	A	B	C	D	E
Exp-10	0.1	50	0.3	0.8	30	0.2
Exp-11	0.2	50	0.1	0.2	60	0.2
Exp-12	0.3	50	0.1	0.2	60	0.2
Exp-13	0.4	50	0.1	0.2	60	0.2
Exp-14	0.5	50	0.1	0.2	60	0.1
Exp-15	0.6	10	0.1	0.2	60	0.1
Exp-16	0.7	10	0.1	0.2	60	0.1
Exp-17	0.8	10	0.1	0.2	60	0.1
Exp-18	0.9	10	0.1	0.4	60	0.1

4.3.4 (DEA) method

DEA is linear programming based technique which is used to empirically measure the productive efficiency of decision making units (DMUs) when the production process presents a structure of multiple inputs and outputs. The efficiency of 'multiple inputs and output factors' can be defined as the following: Ek = weighted sum of outputs/ weighted sum of inputs. Experimental data presented in table (4.2) have been analyzed by aforementioned procedure. For each experiment the relative efficiency has been computed by using equation (2.16), the results show that there are efficient DMUs as given in table (4.9)

Table (4.9) the suggested optimal conditions for combined optimal compressive strength and porosity according to (DEA) method

Experiments	A	B	C	D	E
Exp-19	10%	0.1	0.2	0	0.1
Exp-20	40%	0.1	0.6	90	0.2
Exp-21	50%	0.1	1.0	90	0.3

4.3.5 (DGM) method

The desirability analysis converts the complex multiple quality characteristics optimization into the optimization of a single composite desirability index, thus, simplifies the optimization procedure. At first, the individual desirability (di) for all the compressive strength and porosity results is calculated. The composite desirability index (D) is calculated using Equation (2.24). One-sided desirability transformations for Larger-The-Best (LTB) response type (the estimated response value is expected to be larger than a lower bound L; $y\hat{} > L$) according to equation (2.25). For this, the relative importance of responses is assigned based on

final requirements as 0.1:0.9 for compressive strength and porosity, respectively. The results are given in tables (4.10),(4.11),(4.12).

Table (4.10) the bounded values

No. Exp	Strength	Porosity
1	32.04	29.73
2	32.04	30.07
3	30.52	29.78
4	28.15	29.54
5	26.60	29.54
6	29.60	29.54
7	25.99	29.54
8	15.73	29.54
9	19.99	30.75
10	16.01	29.54
11	17.34	29.54
12	13.97	35.48
13	13.97	36.35
14	27.75	30.88
15	21.86	29.54
16	13.97	37.46
17	15.95	36.29
18	13.97	38.06
19	15.49	29.84
20	13.97	32.27
21	18.93	38.06
22	20.55	35.70
23	13.97	32.46
24	17.71	36.25
25	13.97	37.63

The normalization is done by using equation (2.4) the results are given in table (4.11)

Table (4.11) the normalized values

No. Exp	com/strength	porosity
1	1.00	0.02
2	1.00	0.06
3	0.91	0.02
4	0.78	0.00
5	0.69	0.00
6	0.86	0.00
7	0.66	0.00
8	0.09	0.00
9	0.33	0.14
10	0.11	0.00
11	0.18	0.00
12	0.00	0.69
13	0.00	0.80
14	0.76	0.15
15	0.43	0.00
16	0.00	0.92
17	0.10	0.79
18	0.00	1.00
19	0.08	0.03
20	0.00	0.32
21	0.27	1.00
22	0.36	0.72
23	0.00	0.34
24	0.20	0.78

25	0.00	0.95

Table (4.12) desirability functions (weighted geometric mean), (DGM)

No. Exp	Desirability functions (weighted geometric mean)	DGM
1	0.68	0.68
2	0.75	0.75
3	0.64	0.64
4	0.00	0.00
5	0.00	0.00
6	0.00	0.00
7	0.00	0.00
8	0.00	0.00
9	0.30	0.30
10	0.00	0.00
11	0.00	0.00
12	0.00	0.00
13	0.00	0.00
14	0.65	0.65
15	0.00	0.00
16	0.00	0.00
17	0.13	0.13
18	0.00	0.00
19	0.07	0.07
20	0.00	0.00

21	0.31	0.312
22	0.38	0.38
23	0.00	0.00
24	0.23	0.23
25	0.00	0.00

This method can reduce the number of the suggested optimal conditions to five experiments only as given in table (4.13). The mean plot of compressive strength and porosity with respect to concenteration of H_2O_2, quantity of the yeast, quantity of H_2O_2, polymerization time, quantity of vegetable oil according to (DGM) method are shown in Fig (4.9).

Table (4.13) the suggested optimal conditions for combined optimal compressive strength and porosity according to (DGM) method

Experiments	A	B	C	D	E
Exp-22	50%	0.5	0.4	90	0.1
Exp-23	50%	0.5	0.4	60	0.1
Exp-24	50%	0.1	0.8	60	0.1
Exp-25	10%	0.1	0.8	60	0.1
Exp-26	10%	0.1	0.4	60	0.2

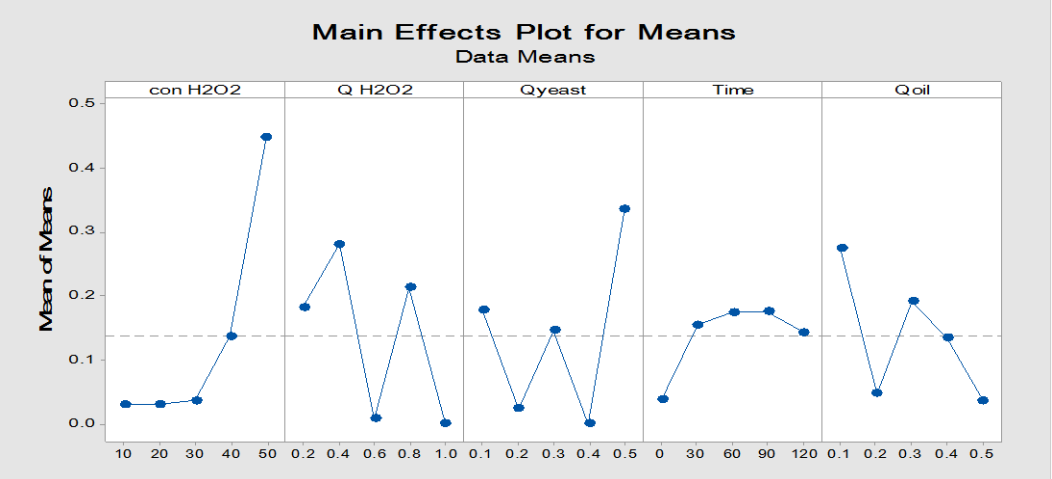

Figure (4.9) the main effect plot for means according to (DGM) method

4.3.6 Engineering Jugdment Method

The results of S/N ratio and normalization are similar to that obtained in tables (4.3) and (4.4). Next the combined response determined using equation (2.34), the results given in table (4.14):

Table (4.14) the combined responses of the engineering judgment method

No. Exp	S/N ratio		Normalized values		Combined response
	strength	porosity	strength	porosity	
1	36.51	29.73	1.00	0.53	0.95
2	34.03	30.07	0.91	0.55	0.87
3	30.52	29.78	0.78	0.53	0.76
4	28.15	26.67	0.70	0.37	0.66
5	26.60	19.57	0.64	0.00	0.58
6	29.60	28.39	0.75	0.46	0.72
7	25.99	24.52	0.62	0.26	0.58
8	15.73	27.72	0.25	0.43	0.27
9	19.99	30.75	0.41	0.59	0.42
10	16.01	25.83	0.26	0.33	0.27
11	17.34	29.02	0.31	0.49	0.33
12	9.79	35.48	0.04	0.84	0.12
13	10.90	36.35	0.08	0.88	0.16
14	27.75	30.88	0.68	0.59	0.67
15	21.86	26.70	0.47	0.37	0.46
16	8.81	37.46	0.01	0.94	0.10
17	15.95	36.29	0.26	0.88	0.32
18	8.46	38.49	0.00	1.00	0.10
19	15.49	29.84	0.25	0.54	0.27
20	12.84	32.27	0.15	0.67	0.20
21	18.93	38.07	0.37	0.97	0.43
22	20.55	35.70	0.43	0.85	0.47
23	13.19	32.46	0.16	0.68	0.22
24	17.71	36.25	0.32	0.88	0.38
25	8.81	37.63	0.01	0.95	0.10

The combined responses are considered for optimizing the multi response parameter design problem by using Taguchi analysis. This method suggested four experiments given in table (4.15). The mean plot of compressive strength and porosity with respect to concenteration of H_2O_2, quantity of the yeast, quantity of H_2O_2, polymerization time, quantity of vegetable oil according to the engineering judgment method are shown in Fig (4.10).

Table (4.15) the suggested optimal conditions for combined optimal compressive strength and porosity according to engineering judgment method.

Experiments	A	B	C	D	E
Exp-27	50%	0.1	0.8	30	0.2
Exp-28	50%	0.1	0.2	60	0.2
Exp-29	10%	0.1	0.2	60	0.1
Exp-30	10%	0.2	0.2	60	0.1

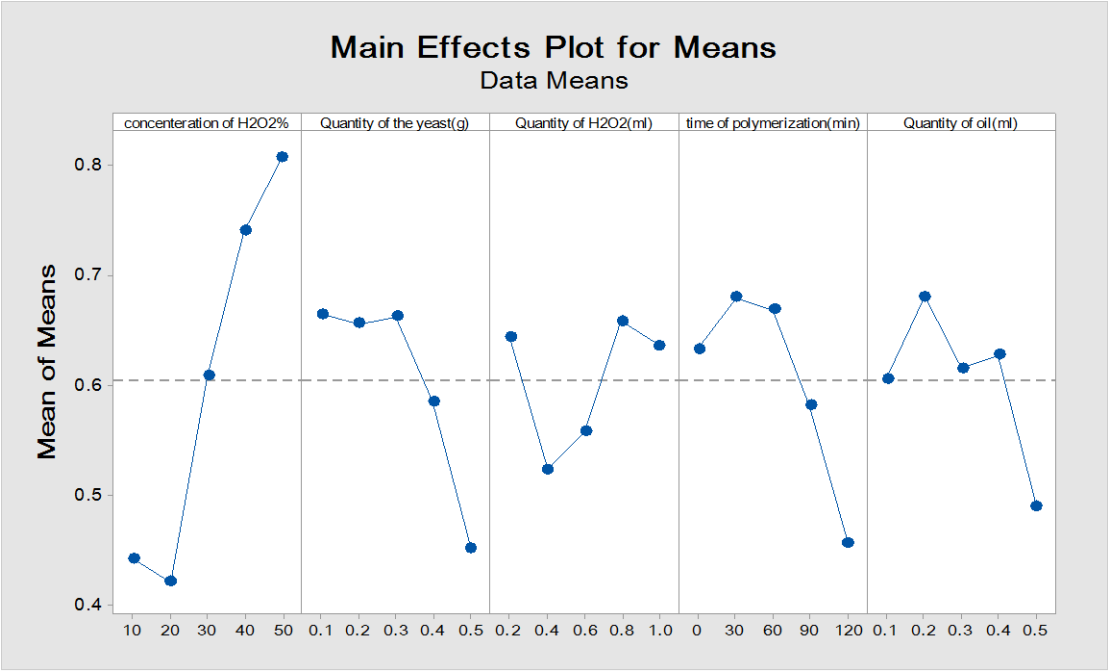

Figure (4.10) the main effects plot for means according to engineering judgment method

4.3.7 Level Weight Method

The S/N ratio, ηj, of response j for each experiment is calculated using Equation (2.3) for all j values and shown in table (4.16) for all of the 25 experiments in L25 array.

Table (4.16) S/N ratio of responses

No. Exp	S/N strength	S/N porosity
1	36.51	29.73
2	34.03	30.07
3	30.52	29.78
4	28.15	26.67
5	26.60	19.57
6	29.60	28.39
7	25.99	24.52
8	15.73	27.72
9	19.99	30.75
10	16.01	25.83
11	17.34	29.02
12	9.79	35.48
13	10.90	36.35
14	27.75	30.88
15	21.86	26.70
16	8.81	37.46
17	15.95	36.29
18	8.46	38.49
19	15.49	29.84
20	12.84	32.27
21	18.93	38.07
22	20.55	35.70
23	13.19	32.46
24	17.71	36.25
25	8.81	37.63

First, the process factors are chosen, these factors assigned at five levels. The average S/N ratios for the levels are estimated from each response j and shown in table (4.17). Similarly, the S/N ratio averages for the levels of factors are calculated from each response j and also displayed in table (4.17) for all j values.

Table (4.17) the S/N ratio averages

Response	Level/factor	Concentration of H_2O_2 (%)	Quantity of H_2O_2(ml)	Quantity of Yeast(g)	Polymerization Time (min)	Oil (ml)
Compressive strength	1	31.17	22.24	21.86	18.47	21.56
	2	21.47	21.27	22.84	17.50	17.73
	3	17.53	15.77	20.89	22.53	18.15
	4	12.32	21.82	14.26	20.68	20.41
	5	15.85	17.23	18.48	19.15	20.47
Porosity	1	27.17	32.54	32.13	32.14	31.34
	2	27.45	32.42	29.5	33.20	33.2
	3	31.69	32.97	30.37	32.60	31.8
	4	34.87	30.88	33	30.90	31.88
	5	36.03	28.41	32.21	28.38	28.98

The level weights for factors A to E are calculated from each response j using Equation (2.39) and displayed in table (4.18) for all j values.

Table (4.18) the level weight

Response	Level/factor	Concentration of H_2O_2 (%)	Quantity of H_2O_2(ml)	Quantity of Yeast(g)	Polymerization Time (min)	Oil (ml)
Compressive strength	1	1.00	1.00	0.95	0.81	1.00
	2	0.68	0.95	1.00	0.77	0.82
	3	0.56	0.70	0.91	1.00	0.84
	4	0.39	0.98	0.62	0.91	0.94
	5	0.50	0.77	0.80	0.84	0.94
Porosity	1	0.75	0.98	0.97	0.96	0.94
	2	0.76	0.98	0.89	1.00	1.00
	3	0.87	1.00	0.92	0.98	0.95
	4	0.96	0.93	1.00	0.93	0.96
	5	1.00	0.86	0.97	0.85	0.87

The anticipated improvements in the five factors calculated and listed in table (4.19).

Table (4.19) anticipated improvement of the proposed approach

	Level/factor	Concentration of H_2O_2 (%)	Quantity of H_2O_2(ml)	Quantity of Yeast(g)	Polymerization Time (min)	Oil (ml)
Level weight	1	0.87	0.99	0.96	0.89	0.97
	2	0.72	0.96	0.94	0.88	0.91
	3	0.72	0.85	0.91	0.99	0.89
	4	0.68	0.95	0.81	0.92	0.95
	5	0.75	0.81	0.89	0.85	0.91

This method suggested one experiment with the optimal conditions (A_1,B_1,C_1,D_3,E_1) as shown in fig (4.11), given in table (4.20).

Table (4.20) the suggested optimal conditions for combined optimal compressive strength and porosity according to level weight method

Experiments	A	B	C	D	E
Exp-31	10%	0.1	0.2	60	0.1

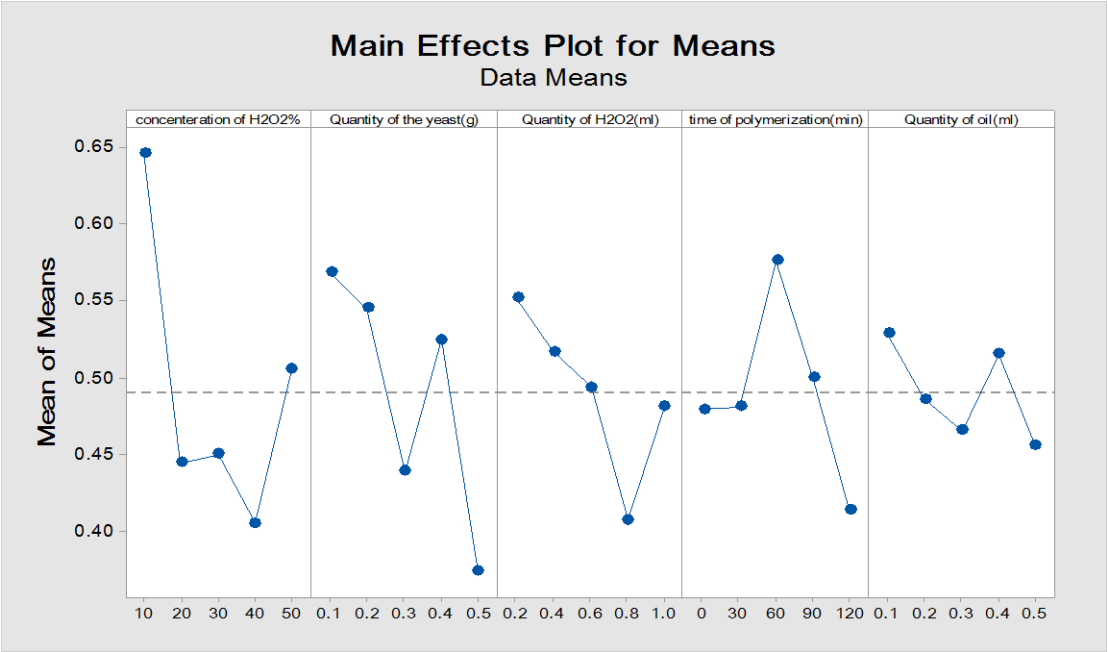

Figure (4.11) the main effects plot for means according to level weight method

4.3.8 The Principal Component Analysis (PCA) Method:

An L25 orthogonal array experiment was used to investigate five variables (A: H_2O_2 concenteration, B: yeast amount, C: H_2O_2 quantity, D: polymerization duration, E: vegetable oil quantity). The responses of interest were compressive strength and porosity. In this example, the two responses belong to the larger-is-better response group. When it comes to consumer importance, the two responses utilize different engineering units and have various relative importance. The NQL values for the two replies are shown in Table (4.21).

Table (4.21) response quality loss values normalized

Exp. no	Compressive strength	porosity
1	1.00	0.54
2	0.91	0.56
3	0.79	0.54
4	0.70	0.38
5	0.65	0.00
6	0.75	0.47
7	0.62	0.26
8	0.26	0.43
9	0.41	0.59
10	0.27	0.33
11	0.32	0.49
12	0.05	0.84
13	0.09	0.89
14	0.69	0.59
15	0.48	0.38
16	0.01	0.94
17	0.27	0.88
18	0.00	1.00
19	0.25	0.54
20	0.16	0.67
21	0.37	0.98
22	0.43	0.85
23	0.17	0.68
24	0.33	0.88
25	0.01	0.95

The NQL values are subsequently subjected to PCA. PCA may be done with a variety of statistical software. Minitab, one of the most widely used statistical software, is employed here. The eigenvector for the principal components is listed in Table (4.22).

Table (4.22) eigenvectors for principal components

component	eigenvector
a11	0.707
a12	0.707

The study' objective is to discover a limited number of straight and statistically independent mixes of the two responses that explain for the bulk of the variance in the data. Only one factor was retrieved in this case since it has an eigenvalue greater than or equal to one. The multi-response performance parameter (Z) for each trial condition is shown in Table (4.23).

Table (4.23) multi-response performance statistic values

Exp. no	Principal component(z)
1	1.08
2	1.03
3	0.93
4	0.76
5	0.45
6	0.86
7	0.62
8	0.48
9	0.70
10	0.42
11	0.57
12	0.62
13	0.68
14	0.90
15	0.60
16	0.67
17	0.81
18	0.70
19	0.56
20	0.58
21	0.95
22	0.90
23	0.60
24	0.85
25	0.68

In order to identify which of the factor effects had a substantial impact on the multi-response performance parameter, an analysis of

variance (ANOVA) was performed on Z. Table (4.24) and (4.25) summarizes the results of the ANOVA.

Table (4.24) major impacts on the performance statistics for multi-response

Analysis of variance for SN ratios						
Source	DF	Seq SS	Adj SS	Adj MS	F	P
A	4	24.84	24.84	6.21	2.30	0.21
B	4	40.26	40.26	10.06	3.73	0.11
C	4	6.31	6.31	1.57	0.59	0.69
D	4	25.60	25.60	6.40	2.37	0.21
E	4	7.65	7.65	1.91	0.71	0.62
Residual erorr	4	10.78	10.78	2.69		
Total	24	115.46				

Table (4.25) shows Response table for signal to noise ratios larger is better

level	A	B	C	D	E
1	-1.73	-1.82	-2.28	-3.07	-2.60
2	-4.40	-2.08	-2.95	-3.02	-2.75
3	-3.45	-3.49	-3.08	-1.55	-3.49
4	-3.57	-2.51	-3.86	-2.84	-2.47
5	-2.06	-5.31	-3.04	-4.73	-3.89
Delta	2.66	3.49	1.58	3.18	1.42
Rank	3	1	4	2	5

The next stage was to determine the best setting for each of the experiment's elements or processing parameters. For each factor, the optimum setting is the one that yields the greatest multi-response performance parameter (or Z) value. According to the (PCA) method, the following factor choices yielded the highest Z number (A_1,B_1,C_1,D_3,E_4), as shown in fig (4.12) and indicated in table (4.26).

Table (4.26) the suggested optimal conditions for combined optimal compressive strength and porosity according to (PCA) method

Experiments	A	B	C	D	E
Exp-32	10%	0.1	0.2	60	0.4

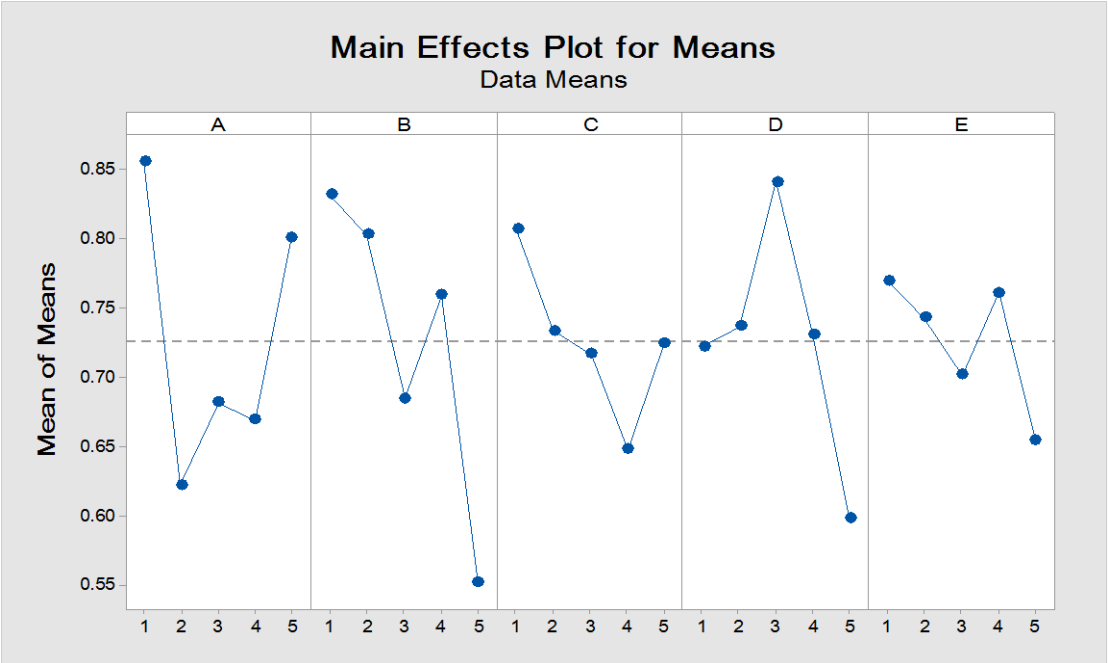

Figure (4.12) the main effects plot for means according to PCA method

4.4 Macrostructure of Optimal Samples

Fig (4.13) shows the porous geopolymer samples produced according to multi response optimization. Those samples foamed with different concenteration of H_2O_2, polymerization time and different amounts of foaming agent, yeast, vegetable oil. The merging of the pores with each other can be seen in fig 4.13 (c-e) which is affected by the viscosity of the paste.

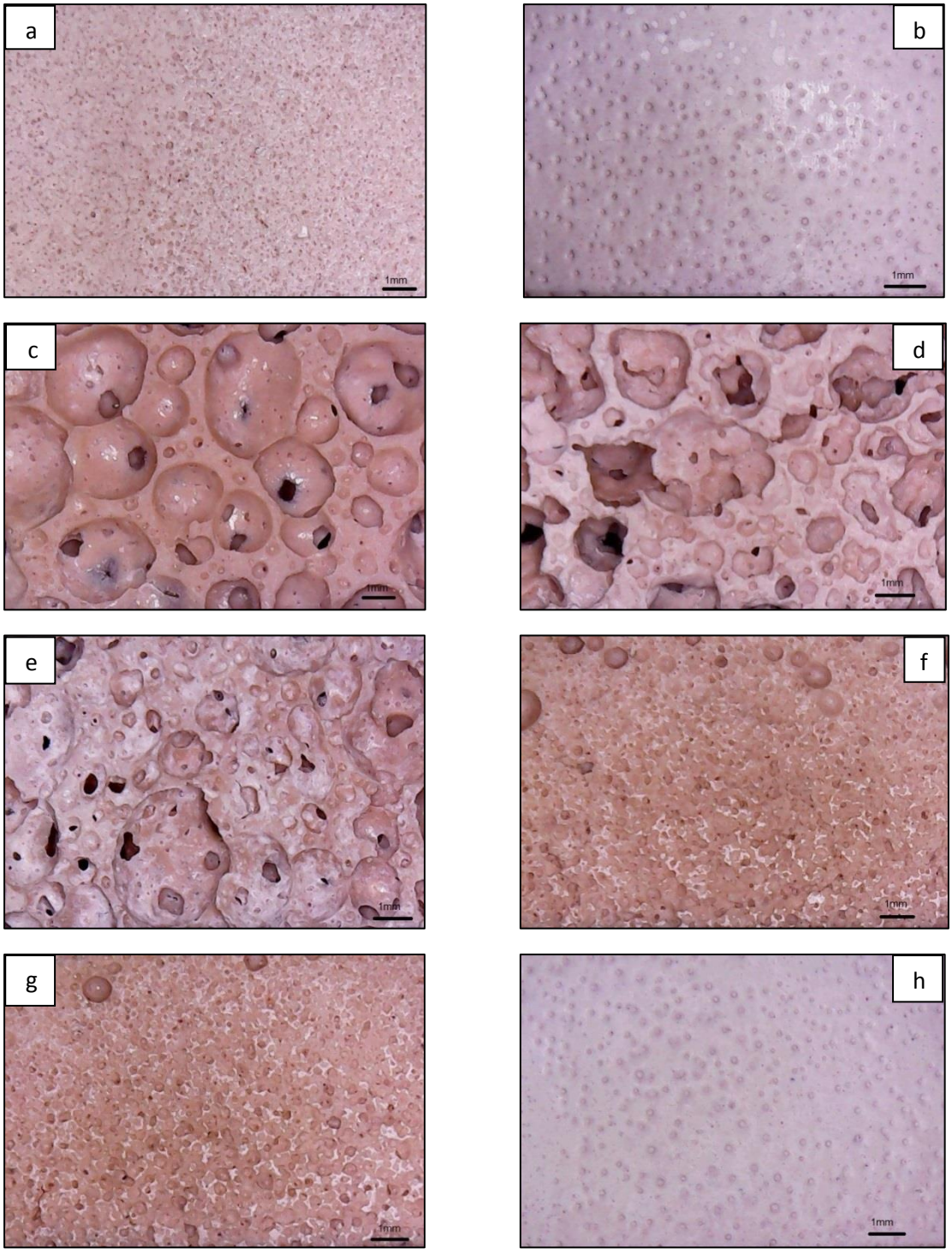

Figure (4.13) optical microscope images of the produced porous geopolymer synthesized according to multi response optimization

4.5 Confirmatory Experiments

The previous tables (4.6, 4.8, 4.9, 4.13, 4.15, 4.20, 4.26) included the results of the different methods in order to obtain the optimum conditions. It can be seen that the suggested optimal conditions are similar for some values of $\boldsymbol{\lambda}$, this indicates that Taguchi method is not sensitive for the minor changes in the values of $\boldsymbol{\lambda}$. Moreover, according to the analysis of variance, it has been found that the factor E has the lowest rank among the studied factors. Keeping these in mind, one can reduce the number of the suggested optimal conditions to eleven experiments only as given in table (4.27). The experimental results of compressive strength and porosity, density, water absorption according to the optimization methods are given in table (4.28). They are superior to that reported for the metakaolin-based geopolymer in the literatures [13] ,[19], [20],[21],[28] as given in table (4.29).

Table (4.27) the suggested optimal conditions for combined optimal compressive strength and porosity

Experiments	A	B	C	D	E
OPT-1	50%	0.1	0.2	90	0.2
OPT-2	50%	0.1	0.2	60	0.2
OPT-3	10%	0.1	0.2	60	0.1
OPT-4	10%	0.1	0.4	60	0.1
OPT-5	50%	0.1	0.8	30	0.1
OPT-6	50%	0.1	0.8	30	0.2
OPT-7	50%	0.5	0.4	90	0.1
OPT-8	50%	0.5	0.4	60	0.1
OPT-9	50%	0.1	0.8	60	0.1
OPT-10	10%	0.1	0.8	60	0.1
OPT-11	10%	0.1	0.4	60	0.2

Table (4.28) the experimental results of the porosity, density, water absorption and compressive strength.

Experiments	Compressive strength(Mpa)	Porosity(%)	Density g/cm^3	Water absorption(%)
OPT-1	15.66	26.3	0.83	31.6
OPT-2	11.42	38.9	0.77	36.0
OPT-3	88.30	22.0	1.26	16.8
OPT-4	45.59	37.6	1.21	11.4
OPT-5	2.36	56.5	0.48	117.0
OPT-6	5.71	58.0	0.71	81.4
OPT-7	6.28	77.0	0.64	68.1
OPT-8	6.38	49.0	0.62	79.3
OPT-9	4.73	59.0	0.47	125.6
OPT-10	34.67	45.2	1.05	15.3
OPT-11	73.43	49.7	1.16	16.8

Table (4.29) the compressive strength and porosity compared with other studied

Reference	Compressive strength(Mpa)	Porosity(%)
[28]	0.57 - 5.9 0.26 - 4.3	28 - 83
[21]	0.3 - 11.6	66 - 83
[20]	3.64 - 7.60	62.5
[19]	1.45	82
[13]	0.35 - 56.5	50 - 86

From table (4.28) the optimal samples are (OPT4, OPT8, OPT10, OPT11), the remaining samples are the lower quality. From the seven optimization methods there are two methods suggested the optimal samples these two methods are (utility concept, DGM), while the other methods (GRA, DEA, PCA, level weight, enginnering judgment) suggested the remaining lower quality samples. From the microscopic images for the optimal samples see fig 4.13 image (h) represents sample (OPT4) it can be noted that the confined pores inside the structure

became more homogeneous, uniformly distributed and rounder pores with lower average pore size results in a compact material with high compressive strength (45.5 Mpa) and high porosity(37.6%). In Fig 4.13 image (g) represents sample (OPT8) in which bubbles tend to coalesce and form larger void, increased porosity resulted in decreased compressive strength. Also, fig 4.13 images (a) and (b) represents (opt10,opt11) in which the pores are evenly distributed, forming a durable structure with high resistance and porosity.

4.6 Single response VIS Multi response

The results can be compared between Taguchi and the multi response optimization method as shown in table (4.30).

Table (4.30) the comparison results

Method	Response	Optimal condition
Single response optimization	Compressive strength	A_1,B_1,C_1,D_3,E_1
	Porosity	A_5,B_3,C_4,D_2,E_2
Multi response optimization	Compressive strength, porosity	A_1,B_1,C_2,D_3,E_1 A_5,B_5,C_2,D_3,E_1 A_1,B_1,C_4,D_3,E_1 A_1,B_1,C_2,D_3,E_2

CHAPTER FIVE
CONCLUSIONS AND RECOMMENDATIONS

5.1 Conclusions

From the results obtained by the current study, the following conclusions can be driven:

1-The experimental results showed that high porosity and adequate compressive strength can be obtained at the same geopolymer body by choosing the suitable values of the processing parameters.

2- The use of yeast as catalyst and the polymerization time are important processing parameters.

3- It has been noticed that the amount of the vegetable oil, which is used as stabilizer, should be kept in low values to obtain the optimal compressive strength and porosity.

4-Optimize both the compressive strength and the porosity of the geopolymer using Taguchi method with the help of several optimization methods are suitable to fulfill the aim; however, the analysis showed that Taguchi method is not sensitive toward the minor changes in the identification coefficient λ of the grey relation analysis.

5- Taguchi method is a suitable tool to design the experiments of metakaolin-based geopolymer with the help of other optimization methods such as the utility concept and DGM method.

6- The multi response optimization approach revealed that in the final step, optimization should begin with establishing the ideal levels of the control parameters.

7- The factors selected for this study: concenteration of H_2O_2, quantity of the yeast, quantity of H_2O_2,polymerization time, quantity of vegetable oil have statistically significant effect on the responses.

8. The compressive strength of the produced porous geopolymer samples equivalent to 88.3 MPa at 28 days with apparent densities (0.47–1.26 g/cm^3), the porosity can be varied between (22- 77%) depending on the mix composition and processing conditions.

5.2 Recommendations

Based on the results obtained in the current study, the following are recommended studies:

1. Conducting a study on improving the porosity of metakaolin based geopolymer using potassium as an alkaline catalyst.
2. Conducting a study on the effect of different types of dispersions on the properties of geopolymers.
3. Conducting a study to learn more about the importance of yeast and its chemical effect as a foaming agent.
4. Conducting a study on the effect of water absorption, pore size, shape and pore distribution on the same composition of geopolymer (Na-geopolymer).

References

[1] C. Jithendra and S. Elavenil, “Influences of Parameters on Slump Flow and Compressive Strength Properties of Aluminosilicate Based Flowable Geopolymer Concrete Using Taguchi Method,” *Silicon*, vol. 12, no. 3, pp. 595–602, 2020.

[2] B. Hökfors, M. Eriksson, and E. Viggh, “Modelling the cement process and cement clinker quality,” *Adv. Cem. Res.*, vol. 26, no. 6, pp. 311–318, 2014.

[3] M. M. Mohsen, “Al-Hussein Bin Talal University Faculty of Engineering Department Of Mining Engineering Cement Manufacturing Relationship between Mining and Cement Manufactaring Submitted to : Dr . Hani Alnawfleh By : Mo ` men Mohsen Anwaar Yousef Al-Farayh Dec / 2015,” no. December, pp. 0–25, 2015.

[4] B. Rangan and D. Hardjito, “Studies on fly ash-based geopolymer concrete,” *Proc. 4th World …*, no. November, 2005.

[5] M. Taylor, C. Tam, and D. Gielen, “Energy Efficiency and CO 2 Emissions from the Global Cement Industry Energy Efficiency and CO 2 Emission Reduction Potentials and Policies in the Cement,” no. September, pp. 4–5, 2006.

[6] B. Afkhami, B. Akbarian, N. Beheshti A., A. H. Kakaee, and B. Shabani, “Energy consumption assessment in a cement production plant,” *Sustain. Energy Technol. Assessments*, vol. 10, pp. 84–89, 2015.

[7] U. Anggarini, S. Pratapa, V. Purnomo, and N. C. Sukmana, “A comparative study of the utilization of synthetic foaming agent and aluminum powder as pore-forming agents in lightweight geopolymer synthesis,” *Open Chem.*, vol. 17, no. 1, pp. 629–638, 2019.

[8] S. Puligilla and P. Mondal, “Role of slag in microstructural development and hardening of fly ash-slag geopolymer,” *Cem. Concr. Res.*, vol. 43, no. 1, pp. 70–80, 2013.

[9] M. I. A. Aleem and P. D. Arumairaj, “Geopolymer Concrete- a Review,” *Int. J. Eng. Sci. Emerg. Technol.*, vol. 1, no. 2, pp. 118–122, 2012.

[10] P. Rovnaník, “Effect of curing temperature on the development of hard structure of metakaolin-based geopolymer,” *Constr. Build. Mater.*, vol. 24, no. 7, pp. 1176–1183, 2010.

[11] C. Tippayasam, S. Boonsalee, S. Sajjavanich, C. Ponzoni, E. Kamseu, and D. Chaysuwan, “Geopolymer Development by Powders of Metakaolin and Wastes in Thailand,” *Adv. Sci. Technol.*, vol. 69, pp. 63–68, 2010.

[12] M. A. Longhi, E. D. Rodríguez, B. Walkley, Z. Zhang, and A. P. Kirchheim, *Metakaolin-based geopolymers: Relation between formulation, physicochemical properties and efflorescence formation*, vol. 182. 2020.

[13] Y. Qiao *et al.*, “Effects of surfactants/stabilizing agents on the microstructure and properties of porous geopolymers by direct foaming,” *J. Asian Ceram. Soc.*, vol. 9, no. 1, pp. 412–423, 2021.

[14] C. Bai and P. Colombo, “Processing , properties and applications of highly porous geopolymers : A review Processing , properties and applications of highly porous geopolymers : A review,” *Ceram. Int.*, no. June, pp. 1–16, 2018.

[15] K. Prałat, J. Ciemnicka, A. Koper, K. E. Buczkowska, and P. Łoś, “Comparison of the thermal properties of geopolymer and modified gypsum,” *Polymers (Basel).*, vol. 13, no. 8, pp. 1–18, 2021.

[16] T. Kovárík and J. Hájek, “Porous geopolymers: processing routes and properties,” *IOP Conf. Ser. Mater. Sci. Eng.*, vol. 613, p.

012048, 2019.

[17] C. Bai, “Highly Porous Geopolymer Components,” p. 145.

[18] T. Ohji and M. Fukushima, “Macro-porous ceramics: Processing and properties,” *Int. Mater. Rev.*, vol. 57, no. 2, pp. 115–131, 2012.

[19] Y. Cui, D. Wang, J. Zhao, D. Li, S. Ng, and Y. Rui, “Effect of calcium stearate based foam stabilizer on pore characteristics and thermal conductivity of geopolymer foam material,” *J. Build. Eng.*, vol. 20, no. June, pp. 21–29, 2018.

[20] N. Lertcumfu, K. Kaewapai, P. Jaita, T. Tunkasiri, S. Sirisoonthorn, and G. Rujijanagul, “Effects of olive oil on physical and mechanical properties of ceramic waste-based geopolymer foam,” *J. Reinf. Plast. Compos.*, vol. 39, no. 3–4, pp. 111–118, 2020.

[21] C. Bai, T. Ni, Q. Wang, H. Li, and P. Colombo, “Porosity, mechanical and insulating properties of geopolymer foams using vegetable oil as the stabilizing agent,” *J. Eur. Ceram. Soc.*, vol. 38, no. 2, pp. 799–805, 2018.

[22] C. Bai and P. Colombo, “High-porosity geopolymer membrane supports by peroxide route with the addition of egg white as surfactant,” *Ceram. Int.*, vol. 43, no. 2, pp. 2267–2273, 2017.

[23] C. Bai *et al.*, “High-porosity geopolymer foams with tailored porosity for thermal insulation and wastewater treatment,” *J. Mater. Res.*, vol. 32, no. 17, pp. 3251–3259, 2017.

[24] C. Bai, H. Li, E. Bernardo, and P. Colombo, “Waste-to-resource Preparation of Glass-containing Foams from Geopolymers Waste-to-resource preparation of glass-containing foams from geopolymers,” *Ceram. Int.*, no. January, pp. 0–1, 2019.

[25] Y. Liu, C. Yan, Z. Zhang, Y. Gong, H. Wang, and X. Qiu, “A facile method for preparation of floatable and permeable fly ash-based geopolymer block,” *Mater. Lett.*, vol. 185, no. September, pp. 370–

373, 2016.

[26] T. Yang, C. Chou, and C. Chien, “The Effects of Foaming Agents and Modifiers on a Foamed-geopolymer,” 2012.

[27] A. Hajimohammadi, T. Ngo, P. Mendis, T. Nguyen, A. Kashani, and J. S. J. van Deventer, “Pore characteristics in one-part mix geopolymers foamed by H2O2: The impact of mix design,” *Mater. Des.*, vol. 130, no. March, pp. 381–391, 2017.

[28] S. Petlitckaia and A. Poulesquen, “Design of lightweight metakaolin based geopolymer foamed with hydrogen peroxide,” *Ceram. Int.*, vol. 45, no. 1, pp. 1322–1330, 2019.

[29] T. W. Haas, “Kinetics of the uncatalyzed, alkaline decomposition of hydrogen peroxide,” *Retrosp. Theses Diss.*, no. 2645, p. 74, 1960.

[30] Z. Zhang, H. Wang, and H. Wang, “The Pore characteristics of geopolymer Foam concrete and Their impact on the compressive strength and Modulus,” vol. 3, no. August, pp. 1–10, 2016.

[31] E. D. Van Rest and D. J. Cowden, “Statistical Methods in Quality Control.,” *Appl. Stat.*, vol. 7, no. 3, p. 202, 1958.

[32] M. A. A. Al-Dujaili, I. A. D. Al-Hydary, and Z. Z. Hassan, “Optimizing the Properties of Metakaolin-based (Na, K)-Geopolymer Using Taguchi Design Method,” *Int. J. Eng. Trans. A Basics*, vol. 33, no. 4, pp. 631–638, 2020.

[33] Z. Z. H. M. A. Ahmed Al-dujaili, I. A. Disher Al-hydary, “Experimental Improvment of Geopolymer-Cement Properties Using Taguchi Method,” University of Babylon, 2019.

[34] G. Masi, W. D. A. Rickard, L. Vickers, M. C. Bignozzi, and A. Van Riessen, “A comparison between different foaming methods for the synthesis of light weight geopolymers,” *Ceram. Int.*, vol. 40, no. 9 PART A, pp. 13891–13902, 2014.

[35] B. A. Ionescu, A.-V. Lăzărescu, and A. Hegyi, “The Possibility of

Using Slag for the Production of Geopolymer Materials and Its Influence on Mechanical Performances—A Review," *Proceedings*, vol. 63, no. 1, p. 30, 2020.

[36] G. N. Kishore and B. Gayathri, "Experimental Study on Rise Husk Ash & Fly Ash Based Geo-Polymer Concrete Using M-Sand," *IOP Conf. Ser. Mater. Sci. Eng.*, vol. 225, no. 1, 2017.

[37] H. I. Riyap *et al.*, "Microstructure and mechanical, physical and structural properties of sustainable lightweight metakaolin-based geopolymer cements and mortars employing rice husk," *J. Asian Ceram. Soc.*, vol. 7, no. 2, pp. 199–212, 2019.

[38] S. K. Das and S. M. Mustakim, "Geopolymer Composites for Bone Tissue Application : A Short Overview," no. July, 2020.

[39] J. Davidovits and D. Comrie, "Long term durability of hazardous toxic and nuclear waste disposals," *1st Eur. Conf. Soft Miner. Compiegne, Fr.*, vol. 1, no. June 1988, pp. 125–134, 1988.

[40] J. Davidovits and M. Davidovics, "GEOPOLYMER : ULTRA-HIGH TEMPERATURE TOOLING MATERIAL," vol. 2, pp. 1–10, 1991.

[41] V. Ducman and L. Korat, "Characterization of geopolymer fly-ash based foams obtained with the addition of Al powder or H2O2 as foaming agents," *Mater. Charact.*, vol. 113, pp. 207–213, 2016.

[42] J. Davidovits, "Geopolymers : Ceramic-Like Inorganic Polymers," vol. 350, pp. 335–350, 2017.

[43] V. D. Cao *et al.*, "Influence of Microcapsule Size and Shell Polarity on the Time-Dependent Viscosity of Geopolymer Paste," *Ind. Eng. Chem. Res.*, vol. 57, no. 29, pp. 9457–9464, 2018.

[44] D. Khale and R. Chaudhary, "Mechanism of geopolymerization and factors influencing its development: A review," *J. Mater. Sci.*, vol. 42, no. 3, pp. 729–746, 2007.

[45] M. Torres-Carrasco and F. Puertas, “Alkaline activation of different aluminosilicates as an alternative to Portland cement: Alkali activated cements or geopolymers,” *Rev. Ing. Construcción*, vol. 32, no. 2, pp. 05–12, 2017.

[46] C. Shi, F. He, S. National, and P. V Krivenko, “classification and characteristics of alkali-activated cements” no. January, 2012.

[47] JianHe, “Synthesis and characterization of geopolymers for infrastructural applications ,Louisiana State University LSU Digital Commons,” 2012.

[48] J. L. Provis, “Activating solution chemistry for geopolymers,” *Geopolymers Struct. Process. Prop. Ind. Appl.*, pp. 50–71, 2009.

[49] Z. Zhang, X. Yao, H. Zhu, S. Hua, and Y. Chen, “Activating process of geopolymer source material: Kaolinite,” *J. Wuhan Univ. Technol. Mater. Sci. Ed.*, vol. 24, no. 1, pp. 132–136, 2009.

[50] G. Varga, “The structure of kaolinite and metakaolinite,” *Epa. - J. Silic. Based Compos. Mater.*, vol. 59, no. 1, pp. 6–9, 2007.

[51] K. Nizar, H. Kamarudin, and M. S. Idris, “Pysical , Chemical & Mineralogical Properties of Fly-ash,” vol. 4, no. January, pp. 47–51, 2015.

[52] J. Temuujin, R. P. Williams, and A. van Riessen, “Effect of mechanical activation of fly ash on the properties of geopolymer cured at ambient temperature,” *J. Mater. Process. Technol.*, vol. 209, no. 12–13, pp. 5276–5280, 2009.

[53] A. R. Krishnaraja, N. P. Sathishkumar, T. S. Kumar, and P. D. Kumar, “Mechanical Behaviour of Geopolymer Concrete under Ambient Curing,” vol. 132, no. 3, pp. 130–132, 2014.

[54] Z. Zhang, J. L. Provis, A. Reid, and H. Wang, “Geopolymer foam concrete: An emerging material for sustainable construction,” *Constr. Build. Mater.*, vol. 56, pp. 113–127, 2014.

[55] X. Peng, H. Li, Q. Shuai, and L. Wang, “Fire resistance of alkali activated geopolymer foams produced from metakaolin and Na2O2,” *Materials (Basel).*, vol. 13, no. 3, pp. 1–8, 2020.

[56] H. Zhao, Q. Xiao, D. Huang, and S. Zhang, “Influence of pore structure on compressive strength of cement mortar,” *Sci. World J.*, vol. 2014, 2014.

[57] A. Pokhrel, D. N. Seo, S. T. Lee, and I. J. Kim, “Processing of porous ceramics by direct foaming: A review,” *J. Korean Ceram. Soc.*, vol. 50, no. 2, pp. 93–102, 2013.

[58] N. Halyag and G. Mucsi, “Functionalized geopolymers: A review,” *Reciklaza i Odrziv. Razvoj*, vol. 11, no. 1, pp. 1–7, 2018.

[59] “JFK 7th Grade Science Bony modeling lab safety protocols !”

[60] "Numerical and Experimental Study the Effect of Alkali Type on the Properties of Modified Geopolymer Concrete" a thesis- 2019

[61] I. Asiltürk and H. Akkuş, “Determining the effect of cutting parameters on surface roughness in hard turning using the Taguchi method,” *Meas. J. Int. Meas. Confed.*, vol. 44, no. 9, pp. 1697–1704, 2011.

[62] D. Manivel and R. Gandhinathan, “Optimization of surface roughness and tool wear in hard turning of austempered ductile iron (grade 3) using Taguchi method,” *Meas. J. Int. Meas. Confed.*, vol. 93, no. grade 3, pp. 108–116, 2016.

[63] S. A. Niknam and V. Songmene, “Simultaneous optimization of burrs size and surface finish when milling 6061-T6 aluminium alloy,” *Int. J. Precis. Eng. Manuf.*, vol. 14, no. 8, pp. 1311–1320, 2013.

[64] L. Tong, C. Su, and C. Wang, “The optimization of multi- response problems in the Taguchi method,” vol. 14, no. 4, pp. 367–380, 1997.

[65] A. A. M. D. Al-tahat, “Solving the multi-response problem in Taguchi method by benevolent formulation in DEA,” pp. 505–521, 2011.

[66] B. Beshah, S. Woldegebriel, and G. Desta, “MULTI-STAGE AND MULTI-RESPONSE PROCESS OPTIMIZATION IN TAGUCHI METHOD,” vol. 33, no. December, pp. 1–12, 2015.

[67] A. N. Haq, P. Marimuthu, and R. Jeyapaul, “Multi response optimization of machining parameters of drilling Al/SiC metal matrix composite using grey relational analysis in the Taguchi method,” *Int. J. Adv. Manuf. Technol.*, vol. 37, no. 3–4, pp. 250–255, 2008.

[68] V. N. Gaitonde, S. R. Karnik, and J. P. Davim, “Multiperformance optimization in turning of free-machining steel using Taguchi method and utility concept,” *J. Mater. Eng. Perform.*, vol. 18, no. 3, pp. 231–236, 2009.

[69] R. Rq, G. Lq, and D. Dqg, “multi-response optimization in dry turning process usingTaguchi’s appraoch and utility concept ” vol. 5, pp. 2142–2151, 2014.

[70] J. L. Lin and C. L. Lin, “The use of the orthogonal array with grey relational analysis to optimize the electrical discharge machining process with multiple performance characteristics,” *Int. J. Mach. Tools Manuf.*, vol. 42, no. 2, pp. 237–244, 2002.

[71] H. C. Liao, “A data envelopment analysis method for optimizing multi-response problem with censored data in the Taguchi method,” *Comput. Ind. Eng.*, vol. 46, no. 4 SPEC. ISS., pp. 817–835, 2004.

[72] C. S. Aksezer, “On the sensitivity of desirability functions for multiresponse optimization,” *J. Ind. Manag. Optim.*, vol. 4, no. 4, pp. 685–696, 2008.

[73] P. Taylor, “Response Surface Methodology and Related Topics,”

Technometrics, vol. 49, no. 4, pp. 501–501, 2007.

[74] G. Derringer and R. Suich, "Simultaneous Optimization of Several Response Variables," *J. Qual. Technol.*, vol. 12, no. 4, pp. 214–219, 1980.

[75] "Madhav S. Phadke - Quality Engineering Using Robust Design (1989, Prentice Hall) - libgen.lc.pdf." .

[76] A. Al-refaie, T. Wu, and M. Li, "An Effective Approach for Solving The Multi-Response Problem in Taguchi Method," vol. 4, no. 2, pp. 314–323, 2010.

[77] J. H. Sheesley, "Quality Engineering in Production Systems," *Technometrics*, vol. 32, no. 4, pp. 457–458, 1990.

[78] S. Maghsoodloo, "The Exact Relation of Taguchi's Signal-to-Noise Ratio to His Quality Loss Function," *J. Qual. Technol.*, vol. 22, no. 1, pp. 57–67, 1990.

[79] K. Pearson, " LIII. On lines and planes of closest fit to systems of points in space ," *London, Edinburgh, Dublin Philos. Mag. J. Sci.*, vol. 2, no. 11, pp. 559–572, 1901.

[80] H. Hotelling, "Analysis of a complex of statistical variables into principal components," *J. Educ. Psychol.*, vol. 24, no. 6, pp. 417–441, 1933.

[81] I. M. Centre, "MULTI-RESPONSE OPTIMIZATION IN INDUSTRIAL EXPERIMENTS USING TAGUCHI ' S QUALITY LOSS FUNCTION AND PRINCIPAL COMPONENT ANALYSIS," no. May 1999, pp. 3–8, 2000.

[82] P. Duxson, J. L. Provis, G. C. Lukey, S. W. Mallicoat, W. M. Kriven, and J. S. J. Van Deventer, "Understanding the relationship between geopolymer composition, microstructure and mechanical properties," *Colloids Surfaces A Physicochem. Eng. Asp.*, vol. 269, no. 1–3, pp. 47–58, 2005.

[83] K. Okada, A. Ooyama, T. Isobe, Y. Kameshima, A. Nakajima, and K. J. D. Mackenzie, “Water retention properties of porous geopolymers for use in cooling applications,” vol. 29, pp. 1917–1923, 2009.

[84] V. Vaou and D. Panias, “Thermal insulating foamy geopolymers from perlite,” *Miner. Eng.*, vol. 23, no. 14, pp. 1146–1151, 2010.

[85] K. Pimraksa, P. Chindaprasirt, A. Rungchet, K. Sagoe-crentsil, and T. Sato, “Lightweight geopolymer made of highly porous siliceous materials with various,” *Mater. Sci. Eng. A*, vol. 528, no. 21, pp. 6616–6623, 2011.

[86] E. Kamseu, B. Nait-Ali, M. C. Bignozzi, C. Leonelli, S. Rossignol, and D. S. Smith, “Bulk composition and microstructure dependence of effective thermal conductivity of porous inorganic polymer cements,” *J. Eur. Ceram. Soc.*, vol. 32, no. 8, pp. 1593–1603, 2012.

[87] M. Olivia and H. Nikraz, “Properties of fly ash geopolymer concrete designed by Taguchi method,” *Mater. Des.*, vol. 36, pp. 191–198, 2012.

[88] P. Steins *et al.*, “Effect of aging and alkali activator on the porous structure of a geopolymer,” *J. Appl. Crystallogr.*, vol. 47, no. 1, pp. 316–324, 2014.

[89] M. S. Cilla, M. R. Morelli, and P. Colombo, “Open cell geopolymer foams by a novel saponification/peroxide/gelcasting combined route,” *J. Eur. Ceram. Soc.*, vol. 34, no. 12, pp. 3133–3137, 2014.

[90] Z. Liu *et al.*, “Fabrication and properties of foam geopolymer using circulating fluidized bed combustion fly ash,” *Int. J. Miner. Metall. Mater.*, vol. 21, no. 1, pp. 89–94, 2014.

[91] P. Palmero, A. Formia, P. Antonaci, S. Brini, and J. M. Tulliani, “Geopolymer technology for application-oriented dense and lightened materials. Elaboration and characterization,” *Ceram. Int.*,

vol. 41, no. 10, pp. 12967–12979, 2015.

[92] D. M. A. Huiskes, A. Keulen, Q. L. Yu, and H. J. H. Brouwers, “Design and performance evaluation of ultra-lightweight geopolymer concrete,” *Mater. Des.*, vol. 89, pp. 516–526, 2016.

[93] R. M. Novais, G. Ascensão, L. H. Buruberri, L. Senff, and J. A. Labrincha, “Influence of blowing agent on the fresh- and hardened-state properties of lightweight geopolymers,” *Mater. Des.*, vol. 108, pp. 551–559, 2016.

[94] A. Mehta, R. Siddique, B. P. Singh, S. Aggoun, G. Łagód, and D. Barnat-Hunek, “Influence of various parameters on strength and absorption properties of fly ash based geopolymer concrete designed by Taguchi method,” *Constr. Build. Mater.*, vol. 150, pp. 817–824, 2017.

[95] M. Łach, D. Mierzwiński, K. Korniejenko, and J. Mikuła, “Geopolymer foam as a passive fire protection,” vol. 00031, pp. 1–6, 2018.

[96] K. Onoue, T. Iwamoto, and Y. Sagawa, “Optimization of the design parameters of fly ash-based geopolymer using the dynamic approach of the Taguchi method,” *Constr. Build. Mater.*, vol. 219, pp. 1–10, 2019.

[97] S. Petlitckaia and A. Poulesquen, “Author ’ s Accepted Manuscript,” *Ceram. Int.*, 2018.

[98] A. Kaddami and O. Pitois, “Cement and Concrete Research A physical approach towards controlling the microstructure of metakaolin- based geopolymer foams,” *Cem. Concr. Res.*, vol. 124, no. June, p. 105807, 2019.

[99] J. B. Saedon, N. Jaafar, and M. Azman, “Multi-objective optimization of titanium alloy through orthogonal array and grey relational analysis in WEDM,” *Procedia Technol.*, vol. 15, pp. 832–

840, 2014.

[100] S. Zhang, W. Qiao, Y. Wu, Z. Fan, and L. Zhang, “Multi-Response Optimization of Ultrafine Cement-Based Slurry Using the Taguchi-Grey Relational Analysis Method,” pp. 1–23, 2021.

[101] N. Costa and J. Lourenço, “a comparative study of multi response optimization criteria working ability,” *Chemom. Intell. Lab. Syst.*, 2014.